



MINISTÉRIO DA CIÊNCIA, TECNOLOGIA, INOVAÇÕES E COMUNICAÇÕES
INSTITUTO NACIONAL DE PESQUISAS ESPACIAIS

sid.inpe.br/mtc-m21c/2019/04.17.16.57-TDI

**MIMETIC GRAVITY DESCRIPTION OF LOOP
QUANTUM COSMOLOGY: REINTERPRETING THE
BOUNCE AND INFLATION FROM A CURVATURE
PERSPECTIVE**

Eunice Valtânia de Jesus Bezerra

Doctorate Thesis of the Graduate
Course in Astrophysics, guided
by Dr. Oswaldo Duarte Miranda,
approved in April 29, 2019.

URL of the original document:

<<http://urlib.net/8JMKD3MGP3W34R/3T62Q42>>

INPE
São José dos Campos
2019

PUBLISHED BY:

Instituto Nacional de Pesquisas Espaciais - INPE
Gabinete do Diretor (GBDIR)
Serviço de Informação e Documentação (SESID)
CEP 12.227-010
São José dos Campos - SP - Brasil
Tel.:(012) 3208-6923/7348
E-mail: pubtc@inpe.br

**BOARD OF PUBLISHING AND PRESERVATION OF INPE
INTELLECTUAL PRODUCTION - CEPPII (PORTARIA Nº
176/2018/SEI-INPE):****Chairperson:**

Dra. Marley Cavalcante de Lima Moscati - Centro de Previsão de Tempo e Estudos
Climáticos (CGCPT)

Members:

Dra. Carina Barros Mello - Coordenação de Laboratórios Associados (COCTE)
Dr. Alisson Dal Lago - Coordenação-Geral de Ciências Espaciais e Atmosféricas
(CGCEA)
Dr. Evandro Albiach Branco - Centro de Ciência do Sistema Terrestre (COCST)
Dr. Evandro Marconi Rocco - Coordenação-Geral de Engenharia e Tecnologia
Espacial (CGETE)
Dr. Hermann Johann Heinrich Kux - Coordenação-Geral de Observação da Terra
(CGOBT)
Dra. Ieda Del Arco Sanches - Conselho de Pós-Graduação - (CPG)
Sílvia Castro Marcelino - Serviço de Informação e Documentação (SESID)

DIGITAL LIBRARY:

Dr. Gerald Jean Francis Banon
Clayton Martins Pereira - Serviço de Informação e Documentação (SESID)

DOCUMENT REVIEW:

Simone Angélica Del Ducca Barbedo - Serviço de Informação e Documentação
(SESID)
André Luis Dias Fernandes - Serviço de Informação e Documentação (SESID)

ELECTRONIC EDITING:

Ivone Martins - Serviço de Informação e Documentação (SESID)
Cauê Silva Fróes - Serviço de Informação e Documentação (SESID)



MINISTÉRIO DA CIÊNCIA, TECNOLOGIA, INOVAÇÕES E COMUNICAÇÕES
INSTITUTO NACIONAL DE PESQUISAS ESPACIAIS

sid.inpe.br/mtc-m21c/2019/04.17.16.57-TDI

**MIMETIC GRAVITY DESCRIPTION OF LOOP
QUANTUM COSMOLOGY: REINTERPRETING THE
BOUNCE AND INFLATION FROM A CURVATURE
PERSPECTIVE**

Eunice Valtânia de Jesus Bezerra

Doctorate Thesis of the Graduate
Course in Astrophysics, guided
by Dr. Oswaldo Duarte Miranda,
approved in April 29, 2019.

URL of the original document:

<<http://urlib.net/8JMKD3MGP3W34R/3T62Q42>>

INPE
São José dos Campos
2019

Cataloging in Publication Data

Bezerra, Eunice Valtânia de Jesus.

B469m Mimetic gravity description of loop quantum cosmology: reinterpreting the bounce and inflation from a curvature perspective / Eunice Valtânia de Jesus Bezerra. – São José dos Campos : INPE, 2019.

xxii + 128 p. ; (sid.inpe.br/mtc-m21c/2019/04.17.16.57-TDI)

Thesis (Doctorate in Astrophysics) – Instituto Nacional de Pesquisas Espaciais, São José dos Campos, 2019.

Guiding : Dr. Oswaldo Duarte Miranda.

1. Mimetic Gravity. 2. Loop Quantum Cosmology. 3. Higgs inflation. 4. Curvature. 5. Primordial universe. I.Title.

CDU 550.312:524.8



Esta obra foi licenciada sob uma Licença [Creative Commons Atribuição-NãoComercial 3.0 Não Adaptada](https://creativecommons.org/licenses/by-nc/3.0/).

This work is licensed under a [Creative Commons Attribution-NonCommercial 3.0 Unported License](https://creativecommons.org/licenses/by-nc/3.0/).

Aluno (a): **Eunice Valtânia de Jesus Bezerra**

Título: "MIMETIC GRAVITY DESCRIPTION OF LOOP QUANTUM COSMOLOGY: REINTERPRETING THE BOUNCE AND INFLATION FROM A CURVATURE PERSPECTIVE"

Aprovado (a) pela Banca Examinadora em cumprimento ao requisito exigido para obtenção do Título de **Doutor(a)** em **Astrofísica**

Dr. Odylio Denys de Aguiar



Presidente / INPE / SJC Campos - SP

() **Participação por Vídeo - Conferência**

Aprovado () **Reprovado**

Dr. Oswaldo Duarte Miranda



Orientador(a) / INPE / SJC Campos - SP

() **Participação por Vídeo - Conferência**

Aprovado () **Reprovado**

Dr. Carlos Alexandre Wuensche de Souza



Membro da Banca / INPE / SJC Campos - SP

() **Participação por Vídeo - Conferência**

Aprovado () **Reprovado**

Dr. Tobias Frederico



Convidado(a) / ITA / São José dos Campos - SP

Participação por Vídeo - Conferência

Aprovado () **Reprovado**

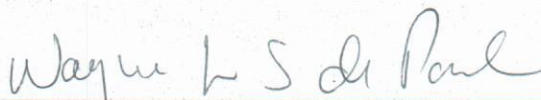
Este trabalho foi aprovado por:

() **maioria simples**

unanimidade

Aprovado (a) pela Banca Examinadora
em cumprimento ao requisito exigido para
obtenção do Título de **Doutor(a)** em
Astrofísica

Dr. Wayne Leonardo Silva de Paula

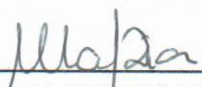


Convidado(a) / ITA / São José dos Campos - SP

() Participação por Vídeo - Conferência

Aprovado () Reprovado

Dr. Marco André Ferreira Dias



Convidado(a) / UNIFESP / Diadema - SP

() Participação por Vídeo - Conferência

Aprovado () Reprovado

Este trabalho foi aprovado por:

() maioria simples

unanimidade

*To my mother **Virgulina**, for all her love and support.*

ACKNOWLEDGEMENTS

I would like to thank my mother Virgulina for all her love and effort to provide me with the best opportunities she could. I am extremely proud to be called her daughter.

I would like to thank my advisor Dr. Oswaldo Duarte Miranda for the honor and privilege to work with him. I could not have asked for a better person to guide me during my PhD.

I am grateful for the support of my blood family, including my father, sister, grandmother, aunts, cousins, uncles and so on.

I am really thankful for the heart family I found at INPE, in particular, Lorena, Carol, Aysses, Isabel, Dinelsa, Fabrícia, Eduardo, Manuel and Fernando.

I would like to thank my teachers for all the teachings I learned along these years.

I thank the INPE staff for the help and kindness I was treated since the start of my master course.

I would like to thank CAPES for the graduate research fellowship.

ABSTRACT

The physics of the early universe remains a mystery to cosmologists. The primordial universe is within energy scales in which the quantum gravity effects may play a significant role. A consistent quantum gravity theory would be composed with the best elements from general relativity and quantum field theory. In our work, we focus on Loop Quantum Gravity (LQG) or being more specific, we are interested in its cosmological counterpart, called Loop Quantum Cosmology (LQC), at the effective level. The results coming from Effective LQC are promising, mainly, the replacement of the initial singularity by a bounce. On the other hand, there is a very powerful approach known as Mimetic Gravity (MG) that can also produce a bounce. The original theory was not built with this purpose, but it was generalized and became capable of reproducing different cosmological evolutionary scenarios. Above all, [Langlois et al. \(2017\)](#) constructed a MG description of LQC in which the Effective LQC dynamics was reproduced. In particular, we explore the treatment employed to obtain the cosmological evolution in a curved Friedmann-Robertson-Walker space-time and the curvature potential presented in it. We build our own formulation reinterpreting the curvature potential role, at the same time, we emphasize its direct relation with matter. After, we apply the developed formalism to Higgs inflationary scenario, taking advantage of the intrinsic relation between the Higgs field and curvature. Moreover, we discuss the primordial gravitational waves and its essential role as fundamental proofs to validate any cosmological model whose aim is to describe the primordial universe dynamics.

Keywords: Mimetic Gravity. Loop Quantum Cosmology. Higgs Inflation. Curvature. Primordial universe.

DESCRIÇÃO DA COSMOLOGIA QUÂNTICA EM LAÇOS PELA GRAVIDADE MIMÉTICA: REINTERPRETANDO O RICOCHETE E A INFLAÇÃO PELA PERSPECTIVA DA CURVATURA

RESUMO

A física do universo primordial permanece um mistério para os cosmólogos. O universo primordial está dentro do intervalo de energia no qual os efeitos gravitacionais quânticos desempenhariam um papel significativo. Uma teoria de gravitação quântica consistente seria composta pelos melhores elementos da relatividade geral e teoria quântica de campo. No nosso trabalho, nós focamos na Gravitação Quântica em Laços (GQL), ou sendo mais específicos, estamos interessados na sua contrapartida cosmológica, denominada Cosmologia Quântica em Laços (CQL), no nível efetivo. Os resultados oriundos da CQL são promissores, principalmente, a substituição da singularidade inicial por um ricochete. Por outro lado, existe uma poderosa abordagem conhecida como Gravidade Mimética (GM) que também pode produzir um ricochete. A teoria original não foi construída com esse propósito, mas foi generalizada, tornando-se capaz de reproduzir diferentes cenários de evolução cosmológica. Sobretudo, [Langlois et al. \(2017\)](#) construiu uma descrição da CQL através da GM, na qual a dinâmica efetiva da CQL pode ser reproduzida. Em particular, exploramos o tratamento empregado para obter a evolução cosmológica de um espaço-tempo Friedmann-Robertson-Walker curvo, além do potencial de curvatura nele apresentado. Construímos nossa formulação própria reinterpretando o papel do potencial de curvatura, ao mesmo tempo em que enfatizamos sua relação direta com a matéria. A seguir, aplicamos nossa formulação para o cenário da inflação de Higgs, usufruindo da relação intrínseca entre o campo de Higgs e a curvatura. Além disso, discutimos as ondas gravitacionais primordiais, bem como seu papel essencial como uma prova fundamental utilizada para confirmar a validade de um modelo cosmológico cujo objetivo é descrever a dinâmica do universo primordial.

Palavras-chave: Gravidade Mimética. Cosmologia Quântica em Laços. Inflação de Higgs. Curvatura. Universo primordial.

LIST OF FIGURES

	<u>Page</u>
1.1 Standard universe evolution timeline	4
1.2 Horizon problem	11
1.3 Solution to the horizon problem	14
1.4 Particle horizon and Hubble radius	14
1.5 Universe evolution	22
2.1 Space-time foliation	27
2.2 Relation between the spacelike hypersurfaces in the universe foliation	27
2.3 Extrinsic curvature of the hypersurface	30
2.4 Spin network	45
2.5 Possible previous configuration of our universe	49
2.6 Scheme evolution of the very early universe	51
4.1 Solutions of the tracking equation	78
4.2 Evolution of the potential terms regarding MG and HI	79
4.3 Evolution of the modified Friedmann equation	87
5.1 BICEP2 CMB power spectrum for B-mode	92
5.2 CMB power spectrum	93
5.3 CMB spectrum for a bounce universe	94
5.4 CMB spectrum from Loop Quantum Cosmology	95
5.5 CMB spectrum from Massive Gravity	96
6.1 MG as the bridge between LQC and HI	101
C.1 Cosmic Microwave Background	125
C.2 CMB polarization patterns	128

LIST OF TABLES

	<u>Page</u>
1.1 Epochs of the standard universe evolution	5
2.1 Variables that plays similar roles	32
2.2 Different pairs of variables from Loop Quantum Cosmology	44
2.3 Evolutionary stages of the primordial universe in Loop Quantum Cos- mology	52

LIST OF ABBREVIATIONS

ADM	–	Arnowitt-Deser-Misner
BEH	–	Brout-Englert-Higgs
CMB	–	Cosmic Microwave Background
DHOST	–	Degenerate Higher-Order Scalar-Tensor
DE	–	dark energy
DM	–	dark matter
EFE	–	Einstein Field Equations
EoM	–	Equations of motion
EoS	–	Equation of state
EW	–	Electroweak
FRW	–	Friedmann-Robertson-Walker
GR	–	General Relativity
GW	–	Gravitational Waves
HBB	–	Hot Big Bang
HI	–	Higgs Inflation
LQC	–	Loop Quantum Cosmology
LQG	–	Loop Quantum Gravity
MG	–	Mimetic Gravity
PGW	–	Primordial Gravitational Waves
SCM	–	Standard Cosmological Model
SMPP	–	Standard Model of Particle Physics
SLS	–	Surface of Last Scattering
Λ CDM	–	Lambda Cold Dark Matter

LIST OF SYMBOLS

$c = \hbar = 1$	–	Natural units
t	–	Proper time
η	–	Conformal time
Greek letters (μ, ν)	–	space-time coordinates
Latin letters (a, b)	–	spatial coordinates
\cdot	–	Derivative with respect to the proper time
(3)	–	Three-dimensional space
∂_μ	–	Partial derivative with respect to the coordinates
∇_μ	–	Covariant derivative with respect to the coordinates
a	–	Scale Factor
$\gamma_{\mu\nu}$	–	Minkowski metric or background metric
$g_{\mu\nu}$	–	Space-time metric
q_{ab}	–	Hypersurface metric
N	–	Lapse function or e-fold number
N^a	–	Shift vector
δ_ν^μ	–	Kronecker delta
$\Gamma_{\mu\nu}^\rho$	–	Christoffel symbol
$R_{\mu\nu\sigma}^\rho$	–	Riemann tensor
$R_{\mu\nu}$	–	Ricci tensor
R	–	Ricci scalar
$G_{\mu\nu}$	–	Einstein tensor
G	–	Newtonian constant
m_{Pl}	–	Planck mass
M_{Pl}	–	Reduced Planck mass
ℓ_{Pl}	–	Planck length
t_{Pl}	–	Planck time
$T_{\mu\nu}$	–	Energy-momentum tensor
ρ	–	Total energy density
ρ_c	–	Critical energy density
ρ_{Pl}	–	Energy density at Planck scales
ρ_{kin}	–	Kinetic energy density
ρ_{eff}	–	Effective energy density
ϵ, η_{SR}	–	Slow-roll parameters
P	–	Pressure
w	–	State parameter
u^μ	–	Four-velocity
Ω	–	Energy density parameter or conformal transformation
Ω_k	–	Curvature parameter
ℓ	–	Loop length or multipole momentum
S	–	Action

H	–	Hubble parameter
\mathcal{H}	–	Comoving Hubble parameter or Hamiltonian density
φ	–	Inflationary scalar field
$V(\varphi)$	–	Potential energy
$V_k(\varphi)$	–	Curvature mimetic potential
$V_{\text{eff}} = 3M_{Pl}^2[V_k(\varphi) - ka^{-2}]$	–	MG effective curvature potential

CONTENTS

	<u>Page</u>
1 INTRODUCTION	1
1.1 Gravity and General Relativity	1
1.2 Standard Cosmological Model	3
1.2.1 Friedmann-Robertson-Walker cosmology	5
1.2.2 Hot Big Bang model	9
1.2.2.1 Horizon problem	10
1.2.2.2 Flatness problem	12
1.3 Inflation	12
1.3.1 How inflation solves the Big Bang puzzles?	13
1.3.2 Conditions to Inflation	15
1.3.3 Slow-roll approximation	16
1.3.4 Cosmological Perturbations	17
1.4 Λ CDM	19
1.5 Motivation and Main Purpose	20
2 LOOP QUANTUM COSMOLOGY	25
2.1 Rewriting General Relativity: the Hamiltonian Formulation of Gravity	25
2.1.1 Space-time foliation	26
2.1.2 Intrinsic and extrinsic curvatures	29
2.1.3 The Hamiltonian and canonical variables	30
2.1.4 Constraints and Lagrange multipliers	33
2.1.5 The electromagnetic Hamiltonian	34
2.1.6 The constrained Hamiltonian	34
2.2 Loop Quantum Gravity	37
2.3 Loop Quantum Cosmology	43
3 MIMETIC GRAVITY	53
3.1 Original proposal and developments	53
3.1.1 Mimetic dark matter	53
3.1.2 Mimetic gravity extension	58
3.2 Mimetic Gravity description of Loop Quantum Cosmology	61

4 APPLICATION OF THE MIMETIC DESCRIPTION OF LOOP QUANTUM COSMOLOGY TO HIGGS INFLATION AND FURTHER DEVELOPMENTS	67
4.1 Curvature Potential from Mimetic Gravity: a new interpretation	67
4.2 Higgs Inflation	70
4.3 Application of MG representation of LQC to Higgs Inflation	75
4.4 Different perspective regarding the energy density components: Dynamic equations with curvature terms	78
4.5 About the conservation of the energy density	83
4.6 A brief note on super-inflationary phase	85
5 A BRIEF DIGRESSION ON GRAVITATIONAL WAVES	89
5.1 Primordial Gravitational Waves	89
5.2 CMB Power Spectrum	92
6 FINAL REMARKS AND PERSPECTIVES	99
REFERENCES	105
APPENDIX A - How to obtain the ADM Lagrangian?	119
APPENDIX B - Some details about the Hamiltonian constraint of Loop Quantum Cosmology and the sine function	123
APPENDIX C - Cosmic Microwave Background: physics and statistics	125

1 INTRODUCTION

In this work, we address the issues regarding the physics of the very early universe in the context of Loop Quantum Cosmology (LQC) from Mimetic Gravity (MG). Therefore, in order to make this a self-consistent text, we start with a brief review of the main elements related to the standard description of the cosmos evolution, focusing on the primordial universe. First, we introduce some particularities of the General Relativity (GR) theory in 1.1, since it is the one used to describe the gravitational interaction. Second, we discuss the universe evolution according to the Standard Cosmological Model (SCM) in 1.2. Next, in section 1.3, we highlight the fundamental aspects of the slow-roll approximation that defines the standard inflationary paradigm. Then, in 1.4, we present a concise explanation of the dark components following the Λ CDM model. Finally, we clarify our main goal and motivation to develop this work in 1.5.

The next chapters contain more technical details. 2 is dedicated to Loop Quantum Gravity (LQG)/Loop Quantum Cosmology, whose concepts are the main actors during the construction of our model. Hence, we will present the fundamental aspects of the Effective LQC that will be reproduced into MG context, the subject of the following chapter. Despite being a relatively new theory, MG has progressed consistently in just a few years, as we will show in 3. Moreover, we discuss our results in 4, explaining the essential features regarding the Higgs Inflation (HI) model. Chapter 5 briefly discusses gravitational waves produced during the primordial universe evolution and their role within the development of a cosmological model. In the end, we emphasize the most important contributions of our formulation and future perspectives related to it in 6.

Along with this Ph.D. thesis, we use the natural systems of units in which the velocity of light c and reduced Planck constant \hbar are equal to one ($c = \hbar = 1$). Therefore, unless we mention a different notation, the Newtonian gravitational constant G , Planck length ℓ_{Pl} , Planck time t_{Pl} , Planck mass m_{Pl} and reduced Planck mass M_{Pl} will be related to one another through expression $m_{Pl} = \ell_{Pl}^{-1} = t_{Pl}^{-1} = (\sqrt{G})^{-1} = \sqrt{8\pi}M_{Pl}$.

1.1 Gravity and General Relativity

In Newtonian Gravitational theory, gravity was interpreted as an attractive force between two massive bodies, however, it does not deal with any aspect regarding the evolution of the universe. Indeed, at this stage, Cosmology was not related to Physics

as it is nowadays, but faced from a philosophical point of view. Notwithstanding, the proposition of Einstein's General Relativity theory with its new perspective about the concepts of space and time besides the observational contribution enables one to study the universe and started a new era referred to as modern cosmology (GRON; HERVIK, 2007; ELLIS, 2018).

GR can be defined as a gravitational theory whose physics remains invariant regardless of the reference frame considered (GAMBINI; PULLIN, 2011). It can be interpreted as a geometric picture described in terms of the space-time and metric, where gravity is neither interaction nor a force, but an effect of the matter's presence in the space-time. Or, from the Quantum Field Theory (QFT) perspective, as a theory dictated by a massless spin-2 particle, the graviton (SEBASTIANI et al., 2017). In other words, the metric tensor is the variable that determines the space-time curvature and it is also the dynamical field of gravity (CARROLL, 2004).

In accordance with the current state of the art, nature is described by four fundamental interactions: weak, strong, electromagnetic and gravitational forces. Among them, the knowledge about gravity still remains the most restrictive one (GAMBINI; PULLIN, 2011). Naturally, GR differs from other theories due to the nature of its basic entity, the metric, that performs two functions. It plays the role of background for the evolution of the physical fields at the same time in which it is a dynamical field itself (BOJOWALD, 2005).

Mathematically speaking, in GR framework, our universe corresponds to a space-time Riemannian manifold \mathcal{M} , which means we live in a space characterized by the pair $(\mathcal{M}, g_{\mu\nu})$ (MARTINS, 2009), where $g_{\mu\nu}$ is the metric tensor. In this framework, regarding the dynamical evolution of the universe, the Einstein Field Equations (EFE) are the most important aspect of GR written as

$$G_{\mu\nu} = 8\pi GT_{\mu\nu}, \tag{1.1}$$

where the Einstein tensor $G_{\mu\nu}$ and the energy-momentum tensor $T_{\mu\nu}$ represent the geometric and matter sectors, respectively. Therefore, EFE establish an intrinsic relation between curvature and matter. Since $g_{\mu\nu}$ is related to the universe curvature, it is employed to construct the Riemann-Christoffel curvature tensor (WEINBERG, 1973),

$$R^\lambda{}_{\mu\nu\kappa} = \frac{\partial\Gamma^\lambda{}_{\mu\nu}}{\partial x^\kappa} - \frac{\partial\Gamma^\lambda{}_{\mu\kappa}}{\partial x^\nu} + \Gamma^\alpha{}_{\mu\nu}\Gamma^\lambda{}_{\kappa\alpha} - \Gamma^\alpha{}_{\mu\kappa}\Gamma^\lambda{}_{\nu\alpha}, \quad (1.2)$$

commonly referred only as Riemann tensor (or curvature tensor), with the Christoffel symbol given by

$$\Gamma^\alpha{}_{\mu\nu} = \frac{1}{2}g^{\alpha\beta}(\partial_\nu g_{\mu\beta} + \partial_\mu g_{\nu\beta} - \partial_\beta g_{\mu\nu}). \quad (1.3)$$

Hence, $R^\lambda{}_{\mu\nu\kappa}$ is the quantity that describes the topology of the manifold we live in, being used to build the Einstein tensor as

$$G_{\mu\nu} \equiv R_{\mu\nu} - \frac{1}{2}g_{\mu\nu}R, \quad (1.4)$$

where $R_{\mu\nu} = R^\nu{}_{\mu\nu\kappa}$ is the Ricci tensor and $R = R^\lambda{}_\lambda$ is the Ricci scalar.

A particular and fundamental property of GR is the principle of diffeomorphism invariance that ensures the invariance of the laws of physics under any change of the coordinate system (BILSON-THOMPSON; VAID, 2014). In chapter 2, we will provide more details about GR. However, for now, we just need to have in mind that the standard cosmology is built under the weak field limit which means the space-time metric differs from the flat Minkowski metric $\gamma_{\mu\nu}$ (used in special relativity) for a small perturbation (MARTINS, 2009).

1.2 Standard Cosmological Model

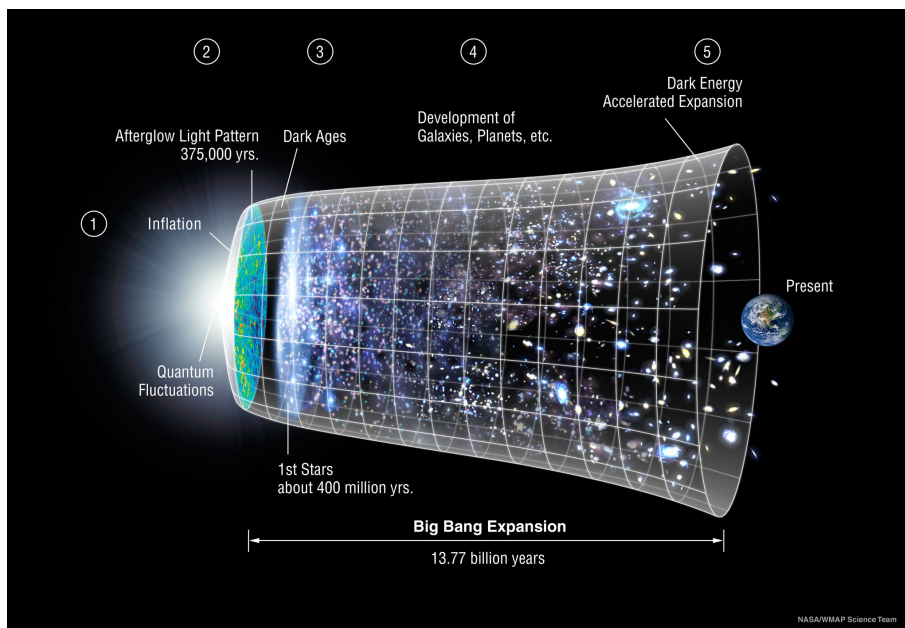
The physics related to the evolutionary history of the universe is currently described by the so-called Standard Cosmological Model. In this scenario, the universe starts from a condition usually referred to as Big Bang initial singularity. After that, it should undergo an accelerated expansion phase known as inflation whose dynamical field would decay into radiation. Therefore, inflation should end giving place to a radiation dominated universe until the amounts of matter and radiation become equal in the so-called equality matter-radiation epoch. Then, the matter overcomes the radiation influence and starts to dictate the universe dynamics. Sometime later, the dark energy is expected to be the one determining the current universe evolution, being responsible by the present accelerated expansion.

In general, the Lambda Cold Dark Matter (Λ CDM) model is used to refer to the standard cosmological model. However, from a dynamic perspective, the SCM can be decomposed into three almost independent approaches: the inflationary paradigm,

Hot Big Bang (HBB) and Λ CDM models. This strategy enables us to analyze the different periods of the universe evolution separately without losing consistency since they have different energy sources.

Figure 1.1 corresponds to a classical representation of the evolutionary history of the universe as mentioned in the previous paragraph. Note that most of the universe evolution is covered by the Big Bang model, leaving the two expansion accelerated phases out of its scope. This wide range is attributed to HBB because the behavior of the decelerated expansion can be described by radiation and matter, which will become clear along with this chapter. Indeed, only the HBB model is well established in cosmology, meanwhile, the inflationary paradigm and Λ CDM model can be interpreted as strategic solutions developed to overcome some discrepancies regarding the cosmological observational results.

Figure 1.1 - Standard universe evolution timeline



SOURCE: NASA/WMAP SCIENCE TEAM (2012)

In Table 1.1, there is a summary of the main epochs of universe evolution according to the SCM. The periods are listed in chronological order since the beginning of the universe until the present. In each phase, the universe may be dominated by a particular type of source, producing different results here referred to as events. Note that the start corresponds to Big Bang singularity, however, the number 1 from

Figure 1.1 would be associated to the inflationary period since it is not possible to obtain any information about a singularity. It is important to mention that the onset of inflation is still not a consensus, nevertheless, the other possible values are not far from 10^{-35} s. Undoubtedly, it must be greater than the Planck time. Relating again Figure 1.1 with Table 1.1, we can identify the HBB with number 2, and the visible universe with 3 and 4. We will not describe these periods because they are outside the scope of this work. Finally, the number 5 represents the current status of our universe, having the dark energy driving the universe in accelerated motion.

Table 1.1 - Epochs of the standard universe evolution

Epoch	Start time	Matter source	Events
Start	Undefined	Unknown	Creation or bounce
Inflation	10^{-35} s	Scalar field	Seed perturbations
HBB	10^{-3} s	Radiation	Nucleosynthesis
Visible universe	380000 years	Dark matter	Structure formation
Accelerating universe	10^9 years	Dark energy	Acceleration

SOURCE: Adapted from Ellis (2018, p. 1229)

The SCM is based on Friedmann–Lemaître–Robertson–Walker (FLRW) cosmology. However, we would rather work with Friedmann-Robertson-Walker (FRW) universe which is constructed from the assumptions of homogeneity and isotropy of the universe in large scales and the validity of general relativity to describe the gravitational interaction (BEBRONNE; TINYAKOV, 2007; GRON; HERVIK, 2007) without considering extra terms from dark energy as it will be exposed in 1.4. Since it is the base of the HBB and the other cosmological isotropic models, we will discuss its general concepts first and only after we are going to highlight the particularities of the HBB model. Despite the great agreement with the observations, the SCM has problems with the two accelerated expansion phases, the primordial and the current ones. Therefore, they will be discussed apart in the following sections. Nonetheless, as we are interested only in the very early universe, our focus is the inflationary period.

1.2.1 Friedmann-Robertson-Walker cosmology

As it was mentioned above, the key aspect of this approach is the assumption of the validity of the cosmological principle that ensures the homogeneity and isotropy of the matter distribution in the universe at scales larger than 200 Mpc. This means the universe should look the same regardless of the position of the observer. Indeed, this

is a good approximation according to the cosmological observations since, statically, the matter distribution in those scales is homogeneous and there is no observational evidence of rotation for our universe. This ansatz is the simplest way to study the universe evolution, enabling to slice the 4-dimensional spacetime of our universe into spatial homogeneous sections Σ associated to each instant of time (BESSADA, 2010; GRON; HERVIK, 2007; MARTINS, 2009; PAPAPETROU, 1974).

The FRW universe is characterized by a space-time whose line element in Cartesian coordinates is given by

$$ds^2 = g_{\mu\nu}dx^\mu dx^\nu = dt^2 - a^2(t)\gamma_{ij}dx^i dx^j = a^2(\eta)(d\eta^2 - \gamma_{ij}dx^i dx^j), \quad (1.5)$$

where $g_{\mu\nu}$ is representing the FRW metric, x^i are the spatial coordinates, t is the proper time, η is the conformal time and a is named scale factor. Note that $g_{\mu\nu}$ differs from $\gamma_{\mu\nu}$ only by the presence of a multiplying the spatial components. Therefore, $g_{\mu\nu}$ is diagonal and the universe dynamics is ruled by a and its evolution (DODELSON, 2003). In a spherical coordinate system, the FRW metric has the following form

$$ds^2 = dt^2 - a^2(t) \left[\frac{dr^2}{1 - kr^2} + r^2(d\theta^2 + \sin^2\theta d\phi^2) \right], \quad (1.6)$$

with k being the real number used to parameterize the space-time curvature, r , θ and ϕ are the spherical coordinates. In accordance with the general consensus, $k = 0$ corresponds to a flat universe, $k = 1$ is equivalent to a closed space-time and $k = -1$ describes a hyperbolic geometry.

A key aspect that we must emphasize is the essential role played by a . It is the quantity that describes how the spacelike hypersurface Σ changes its relative size with time (BAUMANN, 2009). Actually, in terms of dynamics, a is the only variable that can be attributed to the universe itself instead of one of its components. To clarify this, let us think about the universe in analogy with the earth globe. The scale factor could be interpreted as the distance between two points used to define the longitude (or latitude). Now, in order to be more precise, we can imagine the earth globe as a balloon. As it is filling, the distance between two cardinal points d would change, but not the number of meridians. In other words, d would continue to be the distance between the two cardinal points, however, it would be described by a greater value. For example, the Earth radius remains as the Earth radius regardless whether it measures 6400km or 8000km. Accordingly, the time evolution of a determines how the universe expands (or contract).

To begin with, the variation of a is measured by the Hubble parameter,

$$H \equiv \frac{\dot{a}}{a}, \quad (1.7)$$

where the dot represents the derivative with respect to t . H is an essential variable regarding the universe evolution because, as c is unitary, H^{-1} defines the length and age of the universe (BAUMANN, 2009). The expression for H is obtained from the time component of EFE, called the Friedmann equation,

$$H^2 = \left(\frac{\dot{a}}{a}\right)^2 = \frac{8\pi G}{3}\rho - \frac{k}{a^2}, \quad (1.8)$$

in which ρ is the energy density of the elements that fill the universe. In other words, the universe curvature is directly associated with the energy density from both matter and fields that fills the universe (BILSON-THOMPSON; VAID, 2014).

Since the universe is considered homogeneous and isotropic, the energy-momentum tensor must also agree with this picture. Consequently, both pressure P and ρ will not change from one point to another, describing a perfect fluid whose energy-momentum tensor is written as

$$T^{\mu\nu} = (\rho + P)u^\mu u^\nu - P g^{\mu\nu}. \quad (1.9)$$

In this context, the 4-velocity u^μ has only the time component different from zero,

$$T^\mu{}_\nu = \text{diag}(\rho, -P, -P, -P), \quad (1.10)$$

otherwise, the non-null spatial components would imply in privileged directions in the foliation hypersurface, breaking the isotropy of the system (GRON; HERVIK, 2007; GUZZETTI et al., 2016). Furthermore, the fluid is assumed to be a barotropic one, which means it obeys the following equation of state (EoS)

$$P = w\rho, \quad (1.11)$$

with w defined as the state parameter.

Therefore, it is possible to explore the energy content of the universe through measurements of a (DODELSON, 2003) and also its geometry. To clarify this, let us con-

sider the energy density for a flat universe ($k = 0$), named critical energy density, whose definition is given by

$$\rho_c = \frac{3}{8\pi G} H^2. \quad (1.12)$$

Comparing the value of ρ with ρ_c enables to infer whether the universe is curved or not, this is performed through the so-called density parameter,

$$\Omega \equiv \frac{\rho}{\rho_c} = 1 + \frac{k}{(aH)^2} = 1 + \Omega_k, \quad (1.13)$$

where Ω_k is the curvature density parameter. Hence, $\Omega \neq 1$ means the universe would have some curvature, however, recent observations pointed to $|\Omega_k| < 0.005$ (ADE et al., 2016). In this sense, the universe is an Euclidean space section whose energy density is equal to (1.12) (DODELSON, 2003). Consequently, ρ is the parameter that describes how the scale factor evolves with time due to the relation

$$\rho \propto a^{-3(w+1)} \Rightarrow a(t) \propto t^{\frac{2}{3}(w+1)} \quad (1.14)$$

obtained from (1.8).

The energy conservation law implies in the expression $\nabla_\nu T^{0\nu} = 0$, thus, from (1.10), we can obtain the continuity equation as

$$\dot{\rho} + 3 \left(\frac{\dot{a}}{a} \right) (\rho + P) = 0. \quad (1.15)$$

The acceleration equation of the universe (also called second Friedmann equation) can be computed from either the spatial components of the EFE or from combining (1.8) and (1.15), its form is given by

$$\frac{\ddot{a}}{a} = -\frac{4\pi G}{3} (\rho + 3P). \quad (1.16)$$

In summary, the equations (1.8), (1.16) and (1.15) determine the dynamical evolution of the physical system described by the FRW cosmology. The first Friedmann equation (1.8) informs if the universe is expanding, contracting or it is in a stationary state. The second Friedmann equation (1.16) enables to assess if the universe expansion is describing an accelerated, decelerated or constant motion. Finally, (1.15)

is a requirement that must be obeyed by any cosmological model.

Another key thing to remember is that, once the universe is evolving, it just makes sense to choose a coordinate system whose distances do not change with the expansion. This system is called the comoving coordinate system and it is largely used in cosmology. Moreover, the comoving or conformal time η (already mentioned) plays an important role. In reality, it has two essential meanings: a time variable and a comoving horizon. In other words, the fact that no information could travel faster than light implies the existence of a horizon whose size is the total comoving distance light went through since $t = 0$ (DODELSON, 2003). This distance is expressed as

$$\eta = \int_0^t \frac{dt'}{a(t')}. \quad (1.17)$$

Therefore, when you look at two regions whose distance between them is bigger than η , they are not causally connected (DODELSON, 2003) which means these regions have never been in contact at any previous time. It is also advantageous to rewrite some variables in terms of η instead of t like the comoving Hubble parameter \mathcal{H} defined as

$$\mathcal{H} = \frac{a'}{a} = aH, \quad (1.18)$$

where the apostrophe represents the derivative with respect to η .

1.2.2 Hot Big Bang model

The expanding universe, the light element abundance and the cosmic microwave background (CMB) are the reasons why the Hot Big Bang model is such a successful approach to describe the universe evolution (DODELSON, 2003). From (1.14), note that as we regress in time a is getting smaller. Thus, for values of time close to zero, $a(t) \rightarrow 0$, leading the universe to a singularity. Note also that $a(t) \rightarrow 0$ implies infinite values for both density and temperature T since the universe cools as it expands ($T \propto a^{-1}$). Consequently, GR formulation breaks at this point as the dynamical equations and even the relations between a and ρ have no physical meaning.

Since HBB just allows ordinary matter (baryonic matter) and radiation as energy content for the universe, it is not able to produce an accelerated expansion phase.

This can be directly observed from (1.16) and (1.11) that require $w < 0$ to obtain $\ddot{a} > 0$. Therefore, neither ordinary matter nor radiation (with $w = 0$ and $w = \frac{1}{3}$, respectively) are capable to drive the universe to an accelerated expansion phase.

Moreover, HBB model also presents problems commonly referred to as Big Bang puzzles. Here, we will only briefly review the horizon and flatness problems, once they are the more relevant ones regarding the properties of the universe evolution we are going to explore. It is important to mention that neither problem comes from an inconsistency regarding HBB, but they arise from the necessity of special assumptions to solve them (BRAWER, 1995).

1.2.2.1 Horizon problem

As mentioned before, η corresponds to a boundary regarding the distance the fastest particle (a photon or other particle with zero mass) could have traveled since $t = 0$. Thus, it is referred to as the comoving particle horizon or causal horizon. Notwithstanding, there is also the comoving Hubble horizon $\mathcal{H}^{-1} = (aH)^{-1}$, usually called Hubble radius, described by the expression

$$(Ha)^{-1} = H_0^{-1} a^{\frac{1}{2}(1+3w)}, \quad (1.19)$$

where H_0 is the present value of H . From (1.17) and (1.19) it possible to obtain the relation

$$\eta \propto a^{\frac{1}{2}(1+3w)}, \quad (1.20)$$

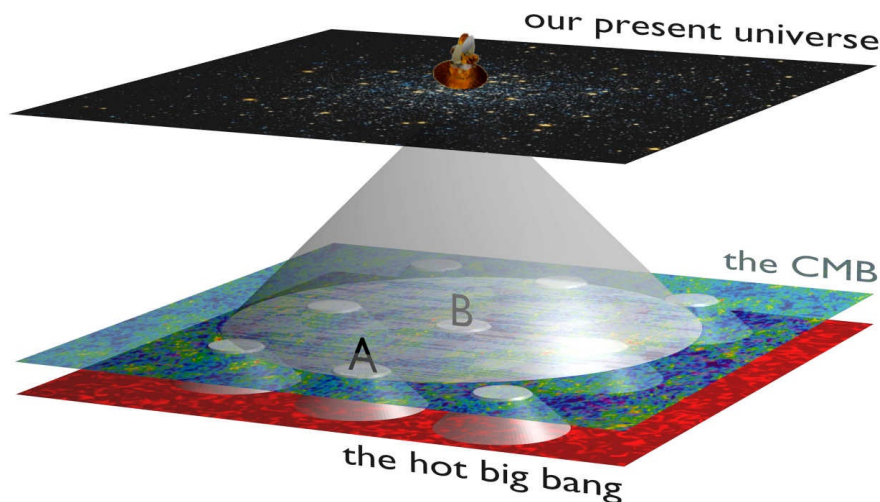
which results in $\eta \propto a$ for the radiation dominated era and $\eta \propto a^{\frac{1}{2}}$ for the matter one, respectively (BAUMANN, 2009).

Before clarifying what is the horizon problem, it is worth to introduce a few aspects of the cosmic microwave background radiation. CMB is the oldest light information available, its photons decoupled from matter when the universe was 380000 years old. Basically, after the Big Bang singularity, the universe started to expand and cool down (remember the inverse relation between T and a). As the universe plasma was cooling, the light atoms (hydrogen and helium) were being formed through the recombination process. Then, the interaction with the radiation was progressively reduced until the photons became free to travel without collisions (KINNEY, 2003; NASA/JAMES WEBB SPACE TELESCOPE, 2019). This process is called decoupling.

Moreover, all photons decoupled approximately at the same time during their last relevant interaction with the electrons, defining the surface of last scattering (SLS). Thus, SLS works as a boundary of the visible universe. All things considered, there would be many regions in the sky that had never established a causal contact when the CMB was formed (BAUMANN, 2009).

As far as one can observe through the universe, the deeper inside its past we are able to see. Figure 1.2 is a simple representation of how the universe can be interpreted from our position, where the Big Bang epoch, decoupling and present time are shown as flat slices. Using η enables us to draw past light cones since now until the Big Bang plan. This means if two regions (A and B) were defined with past light cones that do not touch each other, these regions had never established a causal contact. For example, considering the temperature, A and B did not have time to achieve thermal equilibrium, because they have never been close enough to interact.

Figure 1.2 - Horizon problem



SOURCE: Wang (2014)

Therefore, according to the Big Bang picture, there should exist regions with different values of temperature in the sky. However, the observations show that CMB is homogeneous until one part in 10^5 and may have been even more homogeneous in the past (BAUMANN, 2009). In summary, the horizon problem can be enunciated as the absence of an explanation about how regions causally disconnected, without any opportunity to interact during the time of existence of our universe, presents

similar features.

1.2.2.2 Flatness problem

The flatness problem (also known as fine tuning problem) is directly related to the observational constraints imposed on the value of Ω (BRAWER, 1995). As previously discussed, the density parameter may be close to unity since $|\Omega_k| < 0.005$ (ADE et al., 2016). Therefore, Ω must have been even closer to one during the early times. Otherwise, the monotonic behavior of the Hubble radius regarding matter and radiation would have forced $|\Omega_k|$ to become bigger as \dot{a} was decreasing. To clarify this, equation (1.13) is rewritten like

$$|\Omega - 1| = \frac{k}{(\dot{a})^2}. \quad (1.21)$$

From (1.16), note that matter and radiation decrease the acceleration rate of the scale factor. Thus, $|\Omega_k|$ should have increased its value, leading the universe to assume a curved geometry.

1.3 Inflation

The inflationary paradigm was proposed to provide the initial conditions to the Big Bang model (LIDDLE, 1999). However, it went further, inflation introduced an elegant physical mechanism to explain how large scale structures (LSS) arose. In fact, this paradigm not only solved the well-known Big Bang puzzles, providing an explanation about how the initial seeds of the observable structures were generated but also predicted the anisotropy of CMB temperature (GUZZETTI et al., 2016).

Inflation is based on the assumption that the universe expanded in an exponential accelerated way during the initial instants of its evolutionary history. It is described by a scalar field named inflaton and the metric tensor whose fluctuations and dynamics are the key ingredients that make inflation works in such an elegant way (GUZZETTI et al., 2016). According to Mukhanov et al. (1992), inflation was developed under two main ideas: quantum fluctuations will disturb the classical energy density in an expanding universe and scales within Hubble radius will exponentially grow and extrapolate the visible horizon, returning later as large scale cosmological perturbations.

We split the explanation about inflation to clarify each topic and also to present the background evolution separately. First, we briefly present the strategies applied

to solve the Big Bang puzzles. Second, we expose a few particularities regarding the physics of the inflationary period at background level as well as the necessary conditions to obtain it. Then we discuss inflation's standard picture: the slow-roll approximation. Finally, since in this work we do not deal with the physics at the perturbed level, only the essential aspects of cosmological perturbations will be highlighted.

1.3.1 How inflation solves the Big Bang puzzles?

Once the universe age is not enough to provide the right amount of time required to all currently observed scales causally interact, the idea behind inflation was to extend the causal zone. By construction, Big Bang singularity defines the universe birth at $t = 0$ which is equivalent to $a = 0$ (see equation (1.14)). Notwithstanding, from conformal time expression

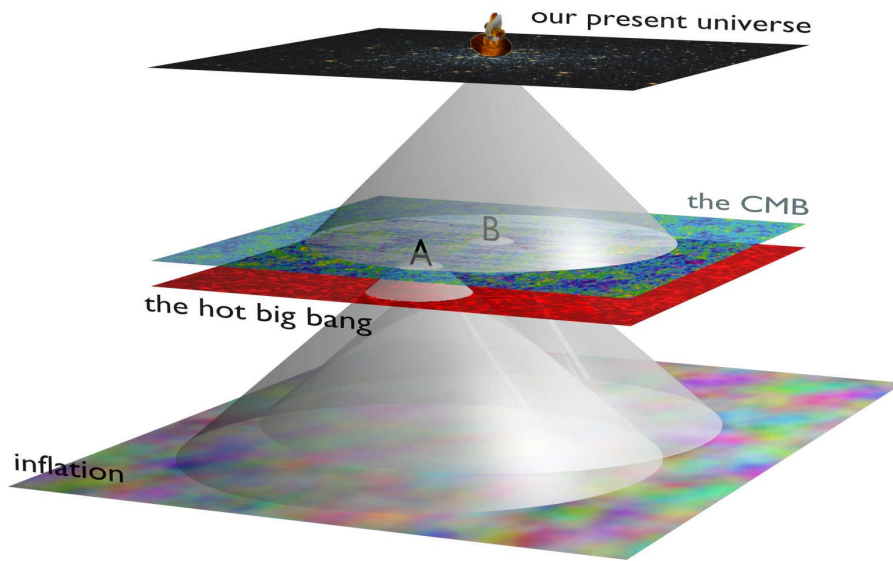
$$dt = a(t)d\eta, \tag{1.22}$$

note that there is no boundary to η , enabling it to assume any value, including $\eta = -\infty$ (BAUMANN, 2009). Consequently, inflation can expand the particle horizon to cover all currently observed LSS, giving enough time for the observed regions to interact. In other words, the two regions (A and B) from Figure 1.2 will have their past light cones extended like presented in Figure 1.3, which allows them to establish a causal connection.

Another way to explain how inflation solves the horizon problem is looking from a quantum fluctuation perspective. In Figure 1.4, see that the red line refers to η , meanwhile, $(aH)^{-1}$ is represented by the grey area. At first, as $(aH)^{-1}$ limits the thermal equilibrium zone, $\eta > (aH)^{-1}$ means there were scales outside $(aH)^{-1}$. Thus, they were not at equilibrium. However, inflation increases the size of $(aH)^{-1}$, making it bigger than η and expanding the thermal equilibrium zone to incorporate all the visible regions in the sky. In this scenario, the cosmological perturbations beyond η are frozen, only recovering their dynamical behavior when the universe achieves the size equivalent to their wavelength.

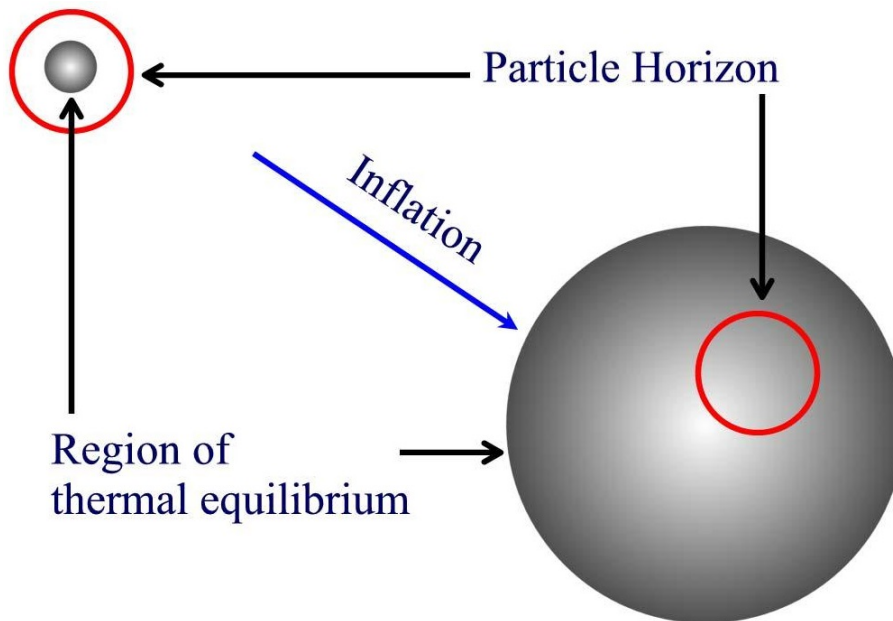
Finally, regarding the flatness problem, inflation naturally solves it due to the accelerated expansion. As we will see next, a evolves exponentially and H is almost constant during the inflationary period. Therefore, regardless the value of k , $|\Omega_k|$ will go to zero due to the large variation of a . This means inflation forced the universe to be flat.

Figure 1.3 - Solution to the horizon problem



SOURCE: Wang (2014)

Figure 1.4 - Particle horizon and Hubble radius



SOURCE: Watson (2000)

1.3.2 Conditions to Inflation

The inflationary paradigm is a proposition that the universe expanded exponentially when it was around 10^{-35} seconds old. This is a fundamental and indispensable requirement for the success of the inflationary mechanism. Nevertheless, from equation (1.16), $\ddot{a} > 0$ demands a fluid with $P < -\frac{\rho}{3}$. Therefore, a matter content different from ordinary radiation and matter may have driven the universe dynamic during inflation (GUZZETTI et al., 2016).

A de Sitter type expansion is the simplest approach to obtain a suitable behavior for the scale factor evolution (GUZZETTI et al., 2016). This happens because a de Sitter expansion requires $P = -\rho$ which agrees with the previous requirement. Nevertheless, during inflation, the evolution must be almost de Sitter. Otherwise, inflation would have lasted forever. Following in this direction, the Hubble parameter is almost constant, $P \simeq -\rho$ and a obeys the relation

$$a(t) \propto e^{H_I(t-t_I)}, \quad (1.23)$$

where the subscript I indicates the beginning of inflation. The usual procedure to implement a perfect fluid with $P \simeq -\rho$ is to introduce a scalar field $\varphi = \varphi(t)$. Therefore, the matter content evolution follows the standard Lagrangian

$$\mathcal{L}_\varphi = \frac{1}{2}\partial_\mu\varphi\partial^\mu\varphi - V(\varphi). \quad (1.24)$$

In this case, the scalar field is assumed as minimally coupled to gravity and the potential energy $V(\varphi)$ form should be chosen carefully to achieve the value $w < 0$ (GUZZETTI et al., 2016).

Once the matter Lagrangian was established, the universe dynamics along inflationary epoch could be described by the action

$$S = S_{EH} + S_\varphi = \int d^4x\sqrt{-g} \left(\frac{1}{16\pi G}R + \mathcal{L}_\varphi \right), \quad (1.25)$$

in which S_{EH} is the Einstein-Hilbert action and S_φ is the matter action. Consequently, the equation of motion for the scalar field is obtained from the variation of (A.1) with respect to the inflaton field, resulting in a Klein-Gordon equation,

$$\ddot{\varphi} + 3H\dot{\varphi} + \partial_{\varphi}V(\varphi) = 0, \quad (1.26)$$

where ∂_{φ} represents the derivative related to φ . If the variation is performed with respect to $g^{\mu\nu}$ instead, it will be possible to write the energy-momentum tensor as

$$T_{\mu\nu} = -2\frac{1}{\sqrt{-g}}\frac{\delta S_{\varphi}}{\delta g^{\mu\nu}} = \partial_{\mu}\varphi\partial_{\nu}\varphi - g_{\mu\nu}\mathcal{L}_{\varphi}. \quad (1.27)$$

Hence, the inflaton energy density and pressure could be determined by comparing the equations (1.9) and (1.27),

$$\rho = \frac{\dot{\varphi}^2}{2} + V(\varphi) \quad \text{and} \quad P = \frac{\dot{\varphi}^2}{2} - V(\varphi), \quad (1.28)$$

enabling to write the state parameter in the form

$$w = \frac{\dot{\varphi}^2 - 2V}{\dot{\varphi}^2 + 2V}. \quad (1.29)$$

From equation (1.29), the requirement $\ddot{a} > 0$ implies $V(\varphi) > \frac{\dot{\varphi}^2}{2}$ and a de Sitter stage ($P \simeq -1$) needs $V(\varphi) \gg \frac{\dot{\varphi}^2}{2}$. In other words, a framework with a scalar field as dominant component, and the potential energy overcomes the kinetic energy of the field, gives rise to an inflationary phase. Moreover, standard inflation reproduces a de Sitter-type evolution through a scalar field rolling down slowly (GUZZETTI et al., 2016) as we will explain next.

1.3.3 Slow-roll approximation

Aiming to obey $V(\varphi) \gg \frac{\dot{\varphi}^2}{2}$, the simplest approach is to impose the existence of a field-configuration space in which the potential is flat enough, $\partial_{\varphi}V(\varphi) \ll V(\varphi)$. Therefore, following these requirements, the equation (1.26) implies that the friction term is the one responsible for driving the evolution of the scalar field, $\ddot{\varphi} \ll 3H\dot{\varphi}$. These restrictions determine boundaries to inflaton's potential and its derivatives (GUZZETTI et al., 2016), being condensed in the so-called slow-roll conditions

$$V(\varphi) \gg \dot{\varphi}^2 \quad \text{and} \quad \ddot{\varphi} \ll 3H\dot{\varphi}. \quad (1.30)$$

Hence, (1.8) and (1.26) can be rewritten in the form

$$H^2 \approx \frac{1}{3M_{Pl}^2}V(\varphi) \quad \text{and} \quad 3H\dot{\varphi} + \partial_\varphi V(\varphi) \approx 0. \quad (1.31)$$

In summary, the slow-roll conditions are related to the flatness of the potential, so that even having a small value for $\partial_\varphi V(\varphi)$, $\ddot{\varphi}$ needs to be negligible comparing to it in order to obtain a de Sitter stage (BEZERRA, 2015).

Another way to express those conditions is to introduce the slow-roll parameters ϵ and η_{SR} like

$$\epsilon \equiv \frac{3}{2} \left(\frac{P}{\rho} + 1 \right) = 4\pi G \left(\frac{\dot{\varphi}}{H} \right)^2 = \frac{1}{H} \frac{dH}{dN} \quad \text{and} \quad \eta_{SR} = -\frac{\ddot{\varphi}}{H\dot{\varphi}}. \quad (1.32)$$

Where N is the time parameter named number of e-foldings commonly used to measure time at inflationary epoch. The slow-roll parameters show directly if the slow-roll conditions are being fulfilled. This could be seen from the acceleration equation written in terms of ϵ ,

$$\frac{\ddot{a}}{a} = H^2(1 - \epsilon), \quad (1.33)$$

in which it is possible to note that $\epsilon < 1$ implies an accelerated expansion, while $\epsilon \ll 1$ gives rise to a slow-roll evolution. Moreover, the parameter $|\eta_{SR}| \ll 1$ ensures the validity of the relation $\ddot{\varphi} \ll 3H\dot{\varphi}$ (BAUMANN, 2009; KINNEY, 2009).

In order to solve the horizon and flatness problems, the inflationary phase must have lasted long enough to enable a causal connection among all regions currently observed. So, being N defined as $dN = Hdt$, a de Sitter-type evolution requires at least $N \sim 60$ to solve the horizon problem. Furthermore, inflation ends when the slow-roll conditions are violated (GUZZETTI et al., 2016).

1.3.4 Cosmological Perturbations

Until now we only talked about the primordial universe physics at background level which is a really good approximation to describe this period. However, we will briefly describe the basic aspects regarding the linearized cosmological perturbation theory in the inflationary context. First of all, inflation is based on the evolution of two dynamical entities: the metric and the inflaton fields. It uses quantum aspects to explain the structure formation and the generation of CMB anisotropy. Quantum fluctuations are expected due to the physical nature of the fields which oscillate with all possible wavelengths. Basically, the wavelengths were extended to scales bigger

than Hubble horizon as a result of inflationary accelerated expansion (GUZZETTI et al., 2016). This subsection is mostly based on the seminal paper of Mukhanov et al. (1992).

The linearized cosmological perturbation theory is based on the assumption that our universe is slightly different from the standard FRW universe. This requirement is necessary due to the successful agreement of the standard cosmology with observations. Therefore, the space-time consists of a manifold whose metric $g_{\mu\nu}$ is described like

$$g_{\mu\nu}(\mathbf{x}, \eta) = \bar{g}_{\mu\nu}(\eta) + \delta g_{\mu\nu}(\mathbf{x}, \eta), \quad (1.34)$$

where $\bar{g}_{\mu\nu}$ is the FRW metric commonly referred to as background part of the metric tensor and $\delta g_{\mu\nu}$ is the metric perturbation whose value is restricted to $\delta g_{\mu\nu} \ll 1$. Since geometry and matter are related, the energy-momentum tensor could also be described by

$$T_{\mu\nu} = \bar{T}_{\mu\nu} + \delta T_{\mu\nu}. \quad (1.35)$$

The bar will always be used to refer to the background variables and δ will be associated to the perturbed quantities. Consequently, EFE can be divided into background and perturbed equations,

$$\bar{G}_{\mu\nu} = 8\pi G \bar{T}_{\mu\nu} \quad \text{and} \quad \delta G_{\mu\nu} = 8\pi G \delta T_{\mu\nu}, \quad (1.36)$$

enabling to study the physics regarding background and perturbation apart from each other.

The metric perturbation $\delta g_{\mu\nu}$ could be separated into a scalar, vector and tensor parts due to its behavior facing spatial coordinate transformations. Hence, they evolve independently in a linear approximation. Scalar perturbations cause the growth of the inhomogeneities which affects the matter dynamics. Vector perturbations are characterized by a fast decay mode making them irrelevant in the cosmological context. Finally, tensor fluctuations or primordial gravitational waves (PGW) dictate the degree of freedom of the gravitational field (MUKHANOV et al., 1992; GUZZETTI et al., 2016).

From time component of the perturbed EFE (1.36), the curvature perturbation is

obtained. They are the ones employed to explain the LSS formation and also the CMB anisotropy. The vector ones come from the mixing terms $\delta G_{0i} = 8\pi G\delta T_{0i}$, which means time-space components. Meanwhile, the spatial components of (1.36) give rise to tensor perturbations or gravitational waves (GW) from the primordial universe. Despite being irrelevant at the background level, the cosmological perturbations are an essential part of modern cosmology and the main focus of the current cosmological experiments.

1.4 Λ CDM

SCM is based on the assumption of the existence of dark matter (DM) and dark energy (DE) besides the evolution of primordial perturbations according to inflation (DODELSON, 2003). As we mentioned before, the Λ CDM model is considered as the standard model of cosmology, including the entire evolutionary history of the universe. However, here, we separate the evolution in three stages because we are only interested in the very early universe.

In principle, the standard inflationary period is only described by the inflaton field and ends with this field decaying into photons. Our work goes until the end of inflation and does not deal with other types of matter beyond scalar fields. Moreover, until the present, there is a gap between the Big Bang singularity and inflation. The first one is related to $a \rightarrow 0$ and $t_{Pl} \rightarrow 0$, meanwhile, inflation must begin only after the Planck scale. Therefore, we do not need to consider dark components to study the primordial universe physics which results in dynamical equations easier than if we have assumed the FLRW metric instead.

Despite the fact that both metrics have the same structure, the FLRW universe differs from the one we have been working with since it considers extra terms due to the presence of dark energy. Regarding the dark matter, it is incorporated into the matter energy density since it should behave like the ordinary matter. Indeed, according to Λ CDM model, the dark components correspond to about 96% of our universe, 73% coming from dark energy and 23% from dark matter. Only, the remaining 4% refers to ordinary matter (BOSE; MAJUMDAR, 2009).

As we repeatedly mentioned, neither radiation nor matter is capable of accelerating the universe expansion. Therefore, the exit was to add new types of fluid to the equation. In the case of inflation, the ordinary matter and radiation still did not exist, living only the inflaton as energy content. Notwithstanding, there are more elements to be considered at present, which means the total energy density is actually given

by the energy density of each of the universe fluid elements, with the dark energy dominating over the others.

In Λ CDM model, the dark energy is Einstein's cosmological constant Λ that is also considered as the vacuum energy density. Initially, Λ was introduced on the left side of Einstein's equations

$$R_{\mu\nu} - \frac{1}{2}Rg_{\mu\nu} - \Lambda g_{\mu\nu} = \frac{8\pi G}{3}T_{\mu\nu} \quad (1.37)$$

as an artifice to obtain a static universe (RYDEN, 2003). However, later it was considered as a new kind of fluid whose pressure must obey $P_\Lambda = -\rho_\Lambda$ to enable the present accelerated expansion, this statement is in agreement with the constrained value $w = -1.006 \pm 0.045$ from Planck satellite data (ADE et al., 2016). Then being moved to the right hand side,

$$R_{\mu\nu} - \frac{1}{2}Rg_{\mu\nu} = \frac{8\pi G}{3}T_{\mu\nu} + \Lambda g_{\mu\nu}. \quad (1.38)$$

Therefore, instead of (1.8) and (1.16), the universe dynamics is dictated by

$$\left(\frac{\dot{a}}{a}\right)^2 + \frac{k}{a^2} = \frac{8\pi G}{3}\rho + \frac{\Lambda}{3}, \quad (1.39)$$

$$\left(\frac{\ddot{a}}{a}\right) = -\frac{4\pi G}{3}(\rho + 3P) + \frac{\Lambda}{3}. \quad (1.40)$$

Despite the fact that the dark energy is dominating the current universe evolution, the matter had dominated the dynamics in recent past and its contribution is not negligible. As we mentioned above, dark matter corresponds to the majority of the matter fluid in the universe. Since it is nonbaryonic, dark matter can not absorb, emit or scatter any kind of radiation (RYDEN, 2003) according to the standard prerogative. Indeed, within this framework, it only interacts gravitationally, which does not allow a direct observation. There are many attempts to describe its nature outside the standard picture, however, this fundamental feature still remains unknown.

1.5 Motivation and Main Purpose

The classical cosmology is based on GR, thus, its prediction power is constrained to its validity limit. Since GR is a nonrenormalizable theory and does not contain the

usual concept of time, it cannot be quantized as it happens with QFT. Notwithstanding GR and QFT are the pillars of modern physics, the results from experiments and surveys have been showing that the universe description by the Standard Model of Particle Physics (SMPP) and SCM is at least incomplete (SEBASTIANI et al., 2017).

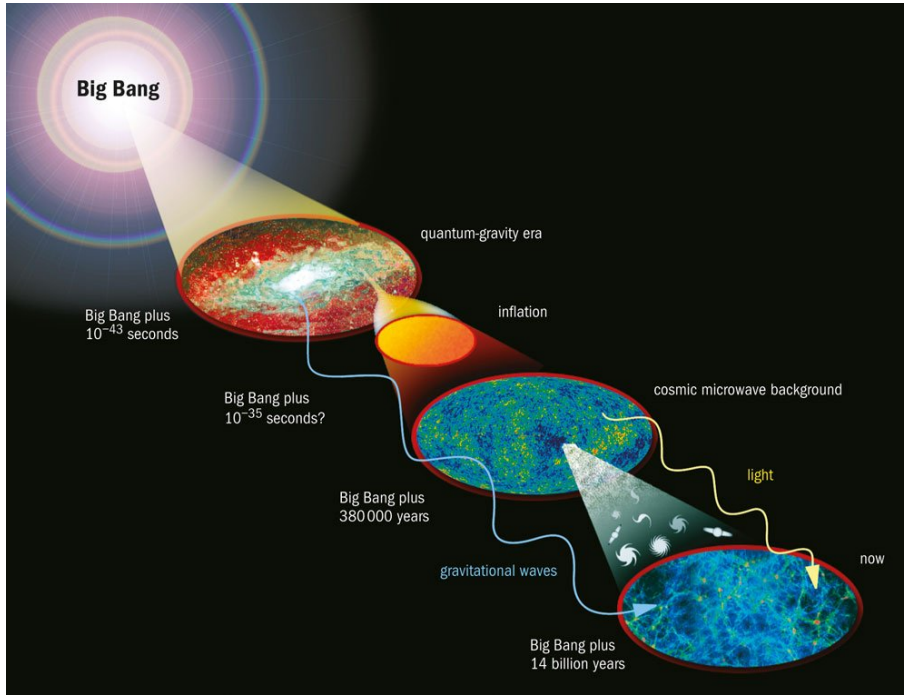
The Big Bang initial singularity is a consequence of every classical solution related to a universe filled with only a massless scalar field (ASHTEKAR et al., 2006b). Since a singularity is usually related to the validity limit of theory and to nonclassical situations, an approach containing the best elements of GR and QFT is expected to shed some light or even eliminate the singularity problem (GAMBINI; PULLIN, 2011).

There is also the question about the inflaton nature that continues without explanation. Indeed, the standard inflaton is supposed to be an extra field whose role ended in a period before the beginning of the range covered by SMPP (HARO et al., 2018a). Moreover, an inflationary period should have been preceded by a Planck epoch in which the initial condition to start an accelerated stage must have been set (MIELCZAREK et al., 2009).

Several challenges arise in the construction of a quantum gravity theory since gravity exhibits proper features as the diffeomorphism invariance and the absent of a background structure. These features in addition to the almost insignificant role played on the atomic scales could lead to questions about whether it is really necessary to quantize gravity. However, there is a particular energy scale that neither general relativity nor quantum mechanics could explain properly, the Planck scale (GAMBINI; PULLIN, 2011).

In other words, the absence of a satisfactory description of the very early universe and a quantum gravity theory may be linked. This stage in the universe evolution corresponds to the exact energy and length scales in which quantum gravity effects must have played a significant role. Figure 1.5 provides a scheme that places when quantum gravity effects should have dictated the universe evolution. Therefore, applications of quantum gravity theories to this epoch could answer questions that the classical theories are not capable of doing.

Figure 1.5 - Universe evolution



SOURCE: Commissariat (2014)

We choose to study loop quantum gravity that provides a discrete description of the spacetime at the kinematic level. Nonetheless, incorporating cosmological dynamics into quantum gravity sector enables one to produce a dynamical discrete scenario, giving rise to loop quantum cosmology, one of the main object in our study. Furthermore, the underlying quantum geometry of LQC results in a quantum bounce instead of a singularity (ASHTEKAR *et al.*, 2006b). Despite the absence of a complete and closed formulation, in LQC framework, it is possible to implement the two most appealing descriptions for the very early universe: inflationary paradigm and bouncing cosmologies (HARO *et al.*, 2018a). However, the LQC scalar field is generally arbitrary, as well as the inflaton.

The natural and logical candidate to play the inflaton role is the Higgs field since it is the only scalar field current observed. However, it is important to emphasize it would be a previous configuration of this elementary particle. An approach called Higgs Inflation provides a chaotic scenario that enables the SMPP Higgs field to be the inflationary scalar field. This model is capable of generating the FRW universe by producing quantum fluctuations as the seeds for the large scale structures and

recovering the HBB evolution (SHAPOSHNIKOV, 2015), besides it reproduces the dynamics expected from the standard slow-roll evolution.

In this work, we will discuss another possible description for the primordial universe coming from the so-called Mimetic Gravity. MG was initially proposed by Chamseddine and Mukhanov (2013) to simulate the dark matter behavior. After, MG was explored as a modification of GR capable of producing a bounce in addition to providing a realistic candidate for dark matter (CHAMSEDDINE et al., 2014; CHAMSEDDINE; MUKHANOV, 2017b). Recently, in a seminal paper, Langlois et al. (2017) demonstrated that MG could reproduce the effective dynamics of LQC. More specifically, they obtained an interesting LQC solution with a curvature potential for closed-universe models.

In summary, the aim is to present our scenario for the very early universe with MG as the link between LQC and HI. Within this framework, we highlight the curvature role during the primordial universe evolution and emphasize the versatility of the MG representation of LQC. Further, we expose our results presented in (BEZERRA; MIRANDA, 2019) and clarify our vision regarding the very early times.

2 LOOP QUANTUM COSMOLOGY

Before we start to discuss Effective LQC, we need to present essential concepts behind the construction of LQG, jumping the unnecessary steps that are beyond the scope of this work. Along section 2.1, we will omit some constants in order to present a simpler mathematical structure to describe the canonical formalism, focusing on the concepts. Nonetheless, in sections 2.2 and 2.3, we continue to follow the notation establish in the chapter 1.

2.1 Rewriting General Relativity: the Hamiltonian Formulation of Gravity

As mentioned earlier, the weak, strong and electromagnetic interactions present a successful description when it comes to the quantum world. Nonetheless, the same statement can not be applied to gravitational force (GAMBINI; PULLIN, 2011). This is reasonable because quantizing gravity will give a quantum meaning to spacetime itself. That is to say, the standard procedure applied to other interactions does not work for gravity once it requires a background in which the fields would evolve. However, the evolution regarding gravity is determined by the space-time that is the background itself (MARTINS, 2009).

Since GR is the theory employed to describe the gravitational interaction, quantizing gravity requires a different treatment. Note that an intrinsic feature of GR is the equal treatment of space-time coordinates. From a GR perspective, there is no difference between time and space components (TAVAKOLY, 2014). The fact that they have the same weight makes difficulty to study the space-time progression once the evolution of a physical system is usually considered in terms of the time coordinate. Therefore, GR has to be restructured in a suitable form in order to implement a quantization process.

There are two main approaches employed to try to quantize general relativity: the covariant description in terms of the elementary variables functional and the canonical path through the Hamiltonian formulation (DONÁ; SPEZIALE, 2010). We are going to follow the second one. Notwithstanding the Lagrangian formalism being the one usually applied to classical field theory, it is a mechanism that strongly depends on the concept of spacetime. Meanwhile, the Hamiltonian formalism is built under the evolution of purely spatial variables for a specific interval of time (ALCUBIERRE, 2008; PEREIRA, 2018).

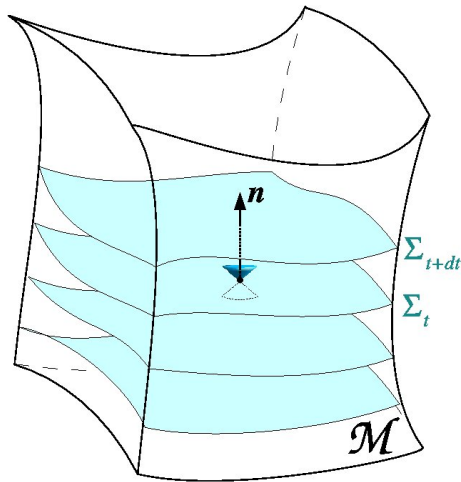
Therefore, the equality between time and space must be broken in order to obtain the gravitational Hamiltonian (TAVAKOLY, 2014), providing a way to follow the evolution of space variables related to our cosmos. This is the proposal of the Arnowitt-Deser-Misner (ADM) formulation which is also referred to as $3 + 1$ formalism. The idea is to change the usual perspective regarding how an observer experiences the laws of physics that, in GR framework, comes from the properties and symmetries of the 4-dimensional manifold \mathcal{M} and its metric $g_{\mu\nu}$ (PEREIRA, 2018). Nonetheless, instead of the spatially homogeneous and isotropic 4-dimensional space-time, the ADM foliation technique splits \mathcal{M} into a family of 3-dimensional space slices Σ parameterized by a global time t . Σ will carry the information about the spatial geometry and its time evolution is going to define the space-time (CARROLL, 2004; MARTINS, 2009; PEREIRA, 2018; TAVAKOLY, 2014).

2.1.1 Space-time foliation

Figure 2.1 provides a clearer picture to understand what means to foliate the space-time. Roughly speaking, we can think about the space-time foliation in analogy with an ordinary ream paper. The envelope that protects the paper leaves is equivalent to the manifold \mathcal{M} , meanwhile, each sheet corresponds to a 3-dimensional hypersurface Σ . Note that each spacelike hypersurface is associated with an instant of time. Moreover, an observer localized in an arbitrary Σ_t has his/her past and future light cone established from the future-pointing (timelike) unit normal vector $\mathbf{n} = n^\mu = (n^0, 0)$ (QUINTIN, 2015) which fully determines the space-time foliation and must obey the relation (BILSON-THOMPSON; VAID, 2014)

$$g_{\mu\nu}n^\mu n^\nu = -1. \tag{2.1}$$

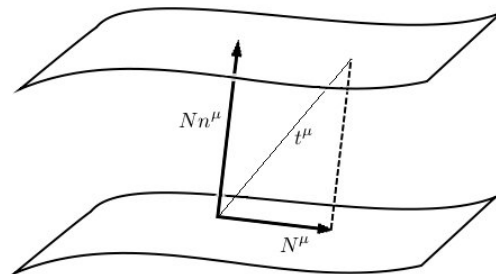
Figure 2.1 - Space-time foliation



SOURCE: Dengiz (2011)

Mathematically speaking, the procedure is to adopt \mathcal{M} as a Lorentzian manifold that is diffeomorphic to $\mathbb{R} \times \Sigma$, where $t \in \mathbb{R}$ (TAVAKOLY, 2014). It is important to emphasize the arbitrariness of the time choice, t can or cannot represent the time variable as we are used to (MOKHTAR, 2014). Besides, although the time direction is usually oriented upwards, this is not necessarily a request. Indeed, the time direction is a fiducial time which means it works as a standard reference and does not affect the dynamics (BILSON-THOMPSON; VAID, 2014).

Figure 2.2 - Relation between the spacelike hypersurfaces in the universe foliation



SOURCE: Bilson-Thompson and Vaid (2014)

To clarify this, let us analyze how to map two points localized in successive hypersurfaces through Figure 2.2. Due to GR diffeomorphism invariance, there is not a canonical choice for the time-like vector field t^μ that should perform the mapping between a point x^μ in Σ_t and another point x'^μ defined in the hypersurface Σ_{t+dt} associated to the next instant of time. Actually, t^μ can be any time-like vector field (BILSON-THOMPSON; VAID, 2014). From Figure 2.2, note that t^μ is generally projected in the hypersurface through the shift vector $N^\mu = (0, N^a)$ and its normal component dictated by the lapse function N . Thus, t^μ could be written as

$$t^\mu = Nn^\mu + N^\mu = Nn^0 + N^a. \quad (2.2)$$

Regarding the hypersurface, the timelike vectors are normal, meanwhile, the space-like vectors are tangent to Σ (TONG, 2006). To put it another way, N provides the information about how far Σ_{t+dt} is from Σ_t , while N^a enables the coordinate propagation from Σ to Σ_{t+dt} (GOURGOULHON, 2007). Hence, N and N^a can be interpreted like a general base from which the variables are decomposed (MARTINS, 2009).

In order to write the space-time metric $g_{\mu\nu}$ considering the splitting $\mathbb{R} \times \Sigma$, the components needs to be adapted. As \mathcal{M} is determined by $g_{\mu\nu}$, its space components should be related to the description of Σ . Hence, there is another key variable in the ADM formalism, the spatial metric q_{ab} of the hypersurface whose relationship with $g_{\mu\nu}$ is dictated by

$$g_{\mu\nu} = q_{\mu\nu} - n_\mu n_\nu. \quad (2.3)$$

Nonetheless, $q_{\mu\nu}$ obviously does not have a time component, since it is only defined in the hypersurface, and $n_a = 0$. Consequently, $g_{\mu\nu}$ acquires the final form

$$g_{\mu\nu} = \begin{pmatrix} -N^2 + q_{ab}N^aN^b & q_{ab}N^b \\ q_{ab}N^a & q_{ab} \end{pmatrix} \quad (2.4)$$

or also

$$ds^2 = g_{\mu\nu}dx^\mu dx^\nu = (-N^2 + q_{ab}N^aN^b)dt^2 + 2N^a dt dx^a + q_{ab}dx^a dx^b, \quad (2.5)$$

usually referred to as ADM decomposition of the metric (BLAU, 2011). In other words, GR has the space-time metric as its main quantity, meanwhile, in the canonical gravity, $g_{\mu\nu}$ is replaced by three quantities N , N^a and q_{ab} of Σ^1 , also called ADM

¹Since the choice regarding the hypersurface is arbitrary, from now on we will use just Σ to refer to the hypersurface defined in an arbitrary constant time t instead of Σ_t .

variables (BOJOWALD; HOSSAIN, 2008). Therefore, instead of the ten independent components of $g_{\mu\nu}$, there are six components of q_{ab} , three from N^a and one related to N (TAVAKOLY, 2014).

After foliating the space-time, the next step is to define the initial conditions. That is to say, we need to specify the space metric q_{ab} , the direction of time and also a variable related to the time derivative of q_{ab} (BLAU, 2011). However, before we follow further, let us first introduce the two curvature concepts that come with this description for a Riemannian manifold: the intrinsic and extrinsic curvatures.

2.1.2 Intrinsic and extrinsic curvatures

Note that now we have a 4-dimensional manifold \mathcal{M} described by $g_{\mu\nu}$ in which a 3-dimensional spacelike hypersurface with induced metric q_{ab} is embedded. In GR, the Riemann tensor (or Ricci tensor) is the one associated with the universe curvature. Notwithstanding, since the computations are performed for an arbitrary hypersurface, it is its curvature we need to pay attention to. Hence, there is a 3-dimensional Riemann tensor ${}^{(3)}R_{abcd}$ to describe the curvature in analogy with the usual 4-dimensional $R_{\mu\nu\alpha\beta}$, this is the concept referred to as intrinsic curvature. As an intrinsic property, ${}^{(3)}R$ is coordinate independent because the measures will be the same regardless if the observation is performed considering \mathcal{M} or Σ (BERTSCHINGER, 2005; CARROLL, 2004; PEREIRA, 2018). An easier way to understand the intrinsic geometry is interpreting it only with respect to the pair (Σ, q_{ab}) , neglecting the embedding around Σ (TAVAKOLY, 2014).

From the embedding of Σ in \mathcal{M} , there is the extrinsic curvature K_{ab} concept to be examined (BERTSCHINGER, 2005). In this case, the position of the observer affects the measures. The simplest example is to consider a paper leaf again. If \mathcal{M} has a box shape or a cylindrical one, the leaf will bend in a different way regarding the observer perspective. Note that the picture of folding a leaf comes from an outside point of view, an observation from inside the leaf will not detect any change once the leaf remains the same (PEREIRA, 2018).

In other words, K_{ab} is directly related to the bending of Σ in \mathcal{M} and defined as the variation of \mathbf{n} along the hypersurface (see Figure 2.3)

$$K_{ab} = D_a n_b. \tag{2.6}$$

Where D_a is a covariant derivative operator associated to Σ that obeys $D_a q_{bc} = 0$

(PEREIRA, 2018) analogously to $\nabla_\mu g_{\nu\lambda} = 0$. Hence, K_{ab} provides the information about how curved Σ is regarding \mathcal{M} (TAVAKOLY, 2014). Despite we have already assumed $n_a = 0$ as an initial value to obtain the standard case, we kept the general definition once it helps to notice how K_{ab} is directly related to the variation of q_{ab} regarding the normal unit vector through a Lie derivative as it follows

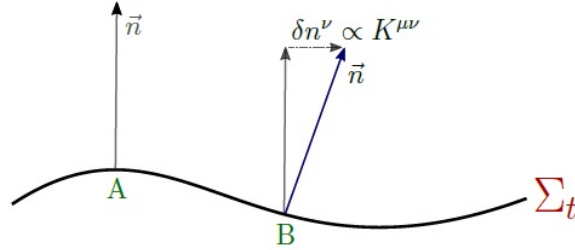
$$K_{ab} = \frac{1}{2} \mathcal{L}_n q_{ab}. \quad (2.7)$$

After some calculation, (2.7) can be written in the form

$$K_{ab} = \frac{1}{N} (\dot{q}_{ab} - D_a N_b - D_b N_a), \quad (2.8)$$

that makes clear the relation between K_{ab} and the time derivative of the metric \dot{q}_{ab} . The reason why we emphasized the extrinsic curvature role is that it will be necessary to rewrite the Einstein-Hilbert action in terms of ${}^{(3)}R$ and K_{ab} , an essential part during the construction of the Hamiltonian.

Figure 2.3 - Extrinsic curvature of the hypersurface



SOURCE: Pereira (2018)

2.1.3 The Hamiltonian and canonical variables

First, the Einstein-Hilbert density Lagrangian \mathcal{L}_{EH} is written considering the ADM variables, which means $g_{\mu\nu}$ will be replaced by N , N_a and q_{ab} , while ${}^{(3)}R$ and K_{ab} are employed to rebuild the 4-dimensional Ricci scalar R (see Appendix A for more details). The result is the ADM Lagrangian given by

$$\mathcal{L}_{\text{ADM}} = N\sqrt{q}[K_{ab}K^{ab} - K^2 + {}^{(3)}R], \quad (2.9)$$

therefore, the ADM action can be expressed like

$$S_{\text{ADM}}[N, N_a, q_{ab}] = \int d^4x \mathcal{L}_{\text{ADM}}(N, N_a, q_{ab}). \quad (2.10)$$

As the variation of the action is performed with respect to $g_{\mu\nu}$ within the Lagrange formulation, in the ADM formalism, the variation is computed considering the variables equivalent to it: N , N^a and q_{ab} . If this is also implemented to the matter action, combining both results will enable to recover the Einstein Field Equations (BERTSCHINGER, 2005).

Since now we have the density Lagrangian, it is possible to perform a Lagrange transformation in order to have the action in the Hamiltonian form. N , N^a and q_{ab} would be equivalent to the generalized variables if we were working with an ordinary mechanic system. Hence, the next step is computing their analog canonical momenta. In this case, the limitation regarding time fixes the field values to a specific spatial position, while the space derivatives enable to relate different field values. For now, let us continue only discussing the gravitational part of the action since the matter sector is assumed to be independent of \dot{N} , \dot{N}^a and \dot{q}_{ab} (BERTSCHINGER, 2005).

From (2.9), it is possible to obtain the momenta π_N , π_a and π_{ab} related to N , N^a and q_{ab} , respectively, as it follows

$$\pi_N = \frac{\partial \mathcal{L}_{\text{ADM}}}{\partial \dot{N}} \approx 0, \quad (2.11)$$

$$\pi^a = \frac{\partial \mathcal{L}_{\text{ADM}}}{\partial \dot{N}_a} \approx 0, \quad (2.12)$$

$$\pi^{ab} = \frac{\partial \mathcal{L}_{\text{ADM}}}{\partial \dot{q}_{ab}} = \sqrt{q}(Kq^{ab} - K^{ab}). \quad (2.13)$$

From (2.11) and (2.12), it can be noticed that the ADM Lagrangian does not depend on the time derivatives of N and N^a . The symbol \approx is the representation of a weak equality, that is to say the equality is true if it is consider over a hypersurface. In this case, N and N^a are not dynamical variables, leaving only q_{ab} and its momentum to define the dynamics of the gravitational sector. Hence, the phase space is com-

posed by all pairs of q_{ab} and π_{ab} (GAMBINI; PULLIN, 2011; MARTINS, 2009). After performing the Lagrange transformation, the gravitational Hamiltonian H_G can be written like

$$H_G = \int d^3x [\dot{N}\pi_N + \dot{N}_a\pi^a + \dot{q}_{ab}\pi^{ab} - \mathcal{L}_{\text{ADM}}] = \int d^3x [\dot{q}_{ab}\pi^{ab} - \mathcal{L}_{\text{ADM}}], \quad (2.14)$$

meanwhile, the total Hamiltonian H_T corresponds to

$$H_T = H_G + H_m = \int d^3x [\dot{q}_{ab}\pi^{ab} - \mathcal{L}_{\text{ADM}} - \mathcal{L}_m], \quad (2.15)$$

where H_m and \mathcal{L}_m are the matter Hamiltonian and density Lagrangian, respectively. Therefore, we can interpret the variables in Σ analogously to the ones from \mathcal{M} (BOOT, 2008), working with them in a similar way as it is identified in Table 2.1.

Table 2.1 - Variables that plays similar roles

General Relativity (\mathcal{M})	Canonical Formulation (Σ)
$g_{\mu\nu}$	q_{ab}
∇_a	D_a
$R_{\mu\nu\alpha\beta}$	${}^{(3)}R_{abcd}$

In the Hamiltonian formulation, the dynamics is dictated by the Hamilton equations whose usual form from analytical mechanics is given by

$$\dot{q}_{ab} = \frac{\partial H_T}{\partial \pi^{ab}}, \quad (2.16)$$

$$\dot{\pi}_{ab} = -\frac{\partial H_T}{\partial q_{ab}}. \quad (2.17)$$

Nevertheless, they could be also expressed in terms of the Poisson bracket between the configuration variables q_{ab} and π_{ab} with H_T . Since the Poisson bracket is defined as

$$\{f, g\} \equiv \frac{\partial f}{\partial q} \frac{\partial g}{\partial \pi} - \frac{\partial f}{\partial \pi} \frac{\partial g}{\partial q} \quad (2.18)$$

for two function of the phase space $f(q, \pi)$ and $g(q, \pi)$, the Poisson bracket between q_{ab} and π_{cb} follows the next expression

$$\{q^{ab}(x), \pi_{cd}(y)\} = \frac{1}{2}(\delta_c^a \delta_d^b + \delta_d^a \delta_c^b) \delta^3(x - y). \quad (2.19)$$

Thus, the equations of motion (EoM) will be described by

$$\dot{q}_{ab} = \{q_{ab}, H_T\} \quad (2.20)$$

and

$$\dot{\pi}_{ab} = \{\pi_{ab}, H_T\}. \quad (2.21)$$

The solution from equations (2.20) and (2.21) can be interpreted as a flow or curve defined in the phase space with $q(t)$ and $\pi(t)$, considering an initial value $q(0)$ and $\pi(0)$ (GAMBINI; PULLIN, 2011). At this point, we need to briefly discuss systems with constraints.

2.1.4 Constraints and Lagrange multipliers

Describing a physical system with more variables than what is actually necessary is a common procedure, particularly, when the true degrees of freedom are unknown. However, these variables are usually attached through restrictions involving the phase-space variables named constraints. Further, the constraints are relations that must hold during the entire evolution, enabling to identify conserved quantities. On the other hand, the presence of conserved quantities is related to physical symmetries. Thus, the constraints indicate the existence of physical symmetries on the system (GAMBINI; PULLIN, 2011).

The standard approach is to incorporate the constraint into the Hamiltonian through the Lagrange multipliers method. Basically, the procedure consists in adding extra terms composed by the constraint multiplied by a Lagrange multiplier to the original Hamiltonian H_{original} , defining a total Hamiltonian like following

$$H_T = H_{\text{original}} + \text{constraints}. \quad (2.22)$$

In case of a generic system, it is possible to identify a constraint by verifying whether the Lagrangian depends on the time derivative of the desired quantity. If a variable y appears in the Lagrangian/Hamiltonian/action, but $\frac{\partial L}{\partial \dot{y}} = 0$, that means y is a Lagrange multiplier and does not contribute to the system dynamics. Hence, the

quantity multiplying it will be a constraint. Moreover, the presence of a Lagrange multiplier means the evolution of the system is not unique due to the arbitrariness they introduce. To put this another way, constraints impose limits to the free parameters of the system, being the generators of the gauge symmetries (GAMBINI; PULLIN, 2011).

2.1.5 The electromagnetic Hamiltonian

An example of a constrained system is the Maxwell electromagnetic theory whose Hamiltonian can be expressed as

$$\begin{aligned} H_{\text{electro}} &\equiv \int (E^a(x)\dot{A}_a - \mathcal{L}_{\text{electro}})d^3x \\ &= \int \left(\frac{1}{2}[E^a(x)E^b(x)\delta_{ab} + B^a(x)B^b(x)\delta_{ab}] - A_0\partial_a E^a \right) d^3x. \end{aligned} \quad (2.23)$$

Here, $\mathcal{L}_{\text{electro}}$ refers to the electromagnetic density Lagrangian, B^a corresponds to the magnetic field defined in terms of the vector potential A_a , which together with the electric field E^b are the canonical variables related by

$$\{A_a(x), E^b(y)\} = \delta_a^b \delta^{(3)}(x - y). \quad (2.24)$$

Therefore, equation (2.24) implies that the variables must be considered at the same spatial point and also for the same vector component. Otherwise, the result would be a null Poisson bracket (GAMBINI; PULLIN, 2011). From (2.23), it is possible to recognize the term $\partial_a E^a$ that, according to Gauss's law, obeys the relation $\partial_a E^a = 0$. Thus, the Gauss law is a constraint, while A_0 is a Lagrange multiplier as it can be observed through computing the EoM of its momentum π^0 :

$$\dot{\pi}^0 = \{A_0, H_{\text{electro}}\} = \partial_a E^a = 0. \quad (2.25)$$

Likewise, the remaining Maxwell equations can be recovered from the values of \dot{A}_a and \dot{E}^a (GAMBINI; PULLIN, 2011).

2.1.6 The constrained Hamiltonian

Unlike the electromagnetic theory, the gravitational Hamiltonian is a purely constrained quantity (ASHTEKAR et al., 2006b). The equations (2.11) and (2.12) imply

that $\pi_N \approx 0$ and $\pi^a \approx 0$ are primary constraints since they are obtained straight from Lagrangian. However, they also give rise to secondary constraints through their time derivatives. Therefore, after rearranging the terms from (2.14), the standard form of the ADM Hamiltonian is given by

$$H_G = \int d^3x [\dot{N}\pi_N + \dot{N}_a\pi^a + N\mathcal{H} + N_a\mathcal{H}^a], \quad (2.26)$$

in which \mathcal{H} and \mathcal{H}^a correspond to secondary constraints defined as

$$\mathcal{H} = \frac{1}{\sqrt{q}} \left(q_{ac}q_{bd} - \frac{1}{2}q_{ab}q_{cd} \right) \pi^{ab}\pi^{cd} - \sqrt{q} {}^{(3)}R, \quad (2.27)$$

$$\mathcal{H}^a = -2\sqrt{q}\nabla_b \left(\frac{\pi^{ab}}{\sqrt{q}} \right), \quad (2.28)$$

with q representing the determinant of q_{ab} .

It is important to emphasize that (2.27) and (2.28) can also be written as functions of K_{ab} instead of π_{ab} . As secondary constraints, $\mathcal{H} \approx 0$ and $\mathcal{H}^a \approx 0$. Thus, in the vacuum, $H_G \approx 0$, where the weak equality should be kept until the computation of the Poisson bracket (MARTINS, 2009). Besides, Equation (2.26) is a direct consequence of GR independence regarding time, because its arbitrariness gives rise to symmetries that make the dynamics obtained arbitrarily as well (GAMBINI; PULLIN, 2011).

Since the Hamiltonian role is to provide the time evolution of the system, in GR case, this means a direct dependence on N and N^a . Despite the absence of proper time, they are the variables to be specified in order to determine the flow evolution at one point of spacetime (TAVAKOLY, 2014), which corresponds to the closest time evolution we can get from GR. Note from (2.11) and (2.12) that N and N_a are Lagrange multipliers (GAMBINI; PULLIN, 2011), in agreement with the arbitrary nature of time.

Incorporating matter to the equation, we can generalize \mathcal{H} and \mathcal{H}^a to contain it and still respect the restrictions $\mathcal{H} \approx 0$ and $\mathcal{H}^a \approx 0$ that limits the physical phase space. Furthermore, it is also useful to introduce the smeared constraints

$$\mathcal{C}_H[N] = \int d^3x N\mathcal{H} = \int d^3x N(\mathcal{H}_{\text{grav}} + \mathcal{H}_{\text{matter}}), \quad (2.29)$$

$$\mathcal{C}[N_a] = \int d^3x N_a \mathcal{H}^a = \int d^3x N_a (\mathcal{H}_{\text{grav}}^a + \mathcal{H}_{\text{matter}}^a). \quad (2.30)$$

Both $\mathcal{C}_H[N]$ and \mathcal{H} are referred to as Hamiltonian constraint (also known as scalar constraint), while $\mathcal{C}[N_a]$ and \mathcal{H}^a are named diffeomorphism constraint (or vector constraint).

The standard procedure is to define $N^a = 0$ which means to evolve the slice Σ only in the normal direction once now $t^\mu = Nn^0$. Hence, the dynamics is dictated only by \mathcal{H} (TAVAKOLY, 2014). However, the problem regarding the standard canonical formalism is the non-polynomial dependence of the constraint equations with respect to the traditionally canonical conjugated variables (ASHTEKAR, 1986). Here, they would be q_{ab} and π_{ab} (or K_{ab}), but they can also be expressed in a tetrad base using the Palatini formulation.

The canonical formulation presents GR as a gauge theory, enabling to perform a canonical quantization (MARTINS, 2009). This process follows Dirac's quantization rule whose the roughly simplest description consists in promoting the canonical variables (for example, A and B) to operators and to turn the Poisson brackets in commutators (BERTSCHINGER, 2005; DONÁ; SPEZIALE, 2010) as it follows

$$\{A, B\} \rightarrow -i[A, B]. \quad (2.31)$$

Nonetheless, this requires that A and B have well-defined quantum analogs, which is hard to obtain considering the non-trivial form of the Hamiltonian. Due to the fact that the Poisson bracket for q_{ab} and π_{ab} is given by (2.19), their quantum analogs should turn into a form similar to

$$q_{ab} \rightarrow \hat{q}_{ab}, \quad (2.32)$$

$$\pi^{ab} \rightarrow -i\hbar \frac{\delta}{\delta q_{ab}}. \quad (2.33)$$

The Hamiltonian is a natural bridge between the classical and quantum worlds (MARTINS, 2009). Since the Hamiltonian constraint (operator) is the one responsible to describe the dynamics in canonical quantum gravity framework, the equations of motion will be derived from it (BOJOWALD; HOSSAIN, 2008). Thus, \mathcal{H} must also have

a quantum analog well defined. However, the constraint equation implies $\mathcal{H} \approx 0$ whose translation to a Schrodinger equation form would result in $\mathcal{H}|\Psi\rangle = 0$. Or also, from (2.44), $\frac{\partial \mathcal{H}_G}{\partial N}|\Psi\rangle = 0$, which corresponds to a singular functional differential equation without physical solution for this phase space (BOOT, 2008).

We will not detail the aspects regarding the quantization process because they are far more complex than we really need to describe in our work. Nevertheless, what we must have in mind is the necessity of having elementary variables to promote to a quantum operator. Moreover, the Hamiltonian constraint must have a suitable form to enable the quantization process to happen.

2.2 Loop Quantum Gravity

Among the current attempts to quantize gravity, we are interested in the one known as Loop Quantum Gravity. It was developed in the mid-1980s by Ashtekar (1986) when he realized the possibility to rewrite the equations of gravity similar to the formulation applied for theories of particle physics. Basically, these equations were written in terms of proper variables from particle physics (GAMBINI; PULLIN, 2011) and a Hamiltonian formulation was developed using these new variables in (ASHTEKAR, 1987).

Moreover, Barbero (1995) gave a fundamental contribution by ensuring that the Ashtekar variables do not need to assume complex values to describe a space-time with Lorentzian signature. This is the reason why sometimes the Ashtekar variables are also named Ashtekar-Barbero variables in the literature. Here, we will use both nomenclatures indistinctly.

Loop Quantum Gravity is a quantum description of gravity that mixes the Hamiltonian formulation of GR with elements from QFT. LQG formalism is constructed analogously to the canonical formulation in which the space-time manifold is leafed into space manifolds related to each instant of time (LANGLOIS et al., 2017; BOJOWALD; HOSSAIN, 2008). Looking from a pragmatic point of view, LQG can be seen as a strategic approach developed to satisfy all the constraints related to the gravitational Hamiltonian. To achieve this goal, GR was rewritten as a gauge theory based on connections since they are the natural objects related to gauge symmetries. The idea was to use the gauge connection and its conjugate momentum as the canonical pair in analogy to the electromagnetic case and build them from q_{ab} and K_{ab} (BENITO, 2010).

The procedure starts by defining the triad e_i^a and cotriad e_b^j ,

$$e_i^a e_a^j = \delta_i^j \quad \text{and} \quad e_i^a e_b^i = \delta_b^a, \quad (2.34)$$

directly related to the spatial metric by

$$q_{ab} = e_a^i e_b^j \delta_{ij}, \quad (2.35)$$

in which δ_{ij} can be interpreted as the Euclidian metric ($\delta_{ij} = \text{diag}(1, 1, 1)$) or Kronecker delta. At this stage, we need to clarify the use of two set of spatial index: $a, b, c\dots$ and $i, j, k\dots$. Meanwhile the indices a, b, c, \dots refer to Σ , i, j, k, \dots are internal indices associated to the fiducial cell (LANGLOIS et al., 2017), which will be discussed in the sequence.

Since the space-time is intrinsically infinite, the Hamiltonian treatment in LQG is performed by considering a finite elementary cell \mathcal{V} , usually referred to as fiducial cell, in order to avoid integrals over infinite region (BOJOWALD; HOSSAIN, 2008). From (2.35), it can be noted that q_{ab} would be the metric to raise and lower the indices $a, b, c\dots$ and δ_{ij} would do the same for $i, j, k\dots$ (MARTINS, 2009). However, δ_{ij} is being employed as fiducial metric, enabling to identify $i, j, k\dots$ with $a, b, c\dots$. That is to say, using either e_a^i or e_j^b enables us to replace the spatial indexes by the internal ones and vice versa (FLEISCHHACK, 2012).

The next step is to introduce the variable playing the role of *electric field* like

$$E_i^a = \sqrt{q} e_i^a, \quad (2.36)$$

that is named densitized triad. Once now there is a variable associated with the spatial metric, it is necessary to construct another from its conjugated momentum, or in this case, from the extrinsic curvature here written in the form

$$K_a^i = K_{ab} e_i^b. \quad (2.37)$$

However, K_a^i is a vector regarding the internal space \mathcal{V} and does not define a connection. With the purpose to obtain a gauge connection, the strategy was to employ the spin connection Γ_a^i that provides the information about how the gravitational field affects the matter (parallel transport) (BLAS, 2013). Thus, the spin connection is the

one describing the intrinsic curvature whose form is designed so that the expression

$$D_a e_i^a \equiv \partial_a e_i^b + \Gamma_{ac}^b e_i^c + \epsilon_{ij}{}^k \Gamma_a^j e_k^b = 0 \quad (2.38)$$

is satisfied, resembling the role played by the Christoffel symbol Γ_{ac}^b (LANGLOIS et al., 2017) with $\epsilon_{ij}{}^k$ referring to the Levi-Civita symbol.

Note that Γ_a^i and K_a^i contain all the information about curvature which is encoded into Ashtekar connection A_a^i through the definition

$$A_a^i = \Gamma_a^i + \gamma K_a^i, \quad (2.39)$$

where γ represents the Barbero-Immirzi parameter. Notwithstanding γ was originally an unknown constant, Meissner (2004) obtained the value $\gamma \simeq 0.2375$ by comparing the black hole entropy with Hawking-Bekenstein formula (MIELCZAREK, 2010). All things considered, the symplectic structure between A_a^i and E_i^a is determined by

$$\{A_a^i(x), A_b^j(y)\} = 0, \quad (2.40)$$

$$\{E_i^a(x), E_j^b(y)\} = 0, \quad (2.41)$$

$$\{A_a^i(x), E_j^b(y)\} = 8\pi G \gamma \delta_a^b \delta_j^i \delta^{(3)}(x - y), \quad (2.42)$$

which is similar to (2.24).

In other words, LQG is based on the Ashtekar variables instead of the spatial metric itself which makes its structure nearest to Yang-Mills theory (GAMBINI; PULLIN, 2011). Therefore, A_a^i and its conjugated momentum E_i^a , named Ashtekar variables, correspond to the canonical variables of LQG description and encode the information regarding curvature and spatial geometry, respectively (LANGLOIS et al., 2017; MIELCZAREK, 2014; ZHANG; LING, 2007). However, now, instead of a metric space, we are dealing with the connection space (DONÁ; SPEZIALE, 2010).

LQG, as well as the canonical formulation, presents a purely constrained Hamiltonian. Nevertheless, changing the calculations from metric space to the connection

one expands the phase space due to the additional degree of freedom. This means a new constraint

$$\mathcal{G}^i \equiv \partial_a E_i^a + \epsilon_{ij}{}^k A_a^j E_k^a \approx 0 \quad (2.43)$$

arises from Ashtekar gravity (FLEISCHHACK, 2012; BLAS, 2013). In analogy with the electromagnetic case, (2.43) is named Gauss constraint, but can be also referred to as rotation constraint once it defines the invariance of Ashtekar gravity under this kind of transformation. Thus, using the Ashtekar-Barbero connection to describe GR means to write it in a language of a gauge theory (CASARES, 2018).

In this sense, GR was translated to a $SU(2)$ gauge theory with the symplectic structure given by (2.42) that results in a constrained system determined by the Gauss law, space diffeomorphism invariance and Hamiltonian constraint (DONÁ; SPEZIALE, 2010). Consequently, the Hamiltonian can be written as the sum of Gauss, diffeomorphism and Hamiltonian constraints and their respective Lagrange multipliers (BOJOWALD; HOSSAIN, 2007; MIELCZAREK, 2014) like

$$H_{LQG} = \int d^3x [N_i \mathcal{G}^i + N_a \mathcal{H}^a + N \mathcal{H}]. \quad (2.44)$$

Regarding the matter sector, its content is arbitrary. Indeed, LQG does not require a specific type of matter (BOOT, 2008), so that any matter content could be the energy source associated with the geometric sector. The simplest and largely employed assumption is to define a scalar field φ and its conjugate momentum π_φ to satisfy

$$\{\varphi, \pi_\varphi\} = 1, \quad (2.45)$$

and to incorporate them within (2.44). Consequently, its density Lagrangian follows (1.24).

The scalar (or Hamiltonian) constraint continues to be the one determining the time evolution of Σ , once \mathcal{G}^i and \mathcal{H}^a are satisfied by construction (BOJOWALD; HOSSAIN, 2008). There are many ways to write this constraint, here, we will work considering the same formalism implemented by Langlois et al. (2017) since it was the fundamental reference for the development of our work (for more details about how to derive the Hamiltonian constraint see Appendix B). Hence, the Hamiltonian

constraint will be written in the form ²

$$\mathcal{H} = -\frac{E_i^a E_j^b}{16\pi G \gamma^2 \sqrt{q}} \epsilon^{ij k} (F_{ab}{}^k - (1 + \gamma^2) \Omega_{ab}{}^k) + \frac{\pi^2 \varphi}{2\sqrt{q}} + \sqrt{q} V(\varphi) \quad (2.46)$$

where

$$F_{ab}{}^k = 2\partial_{[a} A_{b]}^k + \epsilon_{ij}{}^k A_a^i A_b^j \quad (2.47)$$

and

$$\Omega_{ab}{}^k = 2\partial_{[a} \Gamma_{b]}^k + \epsilon_{ij}{}^k \Gamma_a^i \Gamma_b^j. \quad (2.48)$$

Again, analogously to electromagnetism, $F_{ab}{}^k$ illustrates the field strength of A_a^i and describes the curvature of the connection. Meanwhile, $\Omega_{ab}{}^k$ provides the information about the Σ spatial curvature.

At this point, it seems reasonable to think about starting the quantization process. However, it is still not possible to obtain a well-defined operator for the Hamiltonian and connection itself. Indeed, a polynomial Hamiltonian requires a complex γ which will send GR's phase space to the complex plane (BOOT, 2008). Even though the Ashtekar variables could not play the role of elementary variables directly, they are used to build them. In this sense, the LQG strategy to quantize gravity is to describe it in terms of different variables instead of trying to change the theory itself or the quantum paradigm. Thus, GR is rewritten in a suitable way that enables to implement Dirac's quantization procedure (DONÁ; SPEZIALE, 2010).

First of all, in LQG, the space-time geometry is discrete because of the independence of the theory with respect to the background (BOJOWALD, 2005). According to LQG proposal, the space-time is compound by cells named spin network from which the elementary variables are determined. They are holonomies of edges related to Ashtekar connection A_a^i and fluxes across surfaces associated with densitized triads E_i^a . The holonomy is defined as the exponential of the Ashtekar-Barbero connection

$$h_i(\ell) = \exp \left(\int_0^\ell dx^i A_a \left(\frac{\partial}{\partial x^i} \right)^a \right) \quad (2.49)$$

²For more details regarding how to derive (2.46) from equation (2.44), see the classical references (THIEMANN, 2007), (ASHTEKAR, 1986) and (ASHTEKAR, 1987).

evaluated considering the loop inside the elementary cell. Basically, the procedure consists in to draw a curve parallel to the path $\left(\frac{\partial}{\partial x^i}\right)^a$ that has a length ℓ regarding the fiducial metric (LANGLOIS et al., 2017).

Although the flux F_{flux} is the conjugated variable related to the holonomy, it will not be specified here since its reduced form is already a well-defined quantity in the quantum world. Moreover, both holonomy and flux are implemented as elementary variables due to their invariance under diffeomorphism transformation and metric independence, corresponding to smooth versions of A_a^i and E_i^a (BENITO, 2010; BLAS, 2013).

Once the elementary variables have their quantum analogs well-defined, the constraint constructed from them can be written straightforward as a quantum operator (ASHTEKAR et al., 2006b). This requirement is fulfilled by the holonomy and triads that have unambiguous operators analogs defined in the quantized theory (ASHTEKAR et al., 2006a). In LQG quantization, the curvature operator (or F_{ab}^k) is written in terms of holonomies which are defined around a loop with nonzero area gap Δ (ASHTEKAR et al., 2006b). In this scenario, the space-time is discrete because the limit imposed to LQG fundamental cell, preventing it to assume a zero area value (LANGLOIS et al., 2017).

In summary, Loop Quantum Gravity is usually defined as a Hamiltonian formulation of general relativity based on holonomies and fluxes (MIELCZAREK, 2014). This means the equations of motion of the phase space functions are computed via Poisson brackets, $\dot{f} = \{f, H\}$, which defines the kinematic evolution through the canonical variables (BOJOWALD et al., 2006). The kinematic character comes from the use of the connection space that only allows the description of the interactions. The agents responsible to determine the dynamics requires the metric concept absent in LQG framework.

Moreover, this can be also related to the most discussed conceptual problem that comes from the canonical approach, the problem of time. As we mentioned in the previous section, the time evolution is arbitrary and corresponds to a particular case of gauge transformation regarding GR construction as a theory. Coupled with this is the fact that quantized field theory has gauge-invariant states which ensures the quantum gravity states will be independent of time (WALLACE, 2000). However, it is possible to introduce a dynamic character in the kinematic LQG context through cosmological models. This is the content presented in the following section.

2.3 Loop Quantum Cosmology

LQC can be interpreted as an application of LQG to cosmological space-times and defined as a symmetric reduced model to study the quantization process à la loop for highly symmetrical cosmological models (ASHTEKAR et al., 2006a; BLAS, 2013; SADJADI, 2013). Therefore, LQC is built over the variables and techniques from LQG plus the incorporation of the cosmological dynamics that comes from the symmetry features of FRW space-times (LANGLOIS et al., 2017). Within this configuration, the system dynamics is introduced by the cosmological sector, enabling to overcome the LQG kinematic nature. Further, LQC provides a way to explore the effects of the discrete space-time, in addition, to obtain a consistent quantum theory without classical singularities (BENITO, 2010).

LQC can be described in two levels: purely quantum and semi-classical. Despite being a more complete approach, the purely quantum treatment suffers from interpretation issues. Moreover, the semi-classical approach, also called effective, is capable of reproducing the main aspects related to LQG and provides a better fit for cosmological framework (MIELCZAREK, 2010; BOJOWALD; MORALES-TÉCOLT, 2004).

Roughly speaking, the semi-classical approach treats the quantum gravity effects through corrections in the classical equations of motion (MIELCZAREK, 2009) and it is the one constructed from the canonical formalism. Furthermore, the effective theory is a good approximation for a non-compact universe whose volume is greater than ℓ_{Pl}^3 . This includes the FRW space-time, once its spatial volume must be infinite as long as $a \neq 0$ like happens in LQC (LANGLOIS et al., 2017).

The starting point to study the holonomy effects is to set the cosmological model we will going to work with. The standard LQC is built considering a homogeneous and isotropic universe filled with a massless free scalar field, the FRW universe with the scalar field as the energy source. For a spatially flat FRW space-time, the intrinsic curvature is null ($\Gamma_a^i = 0$), which, from (2.48), also applies to $\Omega_{ab}^k = 0$. Remembering the standard assumption $N^a = 0$, the cross terms in (2.4) are going to be null. Thus, the FRW metric can be written analogously to (2.4) like

$$ds^2 = -N^2 dt^2 + a(t)^2 d\vec{x}^2. \quad (2.50)$$

The Ashtekar variables acquire their simplest reduced form

$$E_i^a = p \left(\frac{\partial}{\partial x^i} \right)^a \quad \text{with } p = a^2 \quad (2.51)$$

and

$$A_a^i = c(dx^i)_a \quad \text{with } c = \frac{\gamma \dot{a}}{N} \quad (2.52)$$

as a consequence of the underlying symmetries of FRW space-time. Therefore, c and p correspond to the symmetry reduced gravitational phase space coordinates. They are independent of the fiducial metric and characterize a two-dimensional phase space (ASHTEKAR et al., 2006b), obeying the symplectic structure

$$\{c, p\} = \frac{8\pi G\gamma}{3}. \quad (2.53)$$

Following LQG, the particular feature that makes LQC different from previous attempts to quantize the space-time is the choice of the elementary variables (LANGLOIS et al., 2017). In other words, the quantities elevated to the status of quantum operators. The obvious choice would be A_a^i and E_i^a , nevertheless, neither A_a^i nor c have a quantum counterpart. Hence, the strategy was to use a function defined as an exponential of A_a^i , the holonomy. In this framework, the matter canonical variables are only the scalar field and its momentum, meanwhile, for the gravitational sector we may recognize three pairs: c and p , A_a^i and E_i^a , h_i and F_{flux} . The table 2.2 provides a clear picture by relating the pair with their respective function. Note that each pair has its own role to play in the à la loop quantization scheme and can actually be mixed during the process.

Table 2.2 - Different pairs of variables from Loop Quantum Cosmology

	Configuration variable	Conjugated momentum
Elementary variables	h_i	F_{flux}
Canonical variables	A_a^i	E_i^a
Reduced variables	c	p

All things considered, the total Hamiltonian density acquires the reduced form (see Appendix ??)

$$\mathcal{H} = -\frac{3}{8\pi G\gamma^2} p^{1/2} c^2 + \frac{\pi_\varphi^2}{2p^{3/2}} + p^{3/2} V(\varphi), \quad (2.54)$$

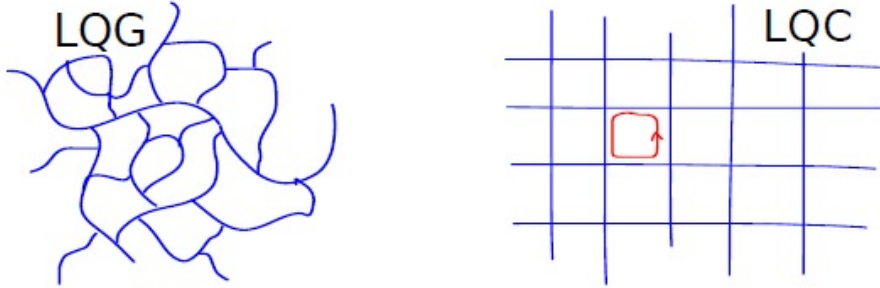
that will be used to obtain the evolution of any observable \mathcal{O} through the relation

$$\frac{d\mathcal{O}}{dt} = \{\mathcal{O}, \mathcal{C}_H\}. \quad (2.55)$$

However, before discussing the EoM from Effective LQC scenario, we will first briefly describe how the quantization process occurs.

To begin with, Figure 2.4 exemplifies the difference between how the space-time is interpreted in the full theory compared with LQC. In the left-hand side, there is a spin network from LQG setup, in which it is possible to identify the space-time cells without any organized structure. In the right-hand side, the spin network seems similar to the picture used to illustrate the space-time concept. Roughly speaking, LQC establishes an organization for the structure of the spin network due to the symmetry properties from cosmological dynamics, usually characterized as homogeneous and isotropic. The loop square shape is a feature that comes with the FRW space-times and makes easy to visualize the holonomy as a parallel transport operator (LANGLOIS et al., 2017). Besides, the holonomy is represented through the red line defined inside the square loop that delimits the elementary cell (MIELCZAREK, 2014).

Figure 2.4 - Spin network



SOURCE: Mielczarek (2014).

The classical relation between holonomy and curvature is associated with a decreasing area loop around which the holonomy is defined. In this case, the area can be shrunk until zero (ASHTEKAR et al., 2006b). The physical length of the square loop is determined from the product of the scale factor a and the square loop length ℓ regarding the fiducial metric. The physical area of the spin network is an expression

of the reduced canonical variable p and a quantity $\bar{\mu}$. The later works as the loop coordinate size and is directly related to quantization of the Ashtekar curvature components F_{ab}^i (BOJOWALD; HOSSAIN, 2008; LANGLOIS et al., 2017). Indeed, the right choice of $\bar{\mu}$ is essential to reach the desired evolution.

In general, $\bar{\mu}$ is defined with respect to the triad component p in order to reflect the space-time discreteness within the dynamics. In spite of being difficult to obtain a precise behavior of the parameter $\bar{\mu}$, there is a favorite value for it, called $\bar{\mu}$ -scheme, that is given by

$$\bar{\mu} = \sqrt{\frac{\Delta}{p}}. \quad (2.56)$$

Δ represents the smallest value that can be used to describe the discrete area of space-time (ASHTEKAR et al., 2006b). It corresponds to the gap area coming from LQG whose form is considered like (MIELCZAREK, 2014)

$$\Delta = 2\sqrt{3}\pi\gamma\ell_{Pl}^2. \quad (2.57)$$

As we mentioned earlier, despite the holonomy operator being well-defined in full LQG, there are not any local operators capable of representing neither the connection nor the curvature. Since the procedure to obtain a quantum constraint should start with a suitable operator to describe the curvature of the gravitational connection, the treatment consists in expressing this curvature as a limit of the holonomy regarding a loop whose minimum area is defined by Δ . Indeed, in quantum geometry, the presence of Δ prevents a zero eigenvalue for the area operator (ASHTEKAR et al., 2006b). Consequently, the area operator has a discrete spectrum defined by a minimum non-zero eigenvalue and F_{ab}^k is written as a function of the holonomy of the connection A_a (LANGLOIS et al., 2017).

The absence of an operator equivalent to c is overcome in the usual procedure by returning to the Hamiltonian (2.46) from full LQG that does not explicitly present A_a^i or c (ASHTEKAR et al., 2006b). It is not necessary to reproduce all this work in order to obtain an operator regarding E_a^i (or the triad flux) once the variable p already determines a well-defined area operator.

The effective dynamics is obtained analogously to the previous proceeding, F_{ab}^k is also described in terms of the holonomy evaluated with respect to a square loop

with minimal area gap Δ . However, as we are considering the semi-classical limit, the Hamiltonian density will be treated at classical level. As a result, the effective scalar constraint is going to be determined by

$$\mathcal{H}_{eff} = -\frac{3p^{3/2}}{8\pi G\Delta\gamma^2} \sin^2 \bar{\mu}c + \frac{\pi_\varphi^2}{2p^{3/2}} + p^{3/2}V(\varphi). \quad (2.58)$$

In the effective treatment, the Hamiltonian is built on a continuum spacetime, the quantum fluctuations are neglected and the quantum corrections are implemented into classical dynamics (LANGLOIS et al., 2017; ZHANG; LING, 2007).

The time evolution of the observable p is computed from (2.55), with the Hamiltonian density given by (2.58), resulting in

$$\dot{p} = 2N \frac{p}{\gamma\sqrt{\Delta}} \sin \bar{\mu}c \cos \bar{\mu}c. \quad (2.59)$$

Since \mathcal{H}_{eff} is weakly equal to zero, the square sine function obeys the expression

$$\sin^2 \bar{\mu}c = \frac{\rho}{\rho_c}, \quad (2.60)$$

which establishes a boundary between the values of ρ and ρ_c to the range $0 \lesssim \rho/\rho_c \lesssim 1$ (Appendix C provides further information about the sine function role). The LQC standard energy density is described by the expression for an arbitrary scalar field φ ,

$$\rho = \frac{\pi_\varphi^2}{2p^3} + V(\varphi), \quad (2.61)$$

whose critical value corresponds to

$$\rho_c = \frac{3}{8\pi G\gamma^2\Delta} = \frac{\sqrt{3}}{32\pi^2\gamma^3}\rho_{Pl}, \quad (2.62)$$

where ρ_{Pl} represents the energy density at Planck scale. Therefore, just like in chapter 1, ρ must also satisfy (1.11), (1.15) and (1.26).

All things considered, we can obtain the effective Friedmann equation for a flat FRW space-time through (2.59) and (2.60) which will result in

$$H^2 = \left(\frac{\dot{p}}{2Np}\right)^2 = \left(\frac{\dot{a}}{Na}\right)^2 = \frac{8\pi G}{3}\rho \left(1 - \frac{\rho}{\rho_c}\right), \quad (2.63)$$

usually called Effective Friedmann equation, being also referred to as modified

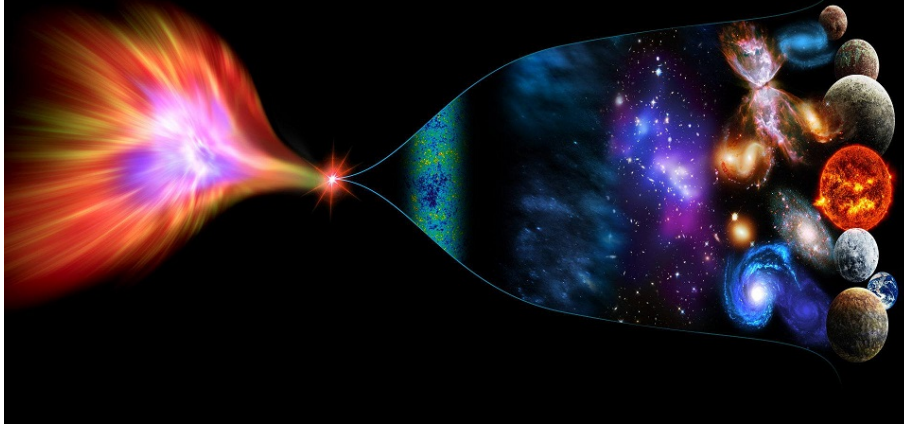
Friedmann equation in the literature. Note that (2.63) only differs from (1.8) by a quadratic term of the energy density $\frac{\rho^2}{\rho_c}$. However, this small difference results in strong implications regarding the primordial universe evolution in LQC framework. First, while in GR, \dot{a} can be only positive or negative, (2.63) also admits $\dot{a} = 0$. In this case, the Hubble parameter vanishes giving rise to a bounce in the universe evolution instead of diverging in a point (ASHTEKAR; SLOAN, 2011).

In this context, a will never assume a null value because (2.60) ensures a finite limit to ρ defined by ρ_c . Consequently, the initial singularity from classical cosmology just does not exist in LQC, being replaced by a bounce when ρ achieves the value of ρ_c (BOJOWALD; HOSSAIN, 2008). This feature may be the most successful aspect regarding effective LQC and it is a purely quantum gravitational effect of LQG since is directly related to the fact that Δ is not able to assume a null value. Otherwise, the universe will collapse in a singularity like in the classical case. Further, the bounce is a straight consequence of the discrete geometry of LQG regardless of the quantum fluctuations and happens apart from initial conditions or the value of the field momentum (ASHTEKAR et al., 2006b; LANGLOIS et al., 2017).

Working with the LQC effective dynamics corresponds to introducing quantum corrections to the classical equations of motion. Therefore, considering the effective EoM, the classical cosmological dynamics receives nonperturbative corrections due to its quantum gravitational nature, only significant in high energy regimes. Indeed, for energy ranges close to the Planck scale, gravity is expected to present a repulsive nature (MIELCZAREK et al., 2009). Likewise, the LQG/LQC scale of discreteness is close to the Planck one, making its effects only significant at high curvature regimes (BOJOWALD, 2005).

Above all, it is possible to notice how the relation between ρ and ρ_c dictates the evolutionary dynamics. As we just mentioned, their relation is limited by the sine function. In this sense, there are particular values associated with the different stages regarding the Effective LQC universe evolution. From (2.63), note that $\rho = \rho_c$ implies $H = 0$, defining the bounce point. Moreover, $H = 0$ comes from $\dot{a} = 0$ that indicates a turn in the universe motion, opening the possibility of a previous configuration of our universe like can be seen in Figure 2.5.

Figure 2.5 - Possible previous configuration of our universe



SOURCE: Bonoguore (2018).

Right after the bounce, the LQC universe is supposed to enter in a super-inflationary phase that covers the interval $\frac{1}{2} \lesssim \frac{\rho}{\rho_c} \lesssim 1$, during which $\dot{H} > 0$. Notwithstanding the drastic change associated with H , this period should last for an interval of time smaller than t_{Pl} . Otherwise, both a and φ would have varied more than expected according to cosmological observations (ASHTEKAR; SLOAN, 2011).

The Hubble parameter goes from its minimum value in bounce point to its maximum one at the end of super-inflationary phase which consists of the value

$$H^2 = \frac{\rho_c}{12M_{Pl}^2}, \quad (2.64)$$

since $\frac{\rho}{\rho_c} = \frac{1}{2}$. Although the holonomy corrections will play a main role during the bounce phase, they also need to be considered at inflationary epoch as small deviations (LUC; MIELCZAREK, 2017). Actually, Ashtekar and Sloan (2011) showed that the probability of LQC producing a slow-roll inflationary period is very close to one, besides, the bounce phase should be able to provide the suitable initial conditions for inflation to occur.

The inflationary period should take place after ρ reaches half of ρ_c ($\frac{\rho}{\rho_c} \approx \frac{1}{2}$) and ends up when ρ becomes negligible compared to it. Therefore, in Effective LQC, the onset of inflation starts immediately after H achieves (2.64). Moreover, since a correct quantum theory not only must admit a semiclassical regime at the smooth

geometric level but also may have GR as an approximation for low energy regimes (DONÁ; SPEZIALE, 2010), much smaller than ρ_{Pl} , at the end of inflation the quantum effects should be negligible, recovering the standard form

$$H^2 = \frac{\rho}{3M_{Pl}^2}. \quad (2.65)$$

Note that since the beginning, the changes of ρ compared to ρ_c are dictating the primordial universe dynamics. Further, ρ varies as the field evolves, being dominated by its kinetic and potential components in different stages of the early evolution. Consequently, the ratio between the kinetic and potential energy may play an essential role. Notwithstanding the absence of a consensus in the area, the most accepted description of the evolutionary stages with respect to the energy density (see equations (2.58), (2.63) and (2.61)) occurs as it follows:

- at the bounce, the universe is supposed to be dominated by the kinetic energy density;
- during the super-inflationary period, the kinetic energy must lose its strength until the potential term be capable to assume at the end;
- inflation should be driven by the potential energy as well as in the classical case;
- at the end of the inflationary period, the kinetic term is bigger than the potential one, but both components should contribute to ρ .

In order to complete the usual set of dynamic equations to describe the universe evolution, we compute the time derivative of equation (2.63), considering (1.15) and obtaining

$$\dot{H} = -4\pi G(\rho + P) \left(1 - \frac{2\rho}{\rho_c}\right). \quad (2.66)$$

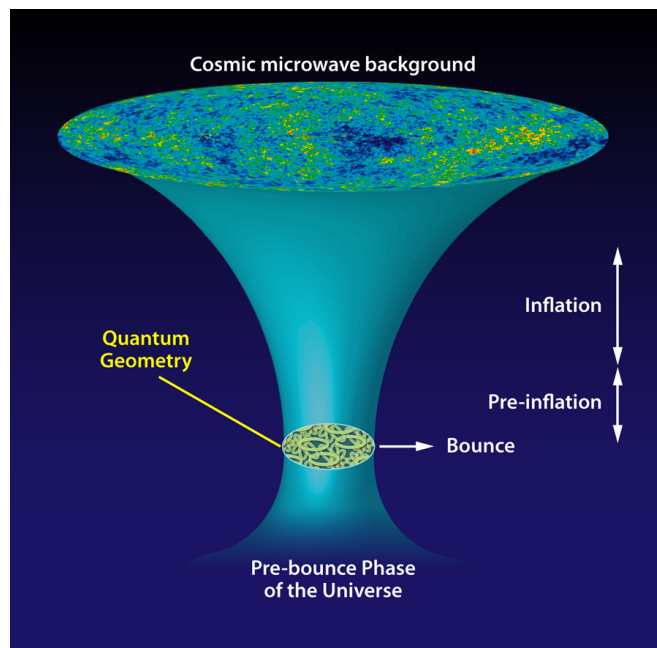
Now, we can write the acceleration equation by adding (2.63) to (2.66) which is going to result in the following expression

$$\dot{H} + H^2 = \frac{4\pi G}{3}\rho \left[-3w - 1 + \frac{2\rho}{\rho_c}(2 + 3w)\right]. \quad (2.67)$$

Thus, (2.63) and (2.67) corresponds to the LQC analogs of the Friedmann equations (1.8) and (1.16).

Figure 2.6 provides a simple picture to describe the evolutionary stages of the Effective LQC primordial universe. First, there would be a previous configuration of our current universe which must end collapsing in a bounce. This happened due to the gravitational effects that compressed the universe until ρ achieves ρ_c . Second, at bounce stage, the universe evolution is dominated by the quantum gravitational effects and represents the turning point in the scale factor evolution, $\dot{a} = 0 \rightarrow H = 0$. Next, the so-called pre-inflationary phase corresponds to the super-inflation period, being a brief overaccelerated stage ($\dot{H} + H^2 > 0$) between the minimum and maximum values of H . Moreover, it seems to be a common point along the different strategies implemented to describe LQC. After, inflation should start right away $\rho = \frac{1}{2}\rho_c$ with the potential in its higher value. The evolution follows the standard premise, which means H is almost constant and $\ddot{a} > 0$. Finally, the inflationary epoch ends with insignificant contribution coming from the quantum gravitational sector. However, their effects could be observed through possible signatures in the cosmic microwave background (vide chapter 5). In Table 2.3, we summarize all this information in a direct manner.

Figure 2.6 - Scheme evolution of the very early universe



SOURCE: Singh (2012).

Table 2.3 - Evolutionary stages of the primordial universe in Loop Quantum Cosmology

Bounce	$\rho = \rho_c$	$H = 0$	$\dot{H} + H^2 = 0$
Super-inflation	$\frac{1}{2} \lesssim \frac{\rho}{\rho_c} \lesssim 1$	$H > 0$	$\dot{H} + H^2 > 0$
Inflation	$\rho \lesssim \frac{1}{2}\rho_c$	$H \simeq \text{const.}$	$\dot{H} + H^2 > 0$
End of Inflation	$\rho \ll \rho_c$	$H > 0$	$\dot{H} + H^2 < 0$

Finally, we conclude this section by emphasizing that holonomy corrections allow the study of the discreteness of the spacetime at the effective level. These corrections are necessary due to the substitution of the Ashtekar connection by the holonomies. Besides, implementing them changes the structure of the classical constraints which becomes effective quantum constraints. Unfortunately, these new constraints do not generate a closed algebra, therefore, there is a mathematical inconsistency within the theory (MIELCZAREK, 2014). Notwithstanding, the LQC healthy properties are too powerful to be ignored, being explored in great number of works throughout the literature.

3 MIMETIC GRAVITY

Mimetic Gravity can be interpreted as a Weyl-symmetry extension of GR capable of providing a unified geometric description regarding the dark sector and inflationary period without extra matter components (SEBASTIANI *et al.*, 2017). Both DE and inflation were already introduced in chapter 1, thus, for completeness, let us briefly discuss the other dark element: dark matter. In order to satisfy the restrictions related to the current observational results, DM should be a non-relativistic fluid whose only source of interaction is via gravitational force (LIN, 2019). There are a variety of models trying to build a suitable candidate to describe the underlying particle physics aspect of DM (like WIMPs model) and also alternative models exploring different viewpoints of gravity itself to explain the effects associated to DM (for example, the MOND framework arose from a modification of Newtonian gravity, see (MILGROM, 1983)).

All things considered, MG is an appealing theory for cosmologists due to its versatility of reproducing different approaches through just adding a scalar degree of freedom. In this section, we will first present the original proposition. Next, we are going to provide a description of its extensions, highlighting the most relevant aspects. Finally, there is a detailed explanation about how MG was explored to be able to represent the Effective LQC dynamics.

3.1 Original proposal and developments

3.1.1 Mimetic dark matter

The mimetic dark matter model is a minimal extension of GR proposed by Chamseddine and Mukhanov (2013) whose original idea was to isolate the conformal degree of freedom of the gravitational field and turning it into a dynamical component capable of mimic the dark matter behavior. In principle, MG should satisfy the cosmological results as well as Λ CDM (ARROJA *et al.*, 2018). The terminology Mimetic Gravity is used indiscriminately to refer to any model built from this proposal. Nevertheless, it worth to mention that there had been previous works approaching scenarios with mimetic properties, see (LIM *et al.*, 2010; GAO *et al.*, 2011; CAPOZZIELLO *et al.*, 2010).

In order to build a modified theory from GR with different dynamic equations, the usual process requires extra fields in addition or substitution of the metric field, increasing the number of dimensions, considering higher derivatives of the metric tensor or breaking the Lorentz invariance. In principle, MG can be categorized as

a theory of modified gravity with an extra scalar degree of freedom. However, this description is not entirely precise since the later is constrained and does not correspond to a proper degree of freedom (SEBASTIANI et al., 2017). This will become clear later.

First, despite the absence of an explicit identification in the original paper, it is important to have in mind that MG was built having the disformal transformations proposed by Bekenstein (1993) as a base. This is a type of transformation that enables to establish a relationship between a physical and a gravitational metric, generalizing the conformal transformation definition. To put this another way, a disformal transformation is a parameterization of an ordinary metric in terms of a fiducial matrix and a scalar field, working as a kind of frame transformation (RABOCHAYA; ZERBINI, 2016; TAKAHASHI et al., 2017).

Following in this direction, constructing the MG formalism is a procedure that begins by performing a Weyl (or conformal) transformation of the metric. Nevertheless, a conformal transformation of a dynamical metric like the FRW one corresponds to a diffeomorphism (TONG, 2012). Thus, the invariance under a diffeomorphism transformation allows parameterizing the physical metric $g_{\mu\nu}$ as a function of an auxiliary metric $\tilde{g}_{\mu\nu}$ and a scalar field φ , later called mimetic field, through the relation

$$g_{\mu\nu} = -(\tilde{g}^{\alpha\beta} \partial_\alpha \varphi \partial_\beta \varphi) \tilde{g}_{\mu\nu}. \quad (3.1)$$

According to GR, the gravitational field has two polarization modes: transverse and longitudinal. Nevertheless, only the transverse has a dynamical role. In the MG framework, the gravitational field keeps its transverse degrees of freedom to describe the graviton, meanwhile, the longitudinal mode also referred to as conformal mode, will be the one used to mimic dark matter (CHAMSEDDINE; MUKHANOV, 2013; SEBASTIANI et al., 2017).

Throughout the MG literature, it is common to find three different names associated with the transformation used to write $g_{\mu\nu}$ like $g_{\mu\nu} = g_{\mu\nu}(\tilde{g}_{\mu\nu}, \varphi)$: disformal, conformal and Weyl transformations. We mentioned above that the conformal transformation corresponds to a particular case of a disformal one. As a conformally invariant theory, MG does not change under transformations performed with respect to an auxiliary metric, which means MG is a Weyl-invariant theory with respect to $\tilde{g}_{\mu\nu}$ (SEBASTIANI et al., 2017). Consequently, MG is a framework in which $g_{\mu\nu}(\tilde{g}_{\mu\nu}, \varphi)$ remains invariant

under any conformal transformation $\Omega^2(t, \mathbf{x})$ performed in $\tilde{g}_{\mu\nu}$, the same statement is also true for φ . In other words, in case of $\tilde{g}_{\mu\nu} \rightarrow \Omega^2(t, \mathbf{x})\tilde{g}_{\mu\nu}$, we have $g_{\mu\nu} \rightarrow g_{\mu\nu}$ and $\varphi \rightarrow \varphi$ (CHAMSEDDINE; MUKHANOV, 2013; LANGLOIS et al., 2017; SEBASTIANI et al., 2017), regardless the way the transformation is called.

Concerning the gravitational action, the mimetic one can be written in the generic structure like (LANGLOIS et al., 2017; CHAMSEDDINE; MUKHANOV, 2013)

$$S[\tilde{g}_{\mu\nu}, \varphi] = S_{EH}[g_{\mu\nu}(\tilde{g}_{\mu\nu}, \varphi)] \equiv \frac{1}{16\pi G} \int d^4x \sqrt{-g(\tilde{g}_{\mu\nu}, \varphi)} R[g_{\mu\nu}(\tilde{g}_{\mu\nu}, \varphi)], \quad (3.2)$$

where $S_{EH}[g_{\mu\nu}(\tilde{g}_{\mu\nu}, \varphi)]$ continues to represent the Einstein-Hilbert action. However, now, we must pay attention to the dependence with respect to $\tilde{g}_{\mu\nu}$ and φ . Furthermore, from (3.1) (and also from the relation between $g^{\mu\nu}$ and $\tilde{g}^{\mu\nu}$), a consistence condition arises in the form

$$g^{\mu\nu} \partial_\mu \varphi \partial_\nu \varphi = -1, \quad (3.3)$$

playing a fundamental role ensuring the equivalence of the EoM whether they are obtained through $g_{\mu\nu}$ or $\tilde{g}_{\mu\nu}$ (CHAMSEDDINE et al., 2014; FOFFANO, 2016).

Just like the procedure exposed in chapter 1, the MG Einstein equations can also be obtained from the variation of the action regarding $g_{\mu\nu}$. Thus, writing the full action as

$$S[\tilde{g}_{\mu\nu}, \varphi] = \int d^4x \sqrt{-g(\tilde{g}_{\mu\nu}, \varphi)} \left\{ \frac{M_{Pl}^2}{2} R[g_{\mu\nu}(\tilde{g}_{\mu\nu}, \varphi)] + \mathcal{L}_m \right\}, \quad (3.4)$$

with \mathcal{L}_m representing an arbitrary matter Lagrangian, and computing the variation of it with respect to $g_{\mu\nu}$, the result is going to be

$$\delta S = \frac{M_{Pl}^2}{2} \int d^4x \sqrt{-g} \left(G^{\mu\nu} - \frac{1}{M_{Pl}^2} T^{\mu\nu} \right) \delta g_{\mu\nu}. \quad (3.5)$$

However, this case requires a more delicate treatment though, since the variation of $g_{\mu\nu}$ would be computed from the variation of both $\tilde{g}_{\mu\nu}$ and φ through (3.1). As a result, the mimetic dark matter EFE are given by the expression

$$G_{\mu\nu} = \frac{1}{M_{Pl}^2} T_{\mu\nu} - \left(G - \frac{1}{M_{Pl}^2} T \right) \partial_\mu \varphi \partial_\nu \varphi, \quad (3.6)$$

here G and T represent the trace of Einstein and energy-momentum tensors, while we are using M_{Pl}^2 instead of $8\pi G$ in order to avoid any confusion between the Einstein tensor and the Newtonian constant along this section.

Note that there is an extra term containing φ explicitly working as an additional matter element (SEBASTIANI et al., 2017), so it will be identified as

$$\tilde{T}_{\mu\nu} = - \left(G - \frac{1}{M_{Pl}^2} T \right) (\partial_\mu \varphi \partial_\nu \varphi). \quad (3.7)$$

This means, (3.6) can be rewritten in the form

$$G_{\mu\nu} = \frac{1}{M_{Pl}^2} T_{\mu\nu} + \tilde{T}_{\mu\nu}. \quad (3.8)$$

Assuming the MG scalar field as a perfect fluid, we can compare (3.7) with (1.9) and distinguish the following relations for its energy density, pressure and 4-velocity

$$\tilde{\rho} \equiv - \left(G - \frac{1}{M_{Pl}^2} T \right), \quad \tilde{P} \equiv 0 \quad \text{and} \quad \tilde{u}^\mu \equiv g^{\mu\alpha} \partial_\alpha \varphi. \quad (3.9)$$

Consequently, in the mimetic dark matter framework, the scalar field corresponds to pressureless dust. At this point, we can recognise that the scalar field describes a collisionless system and only interacts gravitationally which are features associated with dark matter (GRIBEL, 2018). In conclusion, the mimetic nomenclature comes from the scalar mode ability to reproduce the dark matter behavior (GORJI et al., 2018).

The conformal invariance ensures that the EoM continues to be traceless as long as the conformal gauge is fixed like it happens in (3.3). This can be seen by computing the trace of MG Einstein equations (3.6) in which it is possible to identify that a traceless EFE requires

$$\left(G - \frac{1}{M_{Pl}^2} T \right) (1 + g^{\mu\nu} \partial_\mu \varphi \partial_\nu \varphi) = 0. \quad (3.10)$$

This condition is satisfied right away due to (3.3), even if $G \neq M_{Pl}^{-2} T$, giving rise to a

scalar mode regardless the presence of ordinary matter. Therefore, (3.3) defines the conformal gauge condition for an action like (3.2) whose mimetic behavior associated with φ comes from the local Weyl invariance (SEBASTIANI et al., 2017; GORJI et al., 2018; CAROLI, 2018).

In addition to the Einstein equations, there are also the equations of motion related to the mimetic field

$$\frac{1}{\sqrt{-g}}\partial_\alpha \left[\sqrt{-g} \left(G - \frac{1}{M_{Pl}^2} T \right) g^{\alpha\beta} \partial_\beta \varphi \right] = \nabla_\alpha \left[\left(G - \frac{1}{M_{Pl}^2} T \right) \partial^\alpha \varphi \right] = 0, \quad (3.11)$$

whose expression can be obtained not only from the variation of the action with respect to the field but also from $\tilde{T}_{\mu\nu}$ conservation law (CAROLI, 2018). Moreover, the scalar field is the quantity containing the description of the gravitational conformal mode (CHAMSEDDINE et al., 2014). The field alone is not a dynamical variable, the induced longitudinal mode is the one presenting the dynamical behavior (CHAMSEDDINE; MUKHANOV, 2017b). From (3.11), note that the term between brackets is constant regarding the covariant derivative. It corresponds to a geometric effect and does not define a propagation mode.

The reason why MG provides a complete different set of solutions compared to GR ones can be attributed to the Weyl transformations since the mapping $g \rightarrow \tilde{g}, \varphi$ relates a 10 degree of freedom theory with one other described by 11. Consequently, the parameterization $g_{\mu\nu} = g_{\mu\nu}(\tilde{g}_{\mu\nu}, \varphi)$ only goes in one direction, which means we are handling a noninvertible transformation (SEBASTIANI et al., 2017). In summary, MG can be interpreted as a singular limit from a disformal transformation that enables one to write $g_{\mu\nu}$ as a function of $\tilde{g}_{\mu\nu}$ and φ (CHAMSEDDINE; MUKHANOV, 2013; GORJI et al., 2018).

All things considered, (3.3) can be implemented directly in the action through a Lagrange multiplier. Indeed, Golovnev (2014) showed how to obtain a equivalent formulation to the one presented in (CHAMSEDDINE; MUKHANOV, 2013) using a Lagrange multiplier λ to incorporate the consistence condition (3.3) into the full action

$$S[g_{\mu\nu}, \varphi; \lambda] \equiv S_{EH}[g_{\mu\nu}] + \int d^4x \sqrt{-g} [\lambda (g^{\mu\nu} \partial_\mu \varphi \partial_\nu \varphi + 1) + \mathcal{L}_m], \quad (3.12)$$

without considering the presence of the auxiliary metric. Remember from the pre-

vious chapter that the variation of the Lagrangian regarding a Lagrange multiplier will result in a constraint, here this constraint is (3.3).

The singular disformal transformation and Lagrange multiplier formulations are the two main ways to explore the mimetic theory (RABOCHAYA; ZERBINI, 2016). Although, MG can also be studied from a viewpoint of a Brans-Dicke theory (SEBASTIANI et al., 2017). Throughout MG literature, the Lagrange multiplier formulation seems to be present in the majority of the works, which is probably due to its simpler notation. Moreover, it is easier to extend the Lagrange multiplier formalism in comparison to trying to do the same for the singular disformal transformation approach.

As we previously mentioned, despite the fact that Mimetic Gravity is classified as a theory of modified gravity with an extra scalar degree of freedom, this description is not totally accurate because the scalar degree is constrained by a Lagrange multiplier, a feature that differs from approaches with similar definitions (SEBASTIANI et al., 2017). From (3.12), note that the mimetic dark matter model corresponds to GR with a scalar field introduced via a constraint term. Nevertheless, MG provides richer opportunities to explore the cosmological dynamics by just implementing smooth modifications through the conformal sector (GOLOVNEV, 2014).

3.1.2 Mimetic gravity extension

Notwithstanding the initial aim to provide an alternative description to dark matter, the original proposal was extended to be able to produce solutions for inflation, dark energy, non-singular cosmologies, and even black holes. At first, Chamseddine et al. (2014) proposed a minimal extension of MG through the introduction of a potential term associated with the scalar field. Over time, MG was developed in many other directions. Now, it has also been presented as a particular case of higher-order scalar-tensor theories (LANGLOIS et al., 2017; LANGLOIS et al., 2019).

To put it another way, the extended version of the Mimetic Dark Matter can mimic nearly any cosmological background evolution provided that the potential term has a suitable form (CHAMSEDDINE et al., 2014; FOFFANO, 2016). Due to this large range of possible applications, MG has been generalized for many different scenarios. To give an illustration about the versatility of MG formulation we summarize the main extensions following (SEBASTIANI et al., 2017) as:

- **MG with a potential term:**

- MG Inflation;
- Bouncing cosmologies in MG;
- **Mimetic $F(R)$ Gravity** - modified gravity approach containing two extra degrees of freedom, one from mimetic field and another associated with $F(R)$:
 - Late-Time Evolution in Mimetic Gravity;
 - Mimetic $F(R, \varphi)$ Gravity \rightarrow the scalar field is coupled to gravity;
 - Nonlocal Mimetic $F(R)$ Gravity \rightarrow nonlocal approach constructed from two scalars fields and two Lagrange multipliers;
- **Unimodular MG** - geometric vacuum theory in which the relations $\sqrt{-g} = 1$ and (3.3) are considered as constraints:
 - Unimodular Mimetic $F(R)$ Gravity \rightarrow minimal extension of the unimodular MG in which R is replaced by its function $F(R)$;
- **Mimetic Horndeski Gravity** - general scalar-tensor theory with gravitational Lagrangian written in terms of metric and the mimetic field and it is invariant under invertible singular disformal transformations.

The list presented above is just a sample to emphasize the large range covered by MG in its current state of development. However, we are interested in the extension regarding the potential term only. Here, we intend to discuss the potential role in MG description regarding the universe evolution. In this subsection, we change the notation by assuming

$$g^{\mu\nu} \partial_\mu \varphi \partial_\nu \varphi = 1 \quad (3.13)$$

instead of using (3.3) in order to obtain simpler equations. In the next section, we will return to the original form (3.1). For now, we focus on the case in which a potential term is incorporated into a Lagrangian like it can be seen in the action

$$S = \int d^4x \sqrt{-g} \left[\frac{M_{Pl}^2}{2} R(g_{\mu\nu}) + \lambda (g^{\mu\nu} \partial_\mu \varphi \partial_\nu \varphi - 1) - V(\varphi) + \mathcal{L}_m \right]. \quad (3.14)$$

Accordingly, the EoM are computed in analogy with the procedure implemented in the previous subsection, but now considering the Lagrange multiplier formulation. Thus, the Einstein equations obey

$$G_{\mu\nu} - 2\lambda\partial_\mu\varphi\partial_\nu\varphi - \frac{1}{M_{Pl}^2}g_{\mu\nu}V(\varphi) = \frac{1}{M_{Pl}^2}T_{\mu\nu}, \quad (3.15)$$

meanwhile, the EoM for the mimetic field corresponds to the expression

$$\nabla_\alpha \left[\left(G - \frac{1}{M_{Pl}^2}T - \frac{4}{M_{Pl}^2}V(\varphi) \right) \partial^\alpha\varphi \right] = -\frac{\partial V(\varphi)}{\partial\varphi}. \quad (3.16)$$

since the trace of (3.15) allows us to write the Lagrange multiplier like

$$\lambda = \frac{1}{2} \left(G - \frac{1}{M_{Pl}^2}T - \frac{4}{M_{Pl}^2}V(\varphi) \right). \quad (3.17)$$

Again, if we compare the mimetic energy-momentum tensor, now written in the form

$$\tilde{T}_{\mu\nu} = 2\lambda\partial_\mu\varphi\partial_\nu\varphi + \frac{1}{M_{Pl}^2}g_{\mu\nu}V(\varphi), \quad (3.18)$$

with (1.9), it is possible to identify the contribution in terms of its energy density and pressure by the relations

$$\tilde{\rho} \equiv G - \frac{1}{M_{Pl}^2}T - \frac{3}{M_{Pl}^2}V(\varphi) \quad \text{and} \quad \tilde{P} \equiv -\frac{1}{M_{Pl}^2}V(\varphi). \quad (3.19)$$

Note from (3.19) that the potential term enables to reproduce the behavior of a negative pressure fluid, a requirement to obtain an accelerated evolution for the universe.

Introducing the scalar field potential does not increase the number of degree of freedom compared to the original mimetic scenario. Instead, the kinetic term keeps its dark matter behavior, while the non-vanishing potential works as a cosmological constant. This means there are two components contributing to the extra energy-momentum tensor, in principle, they can represent both elements expected from the dark sector (FOFFANO, 2016).

In other words, the extra scalar degree of freedom enables to simulate a dark matter behavior, at the same time, an additional potential term is capable of reproducing a Lagrangian similar to the one associated with the cosmological constant (FOFFANO, 2016). Since the potential can have a cosmological constant behavior, it was the

one used to build inflationary models in MG description. Indeed, the MG inflation with potential term can end generating radiation and baryons through gravitational particle production or coupling the mimetic field with other fields (BERTAZZO, 2015).

In summary, MG corresponds to an economic framework to reproduce promising cosmological models associated with the early and later stages of the universe evolution (DUTTA et al., 2018). Note that in mimetic dark matter scenario there is not a matter fluid to describe the usual behavior associated with a dark-matter-type fluid, instead, gravity is modified to emulate the dark matter properties. The additional potential term enables to do the same for the dark energy. Therefore, MG transfers to geometric sector the power to dictate the universe evolution.

In (CHAMSEDDINE; MUKHANOV, 2017b), the authors did not consider the potential term once its general solution would not avoid space-like singularities as the ones found in black holes. They rather opted to introduce a function $f(\square\varphi)$ in a Born-Infeld action, where \square represents the D'Alembertian, as it follows

$$S = \int d^4x \sqrt{-g} \left[\frac{M_{Pl}^2}{2} R(g_{\mu\nu}) + \lambda(g^{\mu\nu} \partial_\mu \varphi \partial_\nu \varphi - 1) + f(\square\varphi) + \mathcal{L}_m \right]. \quad (3.20)$$

Within this setup, they are able to obtain a similar equation to (2.63). Moreover, they introduced the limiting curvature concept that, as its name suggests, means there is a boundary related to the value of the space-time curvature. They also associated corrections due to the presence of this extra term which would be significant near the singularity. Note that this description has familiar concepts to the ones presented in chapter 2.

For a specific configuration, MG is capable of solving the cosmological singularities associated with the Big Bang and black holes. Moreover, its bouncing solution seems to be similar to the ones obtained in LQC scenario, which is a promising achievement due to the covariant character of MG in contrast with the semiclassical LQC approach. Therefore, from MG perspective, LQC action could be described by a higher order expression (CHAMSEDDINE; MUKHANOV, 2017a; CHAMSEDDINE; MUKHANOV, 2017b; LANGLOIS et al., 2017; BODENDORFER et al., 2018; GORJI et al., 2018).

3.2 Mimetic Gravity description of Loop Quantum Cosmology

Among the many extensions of MG, our fundamental focus is the one proposed by Langlois et al. (2017) in which the authors discussed how the mimetic gravity

Lagrangian gave rise to identical equations of motion like the ones obtained in the LQC scenario. On the other hand, it is important to have in mind that there are other works relating MG with LQC, see (HARO et al., 2018c; HARO et al., 2018b; HARO; AMORÓS, 2018; ACHOUR et al., 2018; GORJI et al., 2018). Our choice for this particular formulation is the treatment employed to study curved space-time backgrounds.

Langlois et al. (2017) presented mimetic theories as a special family of Degenerate Higher-Order Scalar-Tensor (DHOST) theories. In fact, they showed that MG formulated in terms of second derivatives of the scalar field in quartic order or higher can be interpreted as a subclass of DHOST theories that contains an extra symmetry. On the other hand, this constraint is an additional restriction in the gravitational Hamiltonian beyond the Hamiltonian and diffeomorphism constraints (LANGLOIS et al., 2019). Moreover, the authors present the conditions under which the effective dynamics of LQC can be recovered from mimetic action.

In order to obtain a class of theories capable of producing the LQC effective Friedmann equation for a spatially flat FRW space-time, Langlois et al. (2017) started by building an action invariant under time reparametrization that has a , N and φ as its dynamical variables. Within this framework, the modified gravity actions must reduce to the following form

$$S[a, N, \varphi] = \int dt \left[-\frac{3a\dot{a}^2}{8\pi GN} + a^3 \frac{\dot{\varphi}^2}{2N} + Na^3 \mathcal{L}\left(a, \frac{\dot{a}}{N}\right) \right]. \quad (3.21)$$

Here, the function $\mathcal{L}\left(a, \frac{\dot{a}}{N}\right)$ will be developed in order to recover (2.63) from (3.21).

First of all, $\mathcal{L}\left(a, \frac{\dot{a}}{N}\right)$ is defined as a function of the Hubble parameter

$$\mathcal{L}\left(a, \frac{\dot{a}}{N}\right) = \mathcal{F}(H), \quad (3.22)$$

due to the shape of the effective Hamiltonian constraint straightly dependent of c/\sqrt{p} (LANGLOIS et al., 2017). The second step is to ensure that N remains a Lagrange multiplier, living a and φ as dynamical variables. Therefore, the non-trivial canonical pairs are

$$\{a, \pi_a\} = \{\varphi, \pi_\varphi\} = 1, \quad (3.23)$$

with π_a and π_φ representing the conjugated momenta of the scale factor and scalar

field, respectively, given by

$$\pi_a = a^2 \left[-\frac{3H}{4\pi G} + a^2 \mathcal{F}'(H) \right] \quad (3.24)$$

and

$$\pi_\varphi = \frac{a^3}{N} \dot{\varphi}. \quad (3.25)$$

At this point an ansatz is established, enabling to write π_a like

$$\pi_a = \alpha a^n \arcsin \left(\beta \frac{\dot{a}}{Na} \right) \quad (3.26)$$

where n , α and β are defined as constants that must obey the relations $n = 2$ and $\alpha\beta = -3/4\pi G$ in order to recover the classical value $\pi_a = -3a\dot{a}/4\pi GN$ (LANGLOIS et al., 2017). Consequently, we can express (3.26) in the form

$$\pi_a = \alpha a^2 \arcsin \left(-\frac{3H}{4\pi G\alpha} \right). \quad (3.27)$$

From (3.26), the function $\mathcal{F}(H)$ acquires the shape

$$\mathcal{F}(H) = \alpha H \arcsin(\beta H) + \frac{\alpha}{\beta} \sqrt{1 - \beta^2 H^2} + \frac{3H^2}{8\pi G} - \frac{\alpha}{\beta}, \quad (3.28)$$

which results in the Hamiltonian density

$$\mathcal{H} = a^3 \left[\frac{\pi_\varphi^2}{2a^6} - \frac{8\pi G}{3} \alpha^2 \sin^2 \left(\frac{\pi_a}{2\alpha a^2} \right) \right]. \quad (3.29)$$

Then, since now the Hamiltonian is available, we repeat the LQC procedure to obtain the MG version of LQC effective Friedmann equation. However, instead of computing the equation of motion for p , the scale factor is directly used. With this in mind, the result is

$$H^2 = \frac{8\pi G}{3} \rho \left(1 - \frac{\rho}{\rho_c} \right), \quad (3.30)$$

with

$$\rho = \frac{\pi\varphi^2}{2a^6} \quad (3.31)$$

and

$$\rho_c = \frac{8\pi G}{3}\alpha^2. \quad (3.32)$$

Thus, (2.63) and (3.30) will describe the same physics only if the relation

$$\alpha = \frac{3}{8\pi G\gamma\sqrt{\Delta}} \quad (3.33)$$

is true during the entire primordial universe evolution, or at least during the range in which the quantum gravitational effects are not negligible. The equation (3.30) represents the Hamiltonian version of the result attained by [Chamseddine and Mukhanov \(2017b\)](#).

All things considered, the modified gravity theories whose dynamics are expressed by an action like

$$S[a, N, \varphi] = \int dt Na^3 \left(\frac{\dot{\varphi}^2}{2N^2} - \frac{\rho_c}{2} \left[\beta H \arcsin(\beta H) + \sqrt{1 - \beta^2 H^2} - 1 \right] \right), \quad (3.34)$$

where $\beta^2 = \frac{3}{2\pi G\rho_c}$, should be able to reproduce LQC effective dynamics for a flat FRW space-time. The problem relies on the fact that any modified approach is capable of producing exactly the form (3.34) in the cosmological sector, due to the non-linearity of the Lagrangian regarding H ([LANGLOIS et al., 2017](#)).

We repeat the previous process to make it easy to follow its generalization for spatially curved space-times whose particular treatment is our fundamental start point. Initially, the process is the same applied to GR, with an extra term related to the spatial curvature parameter k added to the action,

$$S_k[a, N, \varphi] = \int dt \left[-\frac{3a\dot{a}^2}{8\pi GN} + a^3 \frac{\dot{\varphi}^2}{N} + \frac{3Nka}{8\pi G} + Na^3 \mathcal{L}_k \left(a, \frac{\dot{a}}{N} \right) \right]. \quad (3.35)$$

Notwithstanding, in MG description of LQC, a new term is introduced in the gravitational Hamiltonian through

$$\mathcal{L}_k\left(a, \frac{\dot{a}}{N}\right) = \mathcal{F}(H) - \frac{3}{8\pi G}V_k(a), \quad (3.36)$$

where $V_k(a)$ is a potential-like term independent from any scale factor derivatives. Hence, the curvature is directly implemented in the action and also throughout the function \mathcal{L}_k which enables to obtain the Hamiltonian density as

$$\mathcal{H} = a^3 \left[\rho - \rho_c \sin^2\left(\frac{\pi a}{2\alpha a^2}\right) - \frac{3k}{8\pi G a^2} + \frac{3V_k(a)}{8\pi G} \right]. \quad (3.37)$$

Again, repeating the process of defining $\mathcal{H} \approx 0$, we have the sine function restricting the evolution through the expression

$$\sin^2\left(\frac{\pi a}{2\alpha a^2}\right) = \frac{1}{\rho_c} \left[\rho - \frac{3k}{8\pi G a^2} + \frac{3V_k(a)}{8\pi G} \right], \quad (3.38)$$

and the modified Friedmann equation for curved space-times of [Langlois et al. \(2017\)](#) is obtained in the form

$$H^2 = \left[\frac{8\pi G}{3}\rho - \frac{k}{a^2} + V_k(a) \right] \left\{ 1 - \frac{1}{\rho_c} \left[\rho - \frac{3k}{8\pi G a^2} + \frac{3V_k(a)}{8\pi G} \right] \right\}. \quad (3.39)$$

The potential-type term $V_k(a)$ comes from considering a spatially curved FRW space-time and could be obtained as an extra new term

$$- \int d^4x \sqrt{|g|} \mathcal{V}(g_{\mu\nu}, \phi) \quad (3.40)$$

added to the action for scalar-tensor theories. Despite the fact that $\mathcal{V}(g_{\mu\nu}, \phi)$ does not represent a unique solution, there are specific features it must contain. On a curved FRW space-time, the components of the 3-dimensional Riemann tensor are functions of the scale factor only ([LANGLOIS et al., 2017](#)). In particular, the 3-dimensional Ricci scalar is ${}^{(3)}R = 6k/a^2$ which would allow $V_k(a)$ to be expanded as

$$V_k(a) = \sum_{n>0} v_n \left(\frac{6k}{a^2}\right)^n \equiv \tilde{V}({}^{(3)}R). \quad (3.41)$$

Thus, a possible choice for \mathcal{V} could be

$$\mathcal{V}(g_{\mu\nu}, \varphi) = \tilde{V}({}^3R). \quad (3.42)$$

From (3.42), it can be noticed that the MG representation of LQC dynamics enables the spatial curvature R to be described in terms of a scalar field.

Notwithstanding all the advantages that come with mimetic theories, the ghost instability is still open for discussion. There are many works arguing about the stability/instability of mimetic theories, for example, (FIROUZJAH *et al.*, 2017; YOSHIDA *et al.*, 2017; ZHENG *et al.*, 2017). Until now, there is not a consensus in the community. Furthermore, there is also the limitation imposed by the high symmetry associated with FRW space-times, restricting the coverage area in which MG is applicable.

All things considered, Mimetic Gravity is a powerful tool to reproduce a plethora of cosmological evolutionary scenarios. In the next chapter, we will show that the same prerogative also works for the mimetic description of LQC, emphasizing the versatility of the curvature mimetic potential V_k in reproducing any desired inflationary potential. Furthermore, we also intend to highlight the intermediate character of MG as the remaining factor to link a cosmological quantum theory with another based on the SMPP model.

4 APPLICATION OF THE MIMETIC DESCRIPTION OF LOOP QUANTUM COSMOLOGY TO HIGGS INFLATION AND FURTHER DEVELOPMENTS

This chapter is dedicated to expose and reproduce a detailed explanation about how we obtained the results presented in (BEZERRA; MIRANDA, 2019) and what are the physical implications related to it. First, we reinterpret (3.39) according to the different evolutionary stages during early times. Next, we briefly review the Higgs Inflation model, only approaching the necessary features to understand our work. After we follow by matching the two previous approaches and showing their similar behavior. Then, we present two interpretations of the total energy density that incorporate curvature components followed by our analyzes regarding the validity of the conservation law for the energy density in our formulation. Finally, we end discussing the hints that can come with a super-inflationary phase within our formulation.

4.1 Curvature Potential from Mimetic Gravity: a new interpretation

From (3.39), note that there is no potential term related to the matter field φ . Consequently, $V_k(a)$ is the only kind of energy potential in the mimetic description of LQC. In (LANGLOIS et al., 2017), they neglected the potential $V(\varphi)$ for simplicity once its absence makes easy to implement the quantization process. Here, we propose a different perspective. Paying attention to the curved case, see that a potential term received a null value, meanwhile, one arose described in terms of the curvature. It seems like the role played by $V(\varphi)$ in matter sector was attributed to $V_k(a)$ in the gravitational part.

Following this direction, we reinterpret $V_k(a)$ as the potential term describing the space-time response to the presence of matter. To clarify this, let us consider the case of a non-minimally coupling between a fundamental scalar field and the metric field. Note from the previous paragraph that the potential term seems to contain information about both sectors. Thus, we introduce the quantity $V_k(\varphi)$ to represent the mimetic curvature potential associated with the space-time deformation due to φ . Or, $V_k(\varphi)$ can also be interpreted as a result of the field response to the space-time curvature. Both ways are equivalent. All things considered, $V_k(\varphi)$ corresponds to a signature of the matter-curvature fundamental coupling during the primordial universe period.

Within this framework, we rewrote (3.39) as the expression

$$H^2 = \frac{1}{3M_{Pl}^2} \left[\rho_{\text{kin}} + 3M_{Pl}^2 \left(V_k(\varphi) - \frac{k}{a^2} \right) \right] \left\{ 1 - \frac{1}{\rho_c} \left[\rho_{\text{kin}} + 3M_{Pl}^2 \left(V_k(\varphi) - \frac{k}{a^2} \right) \right] \right\}, \quad (4.1)$$

where ρ_{kin} contains the information about the kinetic energy associated with the scalar field,

$$\rho_{\text{kin}} = \frac{\pi_{\varphi}^2}{2a^6}. \quad (4.2)$$

Therefore, the formalism is built with the kinetic and potential contribution in different sectors since the potential term is considered from the curvature perspective. Nonetheless, comparing (2.60) and (3.38), note that the terms between brackets are working as total energy density. We named this quantity as effective energy density ρ_{eff} whose form is given by

$$\rho_{\text{eff}} = \rho_{\text{kin}} + 3M_{Pl}^2 \left[V_k(\varphi) - \frac{k}{a^2} \right]. \quad (4.3)$$

Thus, from (2.60), see that ρ_{eff} is the quantity regulated by the sine function,

$$\sin^2 \left(\frac{\pi_a}{2\alpha a^2} \right) = \frac{\rho_{\text{eff}}}{\rho_c}, \quad (4.4)$$

and now restricted to the range $0 \lesssim \rho_{\text{eff}}/\rho_c \leq 1$. Note that (4.4) is directly related to the validity of the ansatz (3.26).

In spite of the well-known relation between matter and curvature, they are usually studied individually. Here, we consider them as an intrinsically related pair. From (4.3), notice that ρ_{eff} is composed by a kinetic term, plus the curvature potential associated with the mimetic field and the classical parameter describing the general space-time curvature. During early times, these components should evolve and balance each other in order to give rise to the necessary evolutionary stages expected from recent results obtained by cosmological observations.

The idea is to transfer the duty to be the one providing the information about how the space-time reacts to the matter presence from the matter sector to the geometric one. This will enable us to explore fields without knowing their potential form or even treat massive fields as massless from the matter Hamiltonian perspective. This

is possible since the effective mass associated with the field would be an effect of the coupling.

We proceed by substituting (4.3) in (3.39), recovering the original form of the LQC Effective Friedmann equation given by (2.63) through the expression

$$H^2 = \frac{\rho_{\text{eff}}}{3M_{Pl}^2} \left(1 - \frac{\rho_{\text{eff}}}{\rho_c} \right). \quad (4.5)$$

Consequently, any aspect related to the shape of Effective Friedmann equation also applies to (4.5). Remember from chapter 2 that the bounce may be dominated by the field kinetic energy, thus, the potential energy is negligible compared to the kinetic one or it is defined as zero like commonly found in LQC literature. From (4.3), this implies in $\rho_{\text{eff}} = \rho_{\text{kin}}$ or $\rho_{\text{eff}} \approx \rho_{\text{kin}}$. Therefore, (4.5) acquires the form

$$H^2 = \frac{\rho_{\text{kin}}}{3M_{Pl}^2} \left(1 - \frac{\rho_{\text{kin}}}{\rho_c} \right). \quad (4.6)$$

Focusing again in the definition (4.3), note that (4.6) can be obtained through assuming $V_k(\varphi) = k = 0$ or just having the relation $V_k(\varphi) = ka^{-2}$ as true. For a curved space-time, it does not make sense to consider $k = 0$ when the curvature should be an essential element during a period in which the universe is supposed to be extremely tiny. On the other hand, the equality $V_k(\varphi) = ka^{-2}$ suggests there was an equilibrium between the two curvature sources, which would be compatible with the bounce point concept as the instant in which the universe motion stopped.

The LQC bounce phase is followed by a super-inflationary stage after which the universe should be in the right state for inflation to begin. First of all, we have to make clear that the super-inflationary phase was not approached in (BEZERRA; MIRANDA, 2019). We can not affirm if this period happens or not in our formulation since it would require a deeper study. Thus, our focus is indeed the inflationary period within MG description of LQC scenario.

Following LQC energy evolutionary range, inflation may start for $\rho_{\text{eff}} \approx \frac{1}{2}\rho_c$. So, somehow, the universe must have lost half of its energy density. The other half should be contained into $3M_{Pl}^2(V_k(\varphi) - ka^{-2})$ and must be enough to drive the universe along with inflation. To begin with, we follow the standard inflationary paradigm by neglecting the kinetic term, living the Effective Friedmann equation written like

$$H^2 = \left[V_k(\varphi) - \frac{k}{a^2} \right] \left\{ 1 - \frac{3M_{Pl}^2}{\rho_c} \left[V_k(\varphi) - \frac{k}{a^2} \right] \right\}. \quad (4.7)$$

We kept the term ka^{-2} in (4.7) since the universe curvature should have strongly influenced the dynamics during inflation. Actually, for now, we leave explicit the pair $V_k(\varphi)$ and ka^{-2} to emphasize our interpretation about the balanced relationship between them. Even without considering a specific form for $V_k(\varphi)$, it is possible to notice how the term ka^{-2} is becoming weaker as the universe evolves. In other words, the growth of the scale factor is mitigating the curvature contribution until it virtually disappears. Likewise, $V_k(\varphi)$ must also lose its strength, however, it should continue to contribute as a less dominant component.

As the universe evolves, $V_k(\varphi)$ should be reduced enough to be comparable with ρ_{kin} , ending the inflationary period. At this stage, the quantum corrections may be insignificant with $\rho_{\text{eff}} \ll \rho_c$. Consequently, (4.5) reduces to the standard structure

$$H^2 \approx \frac{1}{3M_{Pl}^2} [\rho_{\text{kin}} + 3M_{Pl}^2 V_k(\varphi)]. \quad (4.8)$$

With this, we fulfill the LQC requirement by enabling the universe to follow the classical evolution after inflation. Moreover, we close the description of the mimetic curvature potential $3M_{Pl}^2(V_k(\varphi) - ka^{-2})$ evolution, starting with (4.7) and finishing with (4.8), running through the entire range $0 < \rho_{\text{eff}}/\rho_c < \frac{1}{2}$.

Just like it happens with the usual treatment of MG theories, in principle, our formalism could also be used to mimic any inflationary scalar field evolution. We opted to study how our model behaves in comparison with a scalar field coupled with gravity. This model is called Higgs Inflation and it is the content discussed in the following section.

4.2 Higgs Inflation

Majority of the current available inflationary models are built considering an extra field outside the SMPP as the energy source. In general, its origin is model dependent. To give an illustration, grand unified theories, supersymmetry, string theory, extra dimensions and extensions of SMPP are all listed as possible ways to give rise to the inflationary scalar field (BEZRUKOV; SHAPOSHNIKOV, 2008).

Recently, it was announced the observation of a process named ttH production in

which a Higgs boson is presented as a consequence of Higgs-top coupling (CERN, 2018). This result was obtained and reported independently by two experiments at CERN: CMS and ATLAS, see references (SIRUNYAN et al., 2018) and (ATLAS COLLABORATION, 2018) for more details. Reinforcing the conclusion about the Higgs field predicted by SMPP being the boson detected in 2012 according to Aad et al. (2012) and Chatrchyan et al. (2012).

The discovery of a particle with a mass consistent with the Higgs boson offers a self-consistent description of the universe at the effective level. This particle belongs to the standard theoretical framework that unifies the electromagnetic and weak interactions, named Electroweak (EW). Under the assumption of the validity of SMPP until Planck scale, the Higgs field could have played a significant role during the early evolutionary history of the universe (SHAPOSHNIKOV, 2015; SALTAS, 2016). Indeed, in (BEZRUKOV et al., 2012), the value of the Higgs mass $m_h \simeq 126\text{GeV}$ is pointed as an indication of the influence of the Planck physics into the EW scale, suggesting that they are related in some level. As the first and only scalar field observed until now, the Higgs field as a fundamental particle is the natural and most suitable candidate to dictate inflation.

Since the first inflationary models were proposed, many attempts have been done to implement the Higgs field as an energy source for inflation. The challenge is matching the huge difference between the energy scale of the current observed Higgs field and the inflationary field. Unfortunately, most models were unstable, plagued with ghosts, or presented other serious problems, see (KOLB; TURNER, 1990) for further information. However, Bezrukov and Shaposhnikov (2008) showed that it was possible to have the SMPP Higgs boson as the field driving inflation by building a model compatible with the observational results at cost of adding a coupling between the Higgs field and gravity.

Indeed, the inflationary model characterized by a single scalar field with a slow-roll type of evolution is the simplest one, besides being considered the standard approach to describe the early times. Notwithstanding, models with non-minimal coupling between gravity and matter field are favored according to the combined observations of Planck and BICEP II data (LUC; MIELCZAREK, 2017).

Higgs inflation is a chaotic description of the inflationary period that reproduces the successful flat potential of the slow-roll approach by changing the interaction between gravity and matter (BEZRUKOV, 2013). It explains the accelerated expansion of the primordial universe by incorporating SMPP into the cosmological context

(BEZRUKOV et al., 2011). Moreover, as a chaotic inflationary model, HI does not require the universe to be in thermal equilibrium in order to give rise to inflation (LINDE, 2007).

However, there are a few requirements to be satisfied. First all, we must have in mind that the Higgs field from HI inflation corresponds to an older configuration of the current one. This enables to get over the energy compatibility issue since the primordial Higgs field h must obey the relation $h \gg M_{Pl}/\xi$, where the non-minimally coupling parameter ξ satisfies $\xi \gg 1$. Hence, h would carry a much greater amount of energy, working as a suitable energy source for inflation. In order to accomplish this goal, the values of the self-coupling parameter λ and its relation with ξ are only determined via cosmological observation results (BEZRUKOV, 2013).

Within this framework, the physics from SMPP is mixed with gravity through the term $\xi h^2 R$ (MOSS, 2014) which means the total action (A.1) acquires the form

$$S_J = \int d^4x \sqrt{-g} \left[-\frac{1}{2}(M_{Pl}^2 + \xi h^2)R + g_{\mu\nu} \frac{\partial^\mu h \partial^\nu h}{2} - V(h) \right]. \quad (4.9)$$

with $V(h)$ being the Higgs field potential constructed like

$$V(h) = \frac{\lambda}{4}(h^2 - v^2)^2 \approx \frac{\lambda}{4}h^4. \quad (4.10)$$

Here, the index J is used to refer to the Jordan frame from SCM and v is the vacuum expectation value of h . Furthermore, ξ is restricted to range $1 \ll \xi \ll M_{Pl}^2/v^2$ where the value v is too small compared to h (BEZRUKOV et al., 2018).

The obvious advantage of HI is to avoid additional degrees of freedom beyond SMPP in order to explain the primordial universe evolution (BEZRUKOV et al., 2018). Nonetheless, (4.9) implies on embroiled equations of motion whose physical interpretation is hard to perform comparing to slow-roll approximation (POSTMA; VOLPONI, 2014). The disadvantages related to non-minimal coupling are removed by changing the cosmological frame to the Einstein one via a conformal transformation Ω^2 ,

$$\Omega^2(h) = \frac{M^2 + \xi h^2}{M_{Pl}^2} \approx 1 + \frac{\xi h^2}{M_{Pl}^2}. \quad (4.11)$$

See that M was identified as M_{Pl} , this happened because the definition of M obeys the relation $M^2 = M_{Pl}^2 - \xi v^2$. Even with the large value attributed to ξ , the term ξv is much smaller than M_{Pl} during the entire Higgs inflationary period, enabling us to

consider $M \simeq M_{Pl}$. It is worth to mention that [Postma and Volponi \(2014\)](#) showed the physical equivalence between two frames related by a conformal transformation, focusing on the Jordan and Einstein frames.

The transformation (4.11) allows us to move the dynamical analysis to the Einstein frame whose metric $\tilde{g}_{\mu\nu}$ is given by

$$\tilde{g}_{\mu\nu} = \Omega^2(h)g_{\mu\nu}. \quad (4.12)$$

Remember that, as the standard frame, all the usual quantities related to the metric $g_{\mu\nu}$ we have been working until now belongs to the Jordan frame. Furthermore, this transformation does not change the physics because it consists only in a field redefinition due to the rescheduling of the length scales ([POSTMA; VOLPONI, 2014](#)).

Therefore, rather than working with the action in Jordan frame (4.9), we are going to obtain the dynamics through

$$S_E = \int d^4x \sqrt{-\tilde{g}} \left[-\frac{M_{Pl}^2}{2} \tilde{R} + \left(\frac{\Omega^2 + 6\xi h^2/M_{Pl}^2}{\Omega^4} \right) \tilde{g}_{\mu\nu} \frac{\partial^\mu h \partial^\nu h}{2} - \frac{V(h)}{\Omega^4} \right], \quad (4.13)$$

where E represents the Einstein frame. See that h is invariant under (4.12). However, instead of working with the complicated form of (4.13), the procedure implemented is to normalize the field through the redefinition

$$\frac{d\chi}{dh} = \sqrt{\frac{\Omega^2 + \frac{3}{2}M_{Pl}^2(\Omega^2)'}{\Omega^4}} = \sqrt{\frac{1 + (\xi + 6\xi^2)h^2/M_{Pl}^2}{(1 + \xi h^2/M_{Pl}^2)^2}}, \quad (4.14)$$

in which the prime corresponds to the derivative regarding h . Thus, both h and χ correspond to the primordial version of the Higgs field, one in Jordan's frame while the other is defined in the Einstein one.

Changing the frame is just a strategy to obtain a similar action to (A.1) and does not change the field. Note that writing (4.13) in terms of χ , the action reduces to the form

$$S_E = \int d^4x \sqrt{-\tilde{g}} \left[-\frac{M_{Pl}^2}{2} \tilde{R} + \tilde{g}_{\mu\nu} \frac{\partial^\mu \chi \partial^\nu \chi}{2} - V(\chi) \right]. \quad (4.15)$$

Nevertheless, the scalar field is not the inflaton and the potential associated with

the field χ is given by

$$V(\chi) = \frac{V(h)}{\Omega^4} = \frac{\lambda h^4(\chi)}{4\Omega^4[h(\chi)]}. \quad (4.16)$$

In (4.16), the potential is determined in terms of h , but, thanks to (4.14), it can be rewritten like

$$V(\chi) = V_0 \left(1 - e^{-\sqrt{\frac{2}{3}} \frac{\chi}{M_{Pl}}} \right)^2, \quad (4.17)$$

with

$$V_0 = \frac{\lambda M_{Pl}^4}{4\xi^2}. \quad (4.18)$$

Note that (4.17) corresponds to a Starobinsky-type potential, see (KEHAGIAS et al., 2014) for more details. Moreover, for sufficiently high values of χ , (4.17) implies in $V(\chi) \approx V_0$ which is approximately constant. This is the case of HI because, for large ξ , the potential derivative regarding χ is small as well as it happens in the standard slow-roll approximation (MOSS, 2014). Therefore, translating the Lagrangian of the system from a frame to another enables the recovering a canonical-type evolution (POSTMA; VOLPONI, 2014).

Following (BEZRUKOV, 2013), the inflation begins for $h \gg M_{Pl}/\sqrt{\xi}$ and ends at $h_{\text{end}} \simeq 1,07M_{Pl}/\sqrt{\xi}$ that corresponds to

$$\chi \simeq \sqrt{\frac{3}{2}} M_{Pl} \ln \Omega^2(h) \chi \gg M_{Pl}/\sqrt{\xi} \quad (4.19)$$

and

$$\chi_{\text{end}} \simeq 0,94M_{Pl}, \quad (4.20)$$

respectively. Once the evolution must happen analogously to standard slow-roll inflation in the Einstein frame, the Friedmann equation is expressed as

$$H^2 = \frac{1}{3M_{Pl}^2} \frac{V(h)}{(1 + \xi h^2/M_{Pl}^2)^2} = \frac{1}{3M_{Pl}^2} V(\chi) \simeq \frac{\lambda M_{Pl}^2}{12\xi^2}. \quad (4.21)$$

where it was assumed $\chi \gg \sqrt{\frac{3}{2}}M_{Pl}$. Moreover, the slow-roll parameters ¹ computed from (4.17),

$$\epsilon = \frac{4M_P^4}{3\xi^2 h^4} \quad \text{and} \quad \eta_{SR} \simeq \frac{4M_P^4}{3\xi^2 h^4} \left(1 - \frac{\xi h^2}{M_P^2}\right), \quad (4.22)$$

are in agreement with what is expected from current observations (BEZRUKOV, 2013).

To finish this section, it worth to mention that HI results are in agreement with CMB current observations performed by WMAP and Planck satellites (BEZRUKOV; SHAPOSHNIKOV, 2014; RUBIO, 2015; BEZRUKOV et al., 2018). Moreover, for a value $\xi \sim 10^3$, the HI should lead the universe to the standard model vacuum according to Rubio (2015). Hence, this approach could be the first step towards constructing a unified model with cosmology and particle physics working together.

4.3 Application of MG representation of LQC to Higgs Inflation

Before we start to discuss how we will apply the formalism presented in 4.1 to Higgs inflation, let us first reinforce the statement that our formulation should work, in principle, for any inflationary field. To give an illustration, we could have used the inflaton instead of the Higgs field. However, the mimetic description of the Effective LQC may provide more interesting results if the inflationary field is directly related to gravity.

Note that, by definition, the Higgs field is intricate within the space-time which is reflected in HI construction. Moreover, from the formulations presented in 3.2 and 4.2, it is possible to notice crucial similarities. As we mentioned earlier, the mimetic dark matter is built under the concept of a conformal transformation, a statement that also applies to HI. Both MG and HI have the relationship between matter and gravity as the main part of their description. In MG case, this comes from the extra scalar degree of freedom used to define the longitudinal mode. For HI, it is directly observed in the coupling. Indeed, due to the great number of familiar features, we assume the MG representation of Effective LQC from 3.2 as an Einstein frame description of Effective LQC dynamics.

In this section, we will consider that these two approaches match properly, describing the same physics. Since HI is restricted to the inflationary period, we compare the

¹See subsection 1.3.3 to review their roles.

Hubble parameters at the beginning of inflation respecting the LQC requirements and also the conditions associated with the successful standard evolution. Remember that H acquires its maximum value (2.64) right before the onset of inflation in LQC context. Therefore, establishing the equality between (2.64) and the HI Friedmann equation at the same period (4.21), we obtain the following expression

$$\rho_c \simeq \frac{\lambda M_{Pl}^4}{\xi^2}. \quad (4.23)$$

Now, we move on to the end of inflation, where our Effective Friedmann equation (4.8) must obey

$$H^2 \simeq \frac{\rho_{\text{eff}}}{3M_{Pl}^2}. \quad (4.24)$$

Within the HI framework, if we plug (4.20) into (4.17), it possible to observe that the value obtained was almost seventy percent smaller than the initial one given by (4.18). Consequently, at the end of inflation $V(\chi) \approx 0.287V_0$ and HI Friedmann equation (4.21) can be written as

$$H^2 \approx 0.287 \frac{\lambda M_{Pl}^2}{12\xi^2}. \quad (4.25)$$

Making (4.24) equal to (4.25), we have

$$\frac{\rho_{\text{eff}}}{3M_{Pl}^2} \approx 0.024 \frac{\lambda M_{Pl}^2}{\xi^2}. \quad (4.26)$$

Next, we isolate the effective energy density term and substitute (4.23) into it, gaining the result

$$\rho_{\text{eff}} \approx 0.072 \frac{\lambda M_{Pl}^4}{\xi^2} = 0.072\rho_c. \quad (4.27)$$

Equation (4.27) shows that our formulation is in agreement with the energy range expected from LQC since the value $\rho_{\text{eff}} \approx 0.072\rho_c$ satisfy the requirement $\rho_{\text{eff}} \ll \rho_c$ needed to recover the SCM evolution at the end of inflation.

Basically, the previous procedure consisted in comparing the evolutionary structure of the standard Friedmann equation and its Effective LQC counterpart for the special case dictated by the quantities ρ_{eff} and $V(\chi)$. Therefore, the assumption regarding

the equivalence between the MG description of LQC and HI will be true only if their dynamics match. This means that the equations (4.5) and (4.21) must be equal during the inflationary period, which results in the tracking condition

$$\rho_{\text{eff}}^2 - \rho_{\text{eff}}\rho_c + V(\chi)\rho_c = 0. \quad (4.28)$$

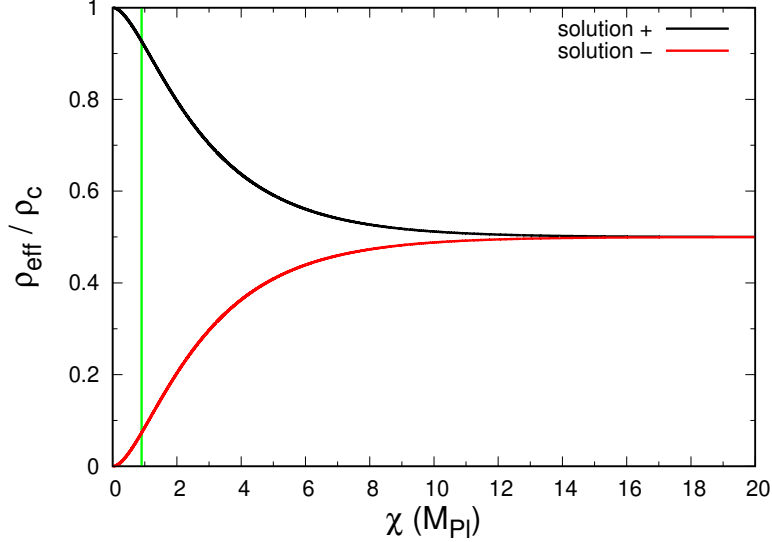
The equation (4.28) enables to verify whether the Higgs inflationary evolution can be mimicked by the mimetic curvature potential that defines ρ_{eff} during this period. To put it another way, $V_k(\varphi)$ would be able to assume the shape needed to reproduce $V(\chi)$ and, at the same time, control the energy variation to respect LQC boundaries. Thus, $V_k(\varphi)$ together with the curvature term ka^{-2} work like $V(\chi)$ and would be the ones dictating the inflationary dynamics.

In order to see whether this is viable or not, let us see how (4.28) behave, which means to evaluate how ρ_{eff} evolves with χ . As a second degree equation, there are two solutions associated with ρ_{eff} , one physical and other not. Figure 4.1 shows both solutions and enables to recognize the red line like the one we are looking for. Note that the black line represents the solution in which ρ_{eff} grows as χ becomes smaller, describing a non-physical evolution. The green line indicates the end of the inflationary period defined at $\chi \simeq 0.94M_{Pl}$. Above all, Figure 4.1 provides the behavior that the term $V_k(\varphi) - ka^{-2}$ must have to make the Hubble parameter exactly the same as the one described by the Higgs potential $V(\chi)$.

Furthermore, at this point, our aim is to compare how $V_k(\varphi) - ka^{-2}$ and $V(\chi)$ evolves separately. Then, the mimetic potential $V_k(\varphi) - ka^{-2}$ is considered with respect to ρ_{eff}/ρ_c . Meanwhile, $V(\chi)$ is evolved within the interval of χ beyond the one covered during inflation. Both potentials are described in Figure 4.2 from which it is possible to observe the clear similarities between them. The mimetic evolution is presented in blue along the x2y2 axes, while the HI one is in red, being related to x1y1 axes. The green line continues to have the same meaning as before.

Figure 4.2 corresponds to one fundamental result of our work since provides a proof that $V_k(\varphi) - ka^{-2}$ can properly mimic the dynamics of a universe driven by $V(\chi)$. Hence, our interpretation of the Langlois et al. (2017) work is able to reproduce the HI scenario. Moreover, the increasing scale factor dilutes the influence of the curvature term ka^{-2} , so that $V_k(\varphi)$ becomes closer and closer to $V(\chi)$ (as it can be seen in Figure 4.2).

Figure 4.1 - Solutions of the tracking equation



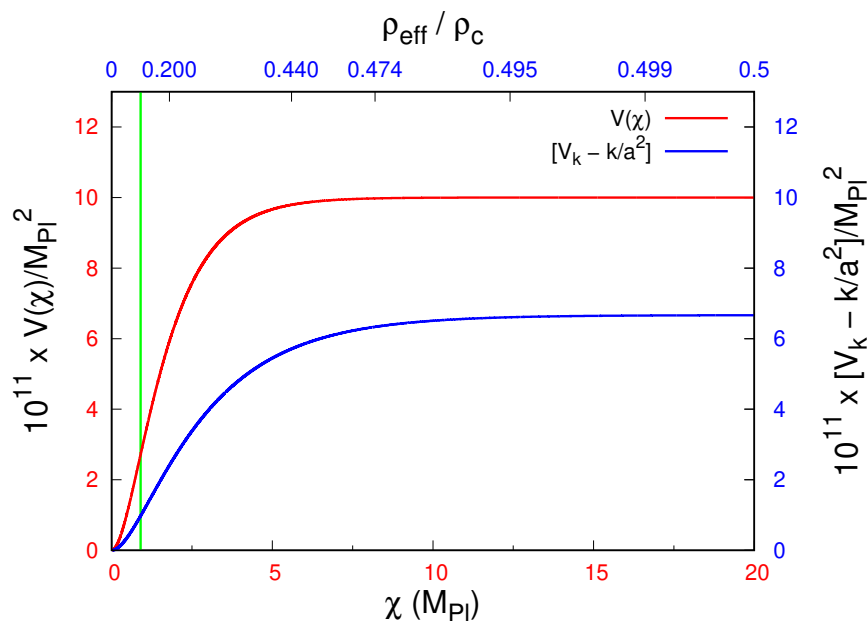
SOURCE: Bezerra and Miranda (2019)

The validity of (4.28) would enable to study the universe evolution during inflation through a unified model LQC-HI with MG as the bridge. Langlois et al. (2017) already linked LQC with MG by rewriting the first one as a formulation of the second. Moreover, Chamseddine and Mukhanov (2018a) inserted the mimetic field into the Brout-Englert-Higgs (BEH) mechanism in order to obtain a massive graviton free of the ghosts. Besides, the strong coupling between the mimetic field and graviton was also associated with scales close to the Planck one. Immediately after, the same authors extended their work to a perturbative level with (CHAMSEDDINE; MUKHANOV, 2018b). Notwithstanding the different application, it is essential to emphasize that this may establish a direct relationship between the mimetic field and Higgs field since the later will be always present when the BEH mechanism is evoked. Here, our goal is to use MG as an intermediary approach, closing this triangle by relating LQC with HI.

4.4 Different perspective regarding the energy density components: Dynamic equations with curvature terms

The relation between matter and curvature reached another level with GR proposal. However, there is no reason why it could not be explored even deeper. Within the

Figure 4.2 - Evolution of the potential terms regarding MG and HI



SOURCE: Bezerra and Miranda (2019)

LQC framework, as well as GR, matter and curvature are analyzed apart from each other. This means the changes implemented in one sector do not directly affect structurally the other. Note that the holonomy corrections as the result of the discrete space-time nature just alter the structure of the gravitational sector. Meanwhile, in case of a matter field self-interacting, in principle, only the matter sector should change.

With our work, we intend to highlight that the matter-curvature relationship could be further explored. Indeed, our focus is to emphasize the curvature as a fundamental element in MG description of LQC. From the possibility of a previous configuration of our universe that would have collapsed into a bounce in LQC framework, it is reasonable to associate this scenario with a closed configuration. Therefore, if the universe collapsed due to gravitational effects, it may have acquired a curved structure. In this case, the role played by the curvature could have been more essential than what was expected from SCM.

During this section, we will show how to obtain the dynamic equations associated with our formalism from subsection 4.1 in analogy with the process exposed in chapter 2 for Effective LQC. First of all, in section 4.1, from a classical perspective,

the only component in the matter side was ρ_{kin} . Following in analogy with the Effective LQC construction, ρ_{eff} is the quantity playing the role of total energy density once it is the one whose value is bounded due to the sine function (4.4). However, what would happen if we change $V_k(\varphi)$ to the matter side since it is supposed to describe the potential energy of the field from a curvature point of view? Here, we are going to analyze these scenarios for the inflationary stage.

In order to respect the dynamic evolution from LQC and standard slow roll approximation, the total energy density ρ cannot be described only as $\rho = \rho_{\text{kin}}$ since there would not have a potential term to lead the universe to accelerated expansion. Therefore, let us start by considering $3M_{Pl}^2 V_k(\varphi)$ as a component of ρ like it follows

$$\rho = \rho_{\text{kin}} + 3M_{Pl}^2 V_k(\varphi), \quad (4.29)$$

see that (4.29) is similar to the standard definition (2.61). In this case, the substitution of (4.29) into (4.1) will obtain an Effective Friedmann equation similar to (2.63),

$$H^2 = \frac{8\pi G}{3} \left[\rho - 3M_{Pl}^2 \frac{k}{a^2} \right] \left\{ 1 - \frac{1}{\rho_c} \left[\rho - 3M_{Pl}^2 \frac{k}{a^2} \right] \right\}, \quad (4.30)$$

with an extra curvature component since we are working with curved space-time.

The next step is to compute the time derivative of equation (4.30), but we need to assume that (4.29) describes a perfect fluid, obeying equations (1.11) and (1.15). After that, the result will be the expression

$$\dot{H} = -\frac{4\pi G}{3} \left[3\rho(1+w) - 6M_{Pl}^2 \frac{k}{a^2} \right] \left[1 - \frac{2}{\rho_c} \left(\rho - 3M_{Pl}^2 \frac{k}{a^2} \right) \right]. \quad (4.31)$$

Then, we sum (4.31) with (4.30) to obtain the acceleration equation

$$\dot{H} + H^2 = \frac{4\pi G}{3} \left\{ \rho(-1-3w) - \frac{2}{\rho_c} \left(\rho - 3M_{Pl}^2 \frac{k}{a^2} \right) \left[\rho(-2-3w) + 3M_{Pl}^2 \frac{k}{a^2} \right] \right\}. \quad (4.32)$$

Finally, from (4.5) and (4.29), (4.32) can be written in the following form

$$\dot{H} + H^2 = \frac{4\pi G}{3} \left\{ \rho(-1 - 3w) - \frac{2\rho_{\text{eff}}}{\rho_c} \left[\rho(-2 - 3w) + 3M_{Pl}^2 \frac{k}{a^2} \right] \right\}. \quad (4.33)$$

Within this configuration, equations (4.30) and (4.32)/(4.33) are the ones determining the universe evolution. From (4.29), it is possible to observe that the universe curvature is treated apart from $V_k(\varphi)$. This scenario has the closest structure to one presented in chapter 2 if it had been applied to curved FRW space-time. Indeed, we had noticed that these results are compatible with the ones from (MIELCZAREK et al., 2009).

Mielczarek et al. (2009) performed a dynamic analysis for Effective LQC considering a curved setup which led to

$$H^2 := \left[\frac{\dot{p}}{2p} \right]^2 = \frac{8\pi G}{3} \frac{1}{\rho_c} [\rho - \rho_1(p)] [\rho_2(p) - \rho], \quad (4.34)$$

with

$$\rho_1(p) \approx \frac{3}{8\pi G a^2} \quad \text{and} \quad \rho_2(p) \approx \rho_c + \frac{3}{8\pi G a^2}. \quad (4.35)$$

It is important to emphasize that (4.34) came from a more complex Hamiltonian than (3.37). However, comparing (4.34) and (3.39), it is possible to identify analog quantities to (4.36) as

$$\rho_1 \approx \frac{3M_{Pl}^2 k}{a^2} \quad \text{and} \quad \rho_2 \approx \rho_c + \frac{3M_{Pl}^2 k}{a^2}, \quad (4.36)$$

that enables to recover exactly (4.30) if they were plugged into (4.34). Even the elements from acceleration equation (4.32) can be recognized in (MIELCZAREK et al., 2009) whose analog form contains extra terms than the ones present in it.

Despite the fact that ka^{-2} has a different origin than $V_k(\varphi)$, it can also compose the total energy density. Indeed, the standard treatment covers the concept of curvature energy density, as it can be seen from (1.13). So, now, $3M_{Pl}^2[V_k(\varphi) - ka^{-2}]$ is the term playing the role of matter potential. For this case, the total energy density corresponds to ρ_{eff} whose Effective Friedmann equation is given by (4.5).

First of all, before trying to compute the acceleration equation, we must assume the validity of the continuity equation

$$\dot{\rho}_{\text{eff}} + 3H(P_{\text{eff}} + \rho_{\text{eff}}) = 0, \quad (4.37)$$

where P_{eff} is the effective pressure associated with ρ_{eff} by the EoS $P_{\text{eff}} = w\rho_{\text{eff}}$. After, the previous process is repeated to compute the time derivative of (4.5) which, considering (4.37), results in

$$\dot{H} = -\frac{4\pi G}{3}\rho_{\text{eff}} \left[3(1+w) \left(1 - \frac{2\rho_{\text{eff}}}{\rho_c} \right) \right]. \quad (4.38)$$

Next, we add (4.5) to (4.38), obtaining the acceleration equation

$$\dot{H} + H^2 = \frac{4\pi G}{3}\rho_{\text{eff}} \left[-3w - 1 + \frac{2\rho_{\text{eff}}}{\rho_c}(2 + 3w) \right]. \quad (4.39)$$

Note that (4.38) and (4.39) have the exact form of the equations (2.66) and (1.16) which should not be different since the Effective Friedmann equation for ρ_{eff} has the same shape compared to LQC, which also applies to (4.37). This part is basically a continuation of the development we started in section 4.1 with the addition of the continuity equation (4.37).

Once we have obtained the acceleration equation, we can now analyze in which condition our formulation can generate inflation through it. See that equation (4.39) implies in the following condition in order to produce an accelerated expansion ($\dot{H} + H^2 > 0$)

$$3w + 1 < \frac{2\rho_{\text{eff}}}{\rho_c}(2 + 3w). \quad (4.40)$$

If we substitute $\frac{\rho_{\text{eff}}}{\rho_c} = \frac{1}{2}$ into (4.40), it is direct to conclude that any value of w will satisfy (4.40) which is in agreement with a similar analysis performed by [Sadjadi \(2013\)](#) for LQC. Therefore, both matter and radiation are able to fulfill (4.40). However, condition (4.40) can also be used to test what values of w would agree with LQC energy range for inflation without substituting it directly. This will become clear in the next section.

Recall that the mimetic potential embedded within ρ_{eff} is the quantity ruling the inflationary stage. In the particular case in which the mimetic potential follows the evolution of the Higgs inflationary potential as presented in [Figure 4.2](#), the value of w may be adjusted in order to reproduce its specific dynamics. Furthermore, it is

the term $3M_{Pl}^2[V_k(\varphi) - ka^{-2}]$ that must satisfy the LQC energy requirement during inflation.

Within certain limits, our work reproduces results exposed by other authors in LQC literature. For the total energy density given by (4.29), the equations obtained would be almost equivalent to the ones from (MIELCZAREK et al., 2009) if they have used the same Hamiltonian as we did. The dynamic equations computed from ρ_{eff} are identical to the ones presented in (SADJADI, 2013) for the flat case. Thus, in principle, we have a curved scenario emulating flat dynamics. Therefore, depending on how we interpret what components should be into the total energy density definition, we can reproduce flat and curved formulation with the mimetic description of LQC. Moreover, note that the pairs (4.5) and (4.30), besides (4.33) and (4.39) are identical for $k = 0$.

4.5 About the conservation of the energy density

The computations performed in the previous section were developed under the assumption that the continuity equation holds for both descriptions of the total energy density. Therefore, the mimetic curvature potential must fulfill this requirement. Here, we will discuss the specific conditions in which this statement is true. In order to do this, we will start from the general case, in which we defined the quantity

$$V_{\text{eff}} = 3M_{Pl}^2[V_k(\varphi) - ka^{-2}], \quad (4.41)$$

and name it as MG effective curvature potential. Now, the effective energy density (4.3) could be written as

$$\rho_{\text{eff}} = \rho_{\text{kin}} + V_{\text{eff}}. \quad (4.42)$$

The next step is to perform a time derivative of equation (4.42), from which we obtain the expression

$$\dot{\rho}_{\text{kin}} + 3H(1+w)\rho_{\text{kin}} + [\dot{V}_{\text{eff}} + 3H(1+w)V_{\text{eff}}] = 0. \quad (4.43)$$

From (4.43), see that we can follow throughout two different paths. The first alternative it is to consider that ρ_{eff} obeys (4.37) due to the teamwork carried out by ρ_{kin} and V_{eff} . This means they evolve in a suitable way to preserve (4.43) as well as

it happens for an ordinary scalar field. Remember from classical mechanics that the energy flows between the kinetic and potential term forms a closed setup. Moreover, V_{eff} reproduces well the matter potential behavior of $V(\chi)$, as we showed in Figure 4.2. Therefore, there is no reason to suppose that it will deviate from this path along with other stages of primordial evolution.

As a second possibility, note that if ρ_{kin} satisfies the continuity equation

$$\dot{\rho}_{\text{kin}} + 3H(1+w)\rho_{\text{kin}} = 0, \quad (4.44)$$

the same statement must also apply to V_{eff} ,

$$\dot{V}_{\text{eff}} + 3H(1+w)V_{\text{eff}} = 0. \quad (4.45)$$

Here, analyzing the continuity equation ρ_{kin} and V_{eff} seems to be a distinct analysis of ρ_{eff} during the bounce and inflation separately. Since ρ_{kin} directly refers to usual matter content, (4.44) must be satisfied. Otherwise, the LQC models whose bounce is dominated by the kinetic energy of the field would face serious problems. Consequently, equation (4.45) corresponds to a condition that the mimetic effective potential must obey.

With this in mind, we substitute (4.41) in (4.45) and obtain the following expression

$$\dot{V}_k(\varphi) + 3H(1+w)V_k(\varphi) - (1+3w)H\frac{k}{a^2} = 0. \quad (4.46)$$

Now, the validity of equation (4.46) is the key to preserve (4.37). Note that for the particular value $k = 0$, (4.46) reduces to

$$\dot{V}_k(\varphi) + 3H(1+w)V_k(\varphi) = 0 \quad (4.47)$$

and corresponds to the requirement for having (4.29) also obeying the continuity equation.

A crucial point to highlight is the fact that considering (4.46) for $w = -\frac{1}{3}$ we can obtain the same dynamic equations for (4.29) and (4.3) without considering $k = 0$. Indeed, this value for the state parameter is able to fulfill the relations

$$\dot{H} = -\frac{4\pi G}{3}\rho_{\text{eff}} \left[3(1+w) \left(1 - \frac{2\rho_{\text{eff}}}{\rho_c} \right) \right] < 0, \quad (4.48)$$

$$\dot{H} + H^2 = \frac{4\pi G}{3}\rho_{\text{eff}} \left[-3w - 1 + \frac{2\rho_{\text{eff}}}{\rho_c}(2 + 3w) \right] > 0 \quad (4.49)$$

and

$$3w + 1 = 0 < \frac{2\rho_{\text{eff}}}{\rho_c}. \quad (4.50)$$

This means that, in a first analysis, $w = -\frac{1}{3}$ is a viable option to describe the fluid responsible to drive inflation.

It is important to note that for the inflationary phase to begin, it must be dominated by a fluid with $w < -1/3$, see (YOKOYAMA, 2014). Coincidentally, our formalism shows that $w = -1/3$ allows preserving the conservation equation for both $k = 0$ and $k = +1$, besides being the value that allows starting the inflationary phase as discussed in Yokoyama (2014). Moreover, the condition $w \gtrsim -1/3$ seemed to be a request to lead the inflationary accelerated expansion to an end. In the reheating phase, w should change from $-1/3$ to a value inside the range $[0, 1/3]$ after an inflationary period dictated by a Higgs mechanism, see reference (COOK et al., 2015) for extended information.

In case of a state parameter depending on the scale factor $w = w(a)$, the equations (4.46) and (4.47) would receive corrections or even completely change as the w evolution goes. All things considered, this last statement is directly related to the introduction of mimetic curvature potential and could be a new element outside the Effective LQC formulation.

4.6 A brief note on super-inflationary phase

Despite the fact that we did not address the super-inflationary phase in (BEZERRA; MIRANDA, 2019), there are hints that naturally arise from our formulation for this specific period. Since the description based on ρ_{eff} as the total energy density produces quite similar results to ones obtained by Sadjadi (2013), there is no reason to the super-inflation stage does not continue into this path.

Recall from chapter 2 that super-inflation happens for $\dot{H} > 0$ because it corresponds to a super-accelerated expansion (SADJADI, 2013). From (4.38), assuming w to be

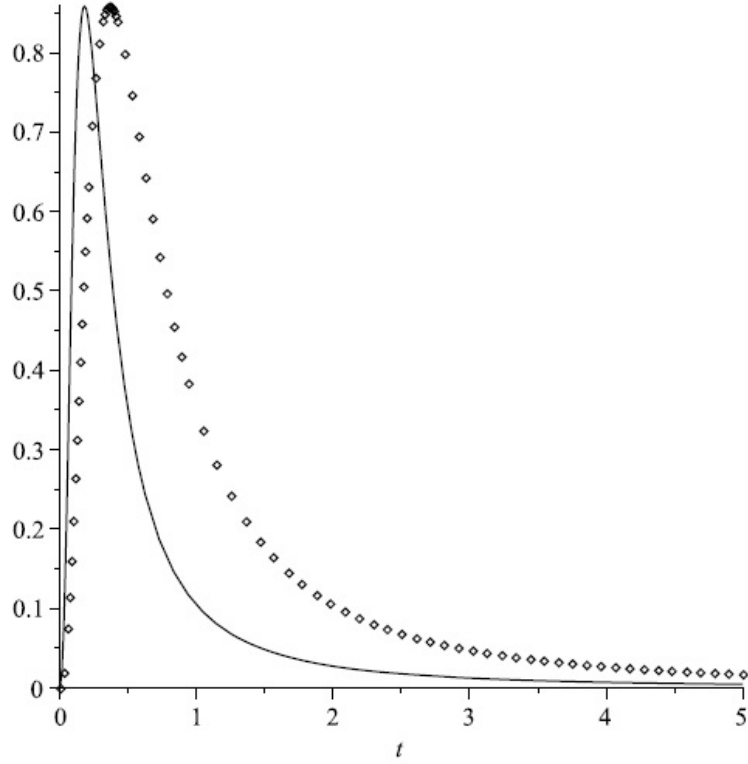
constant, only ρ_{eff} is governing the behavior of the time derivative of the Hubble parameter. On the other hand, since ρ_{eff} is following the evolution regarding the LQC energy range, the super-inflation is placed within the interval $\rho_c/2 < \rho_{\text{eff}} < \rho_c$, enabling any field with $w > -1$ to drive the universe along a super-accelerated expansion. To give an illustration, this covers a range that goes from fluids similar to cosmological constant ($w \gtrsim -1$), radiation-type fields ($w = 1$), fluids with dust-like behavior ($w = 0$) and even Galileon fields ($w > 1$) (BEZERRA; MIRANDA, 2019).

In order to have an idea about how this phase affects the dynamics of H , let us briefly discuss the strategy developed by Sadjadi (2013). The procedure implemented was to introduce a normalized time variable t which is directly related to the ratio ρ/ρ_c , as it follows

$$\frac{\rho}{\rho_c} = \frac{1}{1 + 6\pi G\rho_c(1+w)^2 t^2}. \quad (4.51)$$

Since the dynamic equations are similar to (2.63), (2.67) and (1.15), with a perfect fluid as matter content and $w = \text{constant}$, the Hubble parameter should follow the evolution presented in Figure 4.3. The curves was obtained considering two values of w . The line represents the evolution of the modified Friedmann equation (2.63) for $w = 1$, while the points are related to the case $w = 0$. The vertical axis refers to H^2 that evolves with the normalized time variable t , where $t = 0$ represents the bounce point. Note that there is a huge peak defining the maximum value of H^2 . See also that the super-accelerated period lasts longer for the small value of w (SADJADI, 2013).

Figure 4.3 - Evolution of the modified Friedmann equation



SOURCE: Sadjadi (2013)

Therefore, the function achieves its maximum extremely fast and drop to smaller values also quickly, resembling a delta function. In principle, we could reproduce this plot considering our approach and also assume a constant state parameter. However, there are other points that must be treated carefully, once we are introducing curvature terms to the equation.

In summary, super-inflation remains for discussion in LQC scenario since the explanation behind the loss of half of the kinetic energy after the bounce and how it was transferred to the potential term is still missing. The logical hypothesis would be to use this amount of energy to take the universe outside the bounce phase and lead it to a really fast expansion stage. Moreover, it is worth to mention that models with non-minimal coupling are also capable of producing a super-inflationary phase (SADJADI, 2013). With this in mind, our formulation built under a total energy density ρ_{eff} composed by the pair ρ_{kin} and V_{eff} could provide particular results due to the matter-curvature relationship.

5 A BRIEF DIGRESSION ON GRAVITATIONAL WAVES

A cosmological model is built by steps. First of all, it must be established a foundation, which can be developed from the start or shaped over another theory/model. Next, the model must be checked in order to avoid the presence of undesired features that can take it down like ghosts. This first stage is usually defined at the background level. After, when the model seems to be self-consistent, it should be extended to cover also the perturbative case. Otherwise, the model will lose predictive power once it will not be able to produce essential observable quantities. They are the ones to be compared with cosmological observational results from CMB or future detection of gravitational waves produced during the early times.

Our work is still within its first stage of development. We have the formalism proposed by [Langlois et al. \(2017\)](#) as our base, however, the stability analysis remains an open question even in mimetic gravity itself. Until now, we do not identify any sign of instabilities in general. The treatment we performed is restricted to the background level and it is not completely covered. There are more possibilities associated with bounce and super-inflation (or its absence) that could also be explored before we move on to the level of perturbations. However, in principle, both studies can be approached in parallel without loss of generality.

In this chapter, we review essential aspects regarding the standard picture of primordial gravitational waves. Here, we will use this term to refer to any gravitational wave produced during the early times regardless of the model. Only after, we present a survey containing the CMB power spectrum obtained from models with properties similar to ours. The aim is to illustrate the possibilities to be explored in future works.

5.1 Primordial Gravitational Waves

Gravitational waves are a prediction of Einstein's general relativity theory. They are defined as ripples in the space-time fabric and, in analogy with the usual concept of waves, they can be understood as waves of distorted space that are propagating like radiation from their source ([LIGO COLLABORATION, 2019](#)). Indeed, there are two sources associated with the production of detectable gravitational waves: astrophysics and primordial. The GW from astrophysical objects are the ones detected by LIGO/Virgo collaborations. Nonetheless, there are also GW produced by the physical processes that happened during the primordial universe evolution ([BOJOWALD; HOSSAIN, 2008](#)), being referred to as primordial gravitational waves.

Working with GW is a new way to explore the data available throughout the universe, once they basically do not interact with matter, providing a virtually perfect picture about their source. They correspond to a different and complementary tool which can be used together or apart from electromagnetic observations (LIGO COLLABORATION, 2019). Furthermore, PGW are the ideal lab to study the primordial universe (BOJOWALD; HOSSAIN, 2008) since they are the ones identified as tensor perturbations of the metric tensor.

As it was exposed in chapter 1, the physical metric can be split into the background and perturbed parts. The standard background metric is the FRW one. Meanwhile, the general form to express the metric perturbation is describing it as a sum of all contributions. This means the total perturbation of the metric is given by $\delta g_{\mu\nu} = \delta g_{\mu\nu}^{(S)} + \delta g_{\mu\nu}^{(V)} + \delta g_{\mu\nu}^{(T)}$, with S , V and T indicating the scalar, vector and tensor components.

A fundamental aspect of the linearized cosmological perturbation theory is that the evolution of the scalar, vector and tensor perturbations can be analyzed independently at linear level (MUKHANOV et al., 1992). Since the tensor contribution is the one carrying the information about the PGW, the tensor component is isolated which enables to write the line element in the form

$$ds^2 = a^2(\eta)[d\eta^2 - (\gamma_{ij} + h_{ij})dx^i dx^j], \quad (5.1)$$

where γ_{ij} corresponds to the background metric and h_{ij} corresponds to a transverse and traceless tensor perturbation. Then, in the absence of source $T_{\mu\nu} = 0$, the perturbed Einstein equations (1.36) solved for (5.1) give rise to EoM for tensor perturbations

$$h''_{ij} + 2\mathcal{H}h'_{ij} - \nabla^2 h_{ij} = 0. \quad (5.2)$$

The standard treatment of PGW is built under the assumption of a massless graviton that propagates with two polarization modes (BESSADA; MIRANDA, 2009b). From equation (5.2), it is possible to identify the similarity regarding a wave equation, justifying the name gravitational waves. Consequently, its general solution should be written as

$$h_{ij}(\mathbf{x}, \eta) = h(\eta)e_{ij}^{(+,\times)}(\mathbf{x}) = \sum_{\lambda=(+,\times)} h^{(\lambda)}(\eta)e_{ij}^{(\lambda)}(\mathbf{x}), \quad (5.3)$$

where e_{ij}^λ corresponds to the polarization tensor and it obeys the relations $e_{ij} = e_{ji}$, $\partial^i e_{ji} = 0$, $e_{ii} = 0$. The signals $+$ and \times represent the two GW polarization states expressed in a summarized way by λ (GUZZETTI et al., 2016; BUONANNO, 2007; D'IVERNNO, 1992; FERREIRA, 2014).

A particular feature regarding PGW is that each theory of gravity may provide distinct patterns to describe their behavior. Indeed, the primordial gravitational waves are basically frozen in the super-horizon scales. Thus, PGW's amplitude is the same for all tensor perturbations and it has the inflationary horizon size (GUZZETTI et al., 2016). Therefore, direct observation will provide exclusive information about the primordial universe like its energy range and size.

The aim is to obtain a power-spectrum expression for the quantum fluctuations,

$$\mathcal{P}_T(k) = \frac{k^3}{2\pi^2} \sum_{\lambda} |h_{\mathbf{k}}^{(\lambda)}|^2, \quad (5.4)$$

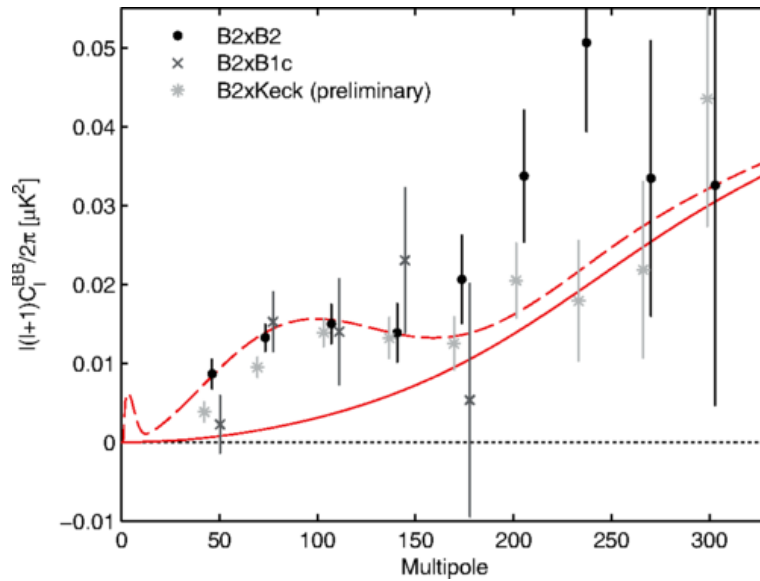
which is the Fourier transform of the two-point correlation function. This quantity is related to the expected value of the quantum field even when they become classic outside the horizon and almost scale-invariant, in agreement with the observational results. The shape of PGW power-spectrum depends on the tensor perturbation equation.

In summary, inflationary models are characterized by the production of a stochastic background of gravitational waves, the tensor perturbations. They are considered the best tool to explore primordial physics since they do not evolve after leaving the universe horizon as well as it happened with the curvature perturbations. Moreover, each inflationary model will have its own power-spectrum. When the PGW return, they bring together the information about how was the universe at the moment they left. This is the reason why they could be seen as a window to observe the early universe, the Planck scale included. Hence, in principle, they will enable us to verify not only the validity of the inflationary models but also the quantum cosmological ones (MIELCZAREK, 2008; GUZZETTI et al., 2016).

5.2 CMB Power Spectrum

Despite the fact that PGW has not been directly detected yet, there is an alternative tool to study them, the cosmic microwave background radiation. Part of the PGW is frozen outside the visible horizon until it returns to the Hubble radius as the universe expand. However, when they come back they should produce signatures in the CMB spectrum due to the interaction with the photons (BESSADA; MIRANDA, 2009b), see Appendix C for further details. The ideal situation would be to observe a B-mode polarization of CMB from the primordial source since it only comes from tensor perturbations. If the B-mode detection from BICEP2 experiment (ADE et al., 2014) would have been as successful as it was first claimed, the PGW power-spectrum would have the form presented in Figure 5.1.

Figure 5.1 - BICEP2 CMB power spectrum for B-mode



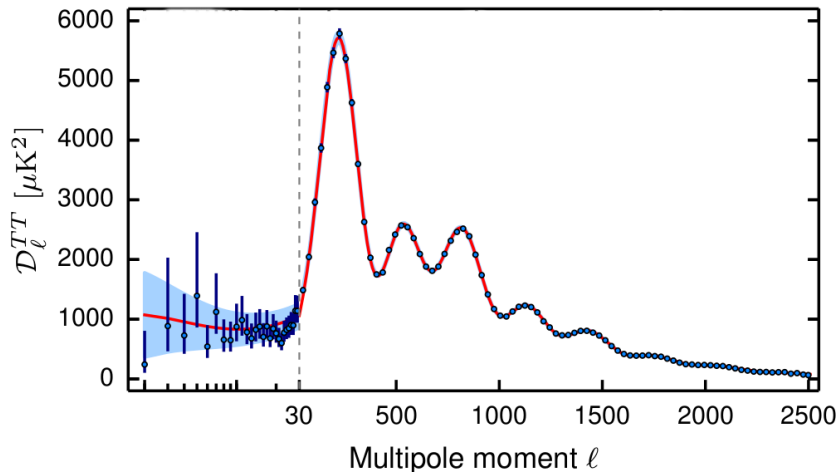
SOURCE: Ade et al. (2014)

However, the B-mode observation from PGW has not happened yet. In fact, the only current possibility is to search for effects within the power spectrum of temperature anisotropies of the CMB. Roughly speaking, the power spectrum can be understood as the amount of anisotropy presented in a determined angular scale, in particular, CMB anisotropies are usually considered with respect to the multipole momentum ℓ (CARROLL, 2006). This is performed by tracing the plot representing the variation

of the correlation function C_ℓ^{TT} regarding ℓ , the double T indicates temperature.

Figure 5.2 shows the Planck satellite results considering the Λ CDM model like in the previous section. The dashed line bounds the region containing the low multipole $\ell < 30$ that is exactly the part of the spectrum associated with possible tensor perturbation signatures. See that this region presents higher error bars compared to the other which is an effect related to the statistic strategy used to obtain C_ℓ^{TT} . This means that any cosmological model must reproduce the spectrum above for $\ell > 30$. Nevertheless, the behavior for very low multipoles could (or should) change since the blue points in Figure 5.2 suggests a possible decaying of the spectrum which could favor other models different from Λ CDM.

Figure 5.2 - CMB power spectrum



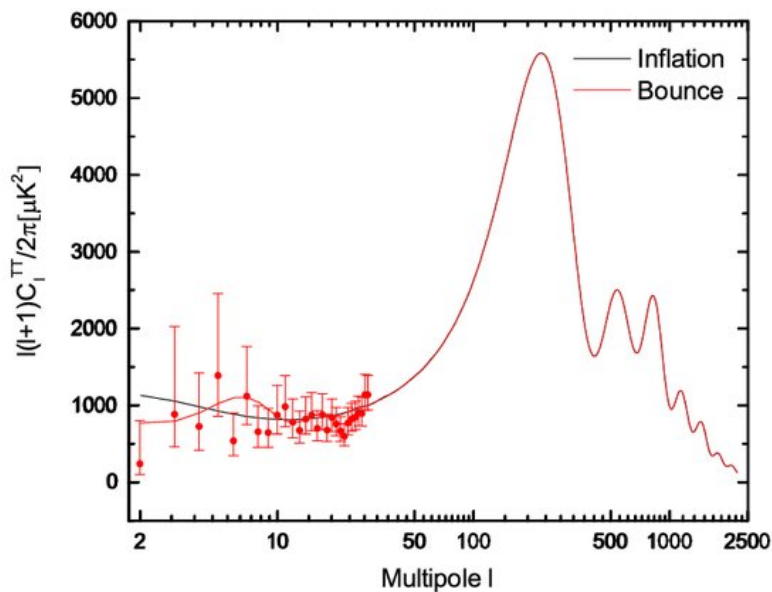
SOURCE: Ade et al. (2016)

Within the same background as Λ CDM, MG models seem to produce indistinguishable power spectrum in comparison to it, at least in linear scales (ARROJA et al., 2018). Therefore, in principle, as a minimal extension of GR, MG's power spectrum should be similar to Figure 5.2. Notwithstanding, there are many extended mimetic approaches discussed throughout the literature whose additional components may bring forth a different pattern.

Our results were built under the Langlois et al. (2017) proposal, and until the writing of this work, there was no publication regarding the shape of its power spectrum.

As the MG representation of LQC was built under high order Lagrangian terms, we should consider the power spectrum for bounce models with high order terms as a starting point to what possibilities we can expect. Figure 5.3 refers to a parameterized bounce inflation model treated in (NI et al., 2018) and modeled according to Horndeski theory. See that power spectrum is suppressed inside the range covered by low values of ℓ ($\ell < 30$), and for this particular case, there are oscillations within the spectrum.

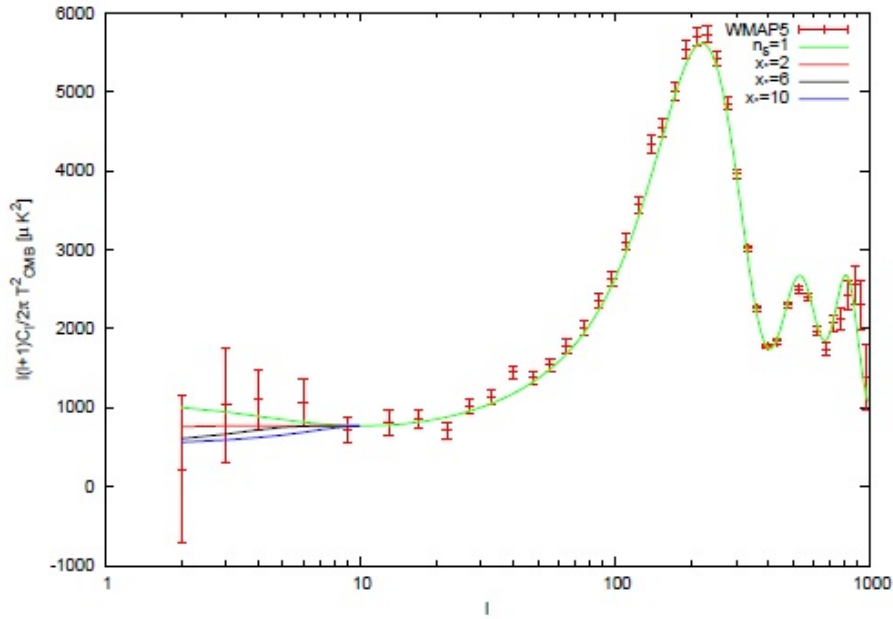
Figure 5.3 - CMB spectrum for a bounce universe



SOURCE: Ni et al. (2018)

Figure 5.4 provides a picture obtained by Mielczarek (2010) considering WMAP data. The green line represents the standard inflationary evolution, meanwhile, the other ones correspond to variants of his Effective LQC model. Note that there is a suppression within the low multipoles region regarding the standard approach, which seems to be a consequence of the replacement of the singularity by the cosmological bounce.

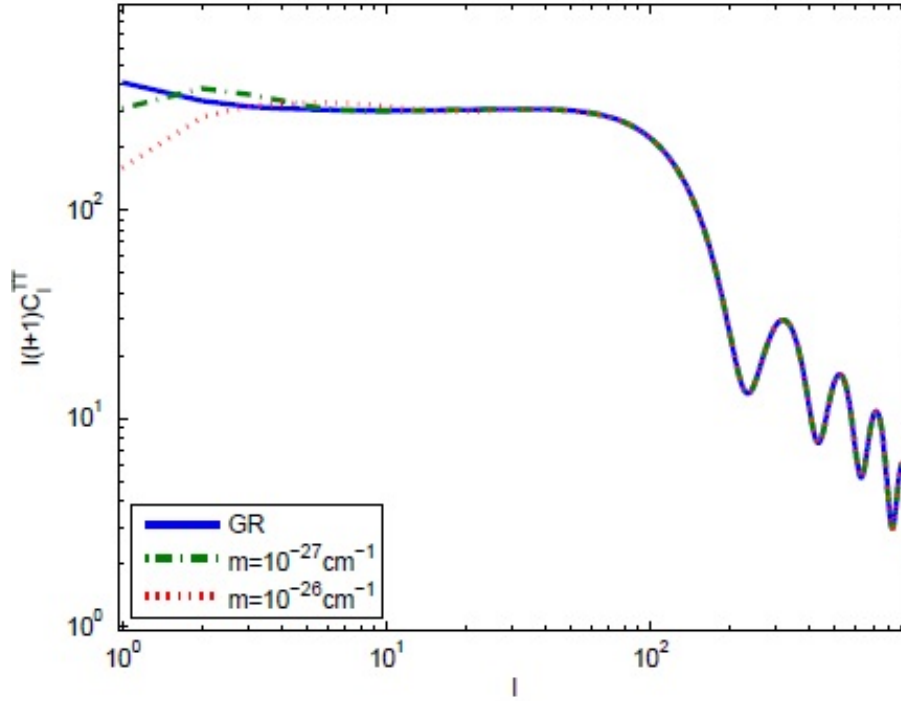
Figure 5.4 - CMB spectrum from Loop Quantum Cosmology



SOURCE: Mielczarek (2010)

Regarding the possible relationship between MG and HI, like in the previous statement, there is no current work available describing the power spectrum for this extension built under the concept of a massive graviton exposed in (CHAMSEDDINE; MUKHANOV, 2018a). Nonetheless, let us briefly discuss the power spectrum from the Massive Gravity approach presented in Figure 5.5 and obtained by Bessada and Miranda (2009a). Here, the plot was also developed in comparison with SCM (expressed by the solid blue line) and included the description of the model for two different values of the graviton mass. In this case, it is also clear the suppression of the correlation function for low multipoles values which is associated with the addition of mass to the standard massless graviton.

Figure 5.5 - CMB spectrum from Massive Gravity



SOURCE: Bessada and Miranda (2009a)

In other words, both previous approaches have a particular behavior when it comes to CMB signatures. Figure 5.5 corresponds to a graph of correlation function C_ℓ^{TT} for massive gravity in comparison to GR. Meanwhile, Figure 5.4 also exposes the difference regarding the correlation function C_ℓ^{TT} from Effective LQC. Although represented in different ways, both results correspond to the temperature anisotropies of the CMB in terms of ℓ . Furthermore, from Figures 5.4 and 5.5, it could be noticed that both show suppression of low CMB multipoles. As our model is kind of in the middle of these two approaches, this behavior is a possibility. However, for now, it is just an initial guess and it requires rigorous tests before any further discussion.

It is worth to mention that the recent works of Casalino et al. (2018), Casalino et al. (2019), Ganz et al. (2019) have shown the compatibility of mimetic gravity with the last results in gravitational waves observations regarding the propagation speed of the tensor perturbations. Further, the matter-curvature coupling has been presented in many papers as a way to stabilize the scalar perturbations. To give an illustration, Hirano et al. (2017) proposed to couple the kinetic term of the scalar

field with curvature in order to make the scalar perturbations stable. Moreover, [Zheng et al. \(2017\)](#) also used the coupling between the higher derivatives of the scalar field with space-time curvature to avoid the instabilities issues, besides their formulation was able to produce observable values compatible with the cosmological observations provided that the potential presented a suitable form. The situation repeats for the work ([TAKAHASHI; KOBAYASHI, 2017](#)), in which it was presented degenerate scalar-tensor theories like an extended mimetic approach. In this case, the scalar perturbation needed to be strongly coupled without allowing additional matter content.

All things considered, we need to perform deeper analyzes of the mimetic curvature potential before trying to address the model behavior regarding the primordial background of gravitational waves. In section 4.4, we discussed how $V_k(\varphi)$ was able to give rise to suitable cosmological solutions from which both super-inflation and inflation can occur. Within this framework, the inflationary phase was capable to imitate the Higgs inflationary evolution. Further, the inflationary dynamic would have been similar for $k = 0$ and $k = +1$ cases as long as the relation $w \approx -1/3$ is preserved by the mimetic curvature. Note that there are gaps related to the role of $V_k(\varphi)$ since the bounce until the end of inflation that must be fulfilled in order to build a consistent cosmological background. This requires a mathematical function to describe the proper behavior of $V_k(\varphi)$ that would not only be consistent with the primordial universe evolution and its energy condition but also free of instabilities (ghosts). Indeed, this is our current challenge to move forward with our model.

6 FINAL REMARKS AND PERSPECTIVES

Along with this text, we have highlighted the advantages of Effective LQC and Mimetic Gravity. Loop quantum cosmology enables to consider the space-time quantization at the effective level, giving rise to a cosmological bounce as a natural solution for the initial singularity. Mimetic gravity is a chameleon theory whose structure can be adapted to emulate a great number of different evolutionary scenarios, besides it enables to reproduce the behavior of the dark components.

Langlois et al. (2017) provided not only an MG formalism capable to mimic the Effective LQC dynamics but also opened a window to further explore the curvature role during primordial universe evolution. The healthy elements of Effective LQC remain intact with the introduction of the mimetic curvature potential, which became the main variable from our formulation. Despite the fact that the mimetic potential was not originally associated explicitly with the matter field, the absence of a matter potential term allowed us to interpret it as the curvature response due to the presence of matter.

Within this framework, we realized that a field strongly coupled with gravity would be a better fit for the scenario we were building in comparison to the standard minimally coupled scalar field. Further, we took advantage of the particular nature of the Higgs field and its inflationary extension proposed by Bezrukov and Shaposhnikov (2008). Our main point was to make clear the intrinsic relation between $V_k(\varphi) - ka^{-2}$ from MG and inflationary potential $V(\chi)$ due to HI. We achieved this goal by showing that the MG curvature potential can reproduce the dynamics from HI universe (see Figure 4.2). Notwithstanding the general form $V_k(\varphi) - ka^{-2}$, we were able to evaluate the behavior required to properly mimic the HI evolution. Indeed, our analysis showed the compatibility between LQC and HI energy scales along with inflation.

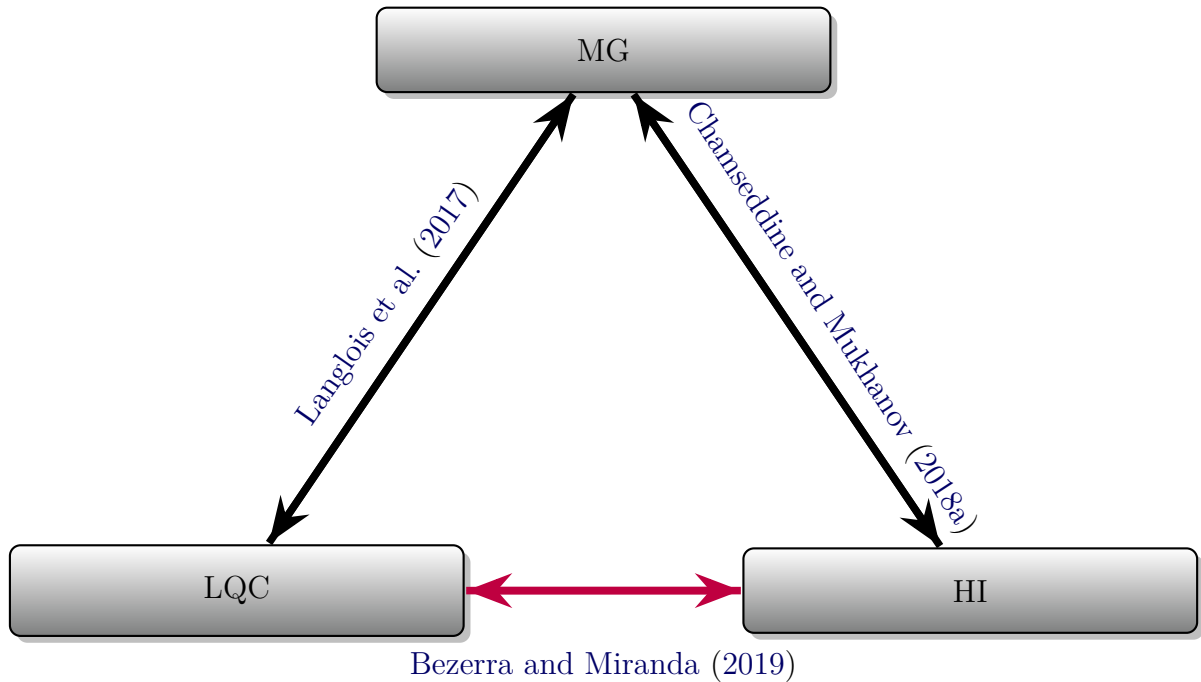
It is worth to mention that Cognola et al. (2016) added a potential term to the mimetic covariant Horava-like model, building a scenario with a Starobinsky-like inflationary epoch and a bounce solution. Moreover, Wan et al. (2015) presented a bounce model constructed from the standard Higgs boson that would be followed by a HI stage, in which the cosmological evolution was considered from the contraction phase (pre-bounce) until inflation ended with the e-fold number close to 60. Our point here is just to make clear that there are aspects of quantum gravity, Higgs inflation, and mimetic gravity which has been related over the literature in different ways.

Through MG description of LQC, in principle, it is possible to obtain a simpler and unified description covering from a natural bounce until an inflationary phase whose dynamics mimics the model with the primordial version of the Higgs field as energy content. The later, according to (RUBIO, 2015), can lead the primordial universe to relax to the vacuum state expected from SMPP. Note that MG basically does not change any structural feature of LQC, likewise, the physics regarding GR is reproduced by the mimetic dark matter model with minimal alteration.

Moreover, our formulation seems to present the versatile behavior of the main theory since we were able to reproduce results from other LQC works for flat and curved space-times just changing the components from total energy density. This is performed by changing the way the curvature is interpreted in both coupling and intrinsic curvature terms. In accordance, the mimetic curvature potential seems to keep the original mimetic potential role as a key element to emulate different cosmological scenarios (see (CHAMSEDDINE et al., 2014; SEBASTIANI et al., 2017)).

As we previously mentioned, MG has been already related to LQC through the work (LANGLOIS et al., 2017). This is also true regarding the Higgs field due to the introduction of the BEH mechanism into MG scenario in (CHAMSEDDINE; MUKHANOV, 2018a; CHAMSEDDINE; MUKHANOV, 2018b). Figure 6.1 is a scheme exposing how we used the MG representation of LQC characterized by its intrinsic matter-curvature foundation to establish a relationship between LQC and HI in (BEZERRA; MIRANDA, 2019). Our aim was to highlight the intermediary character of the MG representation of LQC, focusing on how the curvature interpretation can affect the way the physics during primordial evolution could be understood.

Figure 6.1 - MG as the bridge between LQC and HI



SOURCE: Authors own production.

The link regarding LQC and HI suggests that the formulation could be extrapolated in order to implement the Higgs field as an energy source of LQC. Remember that the standard LQC evolution considers an arbitrary scalar field just like the standard inflationary paradigm. Therefore, if we consider that the Effective LQC dynamics can accept the Higgs field as its possible matter content, using MG as a mediator, we could have a unified and consistent scenario for the very early universe through the MG description of Effective LQC with Higgs field.

To put it another way, Effective LQC can be interpreted as a geometric description of the physics related to scales close to the Planck one. Consequently, the universe dynamics is implemented considering the geometric point of view, having the matter field as a second actor. In HI, the dynamics is concentrated in the field evolution, being the curvature a fundamental part but not the main one. Obtaining the Effective dynamics of LQC from MG highlights the link between matter and curvature and enables the possibility of introducing the Higgs field in LQC framework. Therefore, MG is configured in an interesting formalism to explore the possible connections between LQC, HI and the role of curvature in the primordial universe.

Another key aspect to emphasize is related to the rate $\delta_H = \rho/\rho_c$ which is so-called holonomy corrected term (see (LUC; MIELCZAREK, 2017)). In our case, the correction parameter would be given by $\delta_H = \rho_{\text{eff}}/\rho_c$. Hence, paying attention to evolution dictated by (4.1) over early times, we can think about holonomy as a balanced structure that enables us to measure when quantum effects are significant by comparing the desired energy range with ρ_c . This is a fundamental point since we built the entire formalism giving priority to the evolution of the LQC energy range which is a direct result from holonomy corrections. Recall that the bounce dynamics is dictated by the field kinetic energy density that should lose its strength transferring half of it to the potential term. As the universe expands, the curvature and potential terms are decreasing its leverage. Thence, at end of inflation, the curvature influence virtually disappears, but the potential still continues to contribute as a less dominant component with respect to kinetic energy. However, at this point, the holonomy corrections are already negligible.

Our formulation presented in (BEZERRA; MIRANDA, 2019) has many aspects to be further explored. An explanation regarding the physical processes that gave rise to bounce and super-inflation stages, besides the transition to inflation, is missing throughout the literature in general. Consequently, it is worth to explore whether our model can shed some light within this framework. Considering the MG description of LQC as a versatile tool that allows performing different analysis of the cosmological scenario under the particular LQG perspective. Indeed, in LQG scenario, the fields live on each other, which means the space-time could be interpreted as an image of one specific field, the gravitational one. Thus, MG representation of LQC enables us to assess in a certain way this distinct nature of LQG if we consider it as a tool to explore the primordial physics through the mimetic curvature potential.

In LQC models, there is the hypothesis of a previous arrangement of our universe, see (LIDSEY et al., 2004; SINGH et al., 2006) for instance. Usually, there is an erst-while version of our universe collapsing due to gravitational effects until a certain point that it bounces back and initiates an expansion phase. As the universe was becoming smaller, there must be a limit to define how small the space-time can be. Otherwise, there would have been an instant in which the universe size confined the field in such a way that both position and velocity could be defined. In other words, without a boundary, the universe would have become as small as the field scale itself and eventually collapsed in a singularity. Consequently, the Heisenberg uncertainty principle would have been violated. In order to respect this fundamental principle of quantum mechanics, there must have been a physical process capable of ceasing

the contraction motion.

Following this direction, there is an idea of universe boundaries working like walls in a kind of cosmological Casimir effect. This effect should occur when the vacuum energy density, also called zero-point fluctuations, is distorted by changes in geometry (NAGATANI; SHIGETOMI, 2000). Regarding the primordial evolution, the universe boundaries would correspond to geometry and the vacuum energy would be represented by the energy content. Furthermore, Nagatani and Shigetomi (2000) discussed a generalization of the Casimir effect treating a one-dimensional spherical space with a scale factor similar to the one applied in FRW space-times. This approach was developed for models with a scalar field coupled with gravity. Thus, in principle, the Casimir effect could naturally be integrated into our scenario as the physical process responsible to generate the cosmological bounce.

The aspects related to super-inflationary phase and its transition to usual inflation are still in the research stage. There are some clues to be checked, but they are not our main objective for now. First, we should focus on obtaining an expression to $V_k(\varphi)$ in order to build a self-consistent inflationary evolution. Moreover, the physics behind the bounce is a top priority. After all this, the model would be in a suitable stage to be generalized to the perturbative level.

In its current state, our scenario provides several phenomenological implications about how the physics of the very early universe could be interpreted. Among them, we enumerate the main conclusions remarked during our study:

- a) The curvature could have been a structural balance element that played an essential role in controlling the primordial universe evolution.
- b) The matter-curvature coupling may have worked as the field potential term.
- c) The state parameter $w = -1/3$ commonly related to curvature-type fields seems to be the value in which the space-time evolution does not depend on its own curvature.
- d) The Higgs field could be the missing element to obtain a consistent formulation for LQC.
- e) The incorporation of Higgs inflation in mimic LQC inflationary description provides a consistent picture that could enable to recover both SCM and SMPP.

In conclusion, we must highlight the particular behavior of the mimetic curvature potential $V_k(\varphi) - ka^{-2}$ whose interpretation influences the final result similar to what happened with Einstein's cosmological constant. Note that the mimetic formalism could be the missing component capable to put together the best results obtained by the zoo of cosmological models available in the literature. It can be the interface among quantum gravity, cosmology and particle physics through Effective LQC dynamics that could provide a different perspective forward the study of the universe evolution. Recall that since gravity has its own particular nature beyond the current knowledge compared to the other interactions, a better understanding regarding the gravitational sector could be the key to solve the open problems in cosmology.

REFERENCES

- AAD, G. et al. Observation of a new particle in the search for the Standard Model Higgs boson with the ATLAS detector at the LHC. **Physics Letters B**, v. 716, p. 1–29, sep. 2012. 71
- ACHOUR, J. B.; LAMY, F.; LIU, H.; NOUI, K. Non-singular black holes and the limiting curvature mechanism: a hamiltonian perspective. **Journal of Cosmology and Astroparticle Physics**, v. 2018, n. 05, p. 072, 2018. 62
- ADE, P. A. et al. Planck 2015 results-xiii. cosmological parameters. **Astronomy & Astrophysics**, v. 594, p. A13, 2016. 8, 12, 20, 93
- ADE, P. A. R. et al. Detection of b-mode polarization at degree angular scales by bicep2. **Physical Review Letters**, v. 112, n. 24, p. 241101, 2014. 92
- ALCUBIERRE, M. **Introduction to 3+1 Numerical Relativity**. [S.l.]: Oxford University Press, 2008. 25
- ARROJA, F.; OKUMURA, T.; BARTOLO, N.; KARMAKAR, P.; MATARRESE, S. Large-scale structure in mimetic horndeski gravity. **Journal of Cosmology and Astroparticle Physics**, v. 2018, n. 05, p. 050, 2018. 53, 93
- ASHTEKAR, A. New variables for classical and quantum gravity. **Physical Review Letters**, v. 57, p. 2244–2247, nov. 1986. 36, 37, 41
- _____. New Hamiltonian formulation of general relativity. **Physical Review D**, v. 36, p. 1587–1602, sep. 1987. 37, 41
- ASHTEKAR, A.; PAWLOWSKI, T.; SINGH, P. Quantum nature of the big bang. **Physical Review Letters**, v. 96, n. 14, p. 141301, apr. 2006. 42, 43
- _____. Quantum nature of the big bang: improved dynamics. **Physical Review D**, v. 74, n. 8, p. 084003, oct. 2006. 21, 22, 34, 42, 44, 45, 46, 48
- ASHTEKAR, A.; SLOAN, D. Probability of inflation in loop quantum cosmology. **General Relativity and Gravitation**, v. 43, p. 3619–3655, dec. 2011. 48, 49
- ATLAS COLLABORATION. Observation of Higgs boson production in association with a top quark pair at the LHC with the ATLAS detector. **ArXiv 1806.00425**, jun. 2018. 71

BARBERO, J. F. G. Real Ashtekar variables for Lorentzian signature space-times. **Physical Review D**, v. 51, p. 5507–5510, may 1995. 37

BASKARAN, D.; GRISHCHUK, L. P.; POLNAREV, A. Imprints of relic gravitational waves in cosmic microwave background radiation. **Physical Review D**, v. 74, n. 8, p. 083008, 2006. 127, 128

BAUMANN, D. TASI lectures on inflation. **ArXiv 0907.5424**, jul. 2009. 6, 7, 10, 11, 13, 17

BEBRONNE, M. V.; TINYAKOV, P. G. Massive gravity and structure formation. **Physical Review D**, v. 76, n. 8, p. 084011, oct. 2007. 5

BEKENSTEIN, J. D. Relation between physical and gravitational geometry. **Physical Review D**, v. 48, p. 3641–3647, oct. 1993. 54

BENITO, M. M. **Cosmología cuántica de lazos: anisotropías e inhomogeneidades**. 223 p. Tesis (Doctor in Physics) — Universidad Complutense de Madrid, Madrid, 2010. Available from: <<https://arxiv.org/pdf/1109.5618.pdf>>. Access in: 22 feb. 2019. 37, 42, 43

BERTAZZO, N. **Cosmological implications of mimetic gravity**. 103 p. Thesis (Laurea Magistrale in Fisica) — Università degli Studi di Padova, Padova, 2015. Available from: <http://tesi.cab.unipd.it/50496/1/Tesi_LM_Bertazzo.pdf>. Access in: 21 mar. 2019. 61

BERTSCHINGER, E. **Hamiltonian formulation of general relativity**. 2005. Available from: <<http://web.mit.edu/edbert/GR/gr11.pdf>>. Access in: 12 feb. 2019. 29, 31, 36

BESSADA, D.; MIRANDA, O. D. CMB anisotropies induced by tensor modes in Massive Gravity. **Journal of Cosmology and Astroparticle Physics**, v. 8, p. 033, aug. 2009. 95, 96, 128

_____. CMB polarization in theories of gravitation with massive gravitons. **Classical and Quantum Gravity**, v. 26, n. 4, p. 045005, feb. 2009. 90, 92

BESSADA, D. F. A. **Studying signatures of alternative cosmologies in the cosmic microwave background**. 2010. 214 p. Tese (Doutorado em Astrofísica) — Instituto Nacional de Pesquisas Espaciais (INPE), São José dos Campos, 2010. Available from: <<sid.inpe.br/mtc-m19@80/2010/02.03.11.00-TDI>>. Access in: 13 mar. 2014. 6, 125, 126, 127

BEZERRA, E.; MIRANDA, O. D. Mimetic gravity: mimicking the dynamics of the primeval universe in the context of loop quantum cosmology. **The European Physical Journal C**, v. 79, n. 4, p. 310, 2019. [23](#), [67](#), [69](#), [78](#), [79](#), [85](#), [86](#), [100](#), [101](#), [102](#)

BEZERRA, E. V. J. **Um estudo sobre modelos cosmológicos com campos escalares não-canônicos**. 2015. 74 p. Dissertation (Mestrado em Astrofísica) — Instituto Nacional de Pesquisas Espaciais (INPE), São José dos Campos, 2015. Available from: sid.inpe.br/mtc-m21b/2015/02.05.16.01-TDI. Access in: 01 feb. 2019. [17](#)

BEZRUKOV, F. The Higgs field as an inflaton. **Classical and Quantum Gravity**, v. 30, n. 21, p. 214001, nov. 2013. [71](#), [72](#), [74](#), [75](#)

BEZRUKOV, F.; KALMYKOV, M. Y.; KNIEHL, B. A.; SHAPOSHNIKOV, M. Higgs boson mass and new physics. **Journal of High Energy Physics**, v. 2012, n. 10, p. 140, 2012. [71](#)

BEZRUKOV, F.; MAGNIN, A.; SHAPOSHNIKOV, M.; SIBIRYAKOV, S. Higgs inflation: consistency and generalisations. **Journal of High Energy Physics**, v. 2011, n. 1, p. 16, 2011. [72](#)

BEZRUKOV, F.; PAULY, M.; RUBIO, J. On the robustness of the primordial power spectrum in renormalized higgs inflation. **Journal of Cosmology and Astroparticle Physics**, v. 2018, n. 02, p. 040, 2018. [72](#), [75](#)

BEZRUKOV, F.; SHAPOSHNIKOV, M. The Standard Model Higgs boson as the inflaton. **Physics Letters B**, v. 659, p. 703–706, jan. 2008. [70](#), [71](#), [99](#)

_____. Higgs inflation at the critical point. **Physics Letters B**, v. 734, p. 249–254, 2014. [75](#)

BILSON-THOMPSON, S.; VAID, D. LQG for the Bewildered. **arXiv 1402.3586**, feb. 2014. [3](#), [7](#), [26](#), [27](#), [28](#)

BLAS, D. M. d. **Cosmología cuántica inhomogénea: teoría cuántica de campos y gravedad de lazos**. 2013. 205 p. Tesis (Doctor en Física) — Universidad Complutense de Madrid, Madrid, 2013. Available from: <http://eprints.ucm.es/24119/1/T35058.pdf>. Access in: 22 feb. 2019. [38](#), [40](#), [42](#), [43](#)

BLAU, M. **Lecture notes on general relativity**. Bern, Germany: Albert Einstein Center for Fundamental Physics, 2011. [28](#), [29](#)

BODENDORFER, N.; SCHÄFER, A.; SCHLIEMANN, J. Canonical structure of general relativity with a limiting curvature and its relation to loop quantum gravity. **Physical Review D**, v. 97, n. 8, p. 084057, apr. 2018. 61

BOJOWALD, M. The early universe in loop quantum cosmology. **Journal of Physics Conference Series**, v. 24, p. 77–86, jan. 2005. 2, 41, 48

BOJOWALD, M.; HOSSAIN, G. M. Cosmological vector modes and quantum gravity effects. **Classical and Quantum Gravity**, v. 24, p. 4801–4816, sep. 2007. 40

BOJOWALD, M.; HOSSAIN, G. M. Loop quantum gravity corrections to gravitational wave dispersion. **Physical Review D**, v. 77, n. 2, p. 023508, jan. 2008. 29, 36, 37, 38, 40, 46, 48, 89, 90, 124

BOJOWALD, M.; KAGAN, M.; SINGH, P.; HERNÁNDEZ, H. H.; SKIRZEWSKI, A. Hamiltonian cosmological perturbation theory with loop quantum gravity corrections. **Physical Review D**, v. 74, n. 12, p. 123512, dec. 2006. 42

BOJOWALD, M.; MORALES-TÉCOLT, H. A. Cosmological applications of loop quantum gravity. **Lecture Notes in Physics**, v. 646, p. 421–462, 2004. 43

BONOGUORE, T. **The rise of cosmology’s “big bounce”**. 2018. Available from: <<https://insidetheperimeter.ca/long-read-big-bounce/>>. Access in: 23 mar. 2019. 49

BOOT, T. **The road to loop quantum gravity**. 2008. 40 p. Bachelorscriptie Natuurkunde — Faculteit der Wiskunde en Natuurwetenschappen, Groningen, 2008. Available from: <http://thep.housing.rug.nl/sites/default/files/theses/Bachelor%20thesis_Tom%20Boot.pdf>. Access in: 22 feb. 2019. 32, 37, 40, 41

BOSE, N.; MAJUMDAR, A. S. k-essence model of inflation, dark matter, and dark energy. **Physical Review D**, v. 79, n. 10, p. 103517, may 2009. 19

BRAWER, R. **Inflationary cosmology and horizon and flatness problems: the mutual constitution of explanation and questions**. 1995. 81 p. Dissertation (Master of Science in Physics) — Massachusetts Institute of Technology (MIT), Cambridge, 1995. Available from: <<https://core.ac.uk/download/pdf/4403152.pdf>>. Access in: 06 may 2019. 10, 12

- BUONANNO, A. Gravitational waves. **ArXiv 0709.4682v1**, 2007. 91
- CABELLA, P.; KAMIONKOWSKI, M. Theory of cosmic microwave background polarization. **arXiv astro-ph/0403392**, 2004. 127
- CAPOZZIELLO, S.; MATSUMOTO, J.; NOJIRI, S.; ODINTSOV, S. D. Dark energy from modified gravity with lagrange multipliers. **Physics Letters B**, v. 693, n. 2, p. 198–208, 2010. 53
- CAROLI, R. **Cosmological aspects of mimetic gravity**. 2018. 92 p. Thesis (Master in Cosmology) — Ludwig Maximilians Universitat Munchen, Muchen, 2018. Available from: <<https://www.theorie.physik.uni-muenchen.de/TMP/theses/thesiscaroli.pdf>>. Access in: 25 mar. 2019. 57
- CARROLL, S. M. **Spacetime and geometry. an introduction to general relativity**. [S.l.: s.n.], 2004. 2, 26, 29
- _____. **WMAP results — cosmology makes sense!** 2006. Available from: <<http://www.preposterousuniverse.com/blog/2006/03/16/wmap-results-cosmology-makes-sense/>>. Access in: 12 apr. 2019. 92
- CASALINO, A.; RINALDI, M.; SEBASTIANI, L.; VAGNOZZI, S. Mimicking dark matter and dark energy in a mimetic model compatible with GW170817. **Physics of the Dark Universe**, v. 22, p. 108–115, dec. 2018. 96
- _____. Alive and well: mimetic gravity and a higher-order extension in light of GW170817. **Classical and Quantum Gravity**, v. 36, n. 1, p. 017001, jan. 2019. 96
- CASARES, P. A. M. **An review on loop quantum gravity**. 2018. 75 p. Thesis (Master in Mathematical and Theoretical Physics) — University of Oxford, Trinity, 2018. Available from: <<https://arxiv.org/pdf/1808.01252.pdf>>. Access in: 22 feb. 2019. 40
- CERN. **Higgs boson comes out on top**. 2018. Available from: <<https://home.cern/about/updates/2018/06/higgs-boson-comes-out-top>>. Access in: 06 feb. 2019. 71
- CHAMSEDDINE, A. H.; MUKHANOV, V. Mimetic dark matter. **Journal of High Energy Physics**, v. 11, p. 135, nov. 2013. 23, 53, 54, 55, 57

_____. Nonsingular black hole. **European Physical Journal C**, v. 77, p. 183, mar. 2017. 61

_____. Resolving cosmological singularities. **Journal of Cosmology and Astroparticle Physics**, v. 3, p. 009, mar. 2017. 23, 57, 61, 64

_____. Ghost free mimetic massive gravity. **Journal of High Energy Physics**, v. 6, p. 60, jun. 2018. 78, 95, 100, 101

_____. Mimetic massive gravity: beyond linear approximation. **Journal of High Energy Physics**, v. 6, p. 62, jun. 2018. 78, 100

CHAMSEDDINE, A. H.; MUKHANOV, V.; VIKMAN, A. Cosmology with Mimetic Matter. **Journal of Cosmology and Astroparticle Physics**, v. 6, p. 017, jun. 2014. 23, 55, 57, 58, 100

CHANDRASEKHAR, S. **Radiative Transfer**. Dover Publications, 1960. (Dover Books on Intermediate and Advanced Mathematics). ISBN 9780486605906. Available from: <<https://books.google.com.br/books?id=CK3HDRwCT5YC>>. 125

CHATRCHYAN, S. et al. Observation of a new boson at a mass of 125 GeV with the CMS experiment at the LHC. **Physics Letters B**, v. 716, p. 30–61, sep. 2012. 71

COGNOLA, G.; MYRZAKULOV, R.; SEBASTIANI, L.; VAGNOZZI, S.; ZERBINI, S. Covariant hořava-like and mimetic horndeski gravity: cosmological solutions and perturbations. **Classical and quantum gravity**, v. 33, n. 22, p. 225014, 2016. 99

COMMISSARIAT, T. **BICEP2 finds first direct evidence of cosmic inflation**. 2014. Available from: <<https://physicsworld.com/a/bicep2-finds-first-direct-evidence-of-cosmic-inflation/>>. Access in: 05 feb. 2019. 22

COOK, J. L.; DIMASTROGIOVANNI, E.; EASSON, D. A.; KRAUSS, L. M. Reheating predictions in single field inflation. **Journal of Cosmology and Astroparticle Physics**, v. 2015, n. 04, p. 047, 2015. 85

DENGIZ, S. $3+1$ orthogonal and conformal decomposition of the einstein equation and the adm formalism for general relativity. **arXiv preprint arXiv:1103.1220**, 2011. 27

- D'IVERNNO, R. A. **Introducing Einstein's relativity**. New York: Oxford University Press, 1992. 91
- DODELSON, S. **Modern cosmology**. Massachusetts, USA: Academic Press, 2003. 6, 7, 8, 9, 19, 125, 126
- DONÁ, P.; SPEZIALE, S. Introductory lectures to loop quantum gravity. **arXiv 1007.0402**, jul. 2010. 25, 36, 39, 40, 41, 50
- DUTTA, J.; KHYLLEP, W.; SARIDAKIS, E. N.; TAMANINI, N.; VAGNOZZI, S. Cosmological dynamics of mimetic gravity. **Journal of Cosmology and Astroparticle Physics**, v. 2, p. 041, feb. 2018. 61
- ELLIS, G. The standard cosmological model: achievements and issues. **Foundations of Physics**, p. 1–20, 2018. 2, 5
- FERREIRA, C. G. V. **Confrontando modelos de energia escura com a taxa de formação estelar cósmica, LGRB e fundos estocásticos de ondas gravitacionais**. 2014. 214 p. Dissertation (Mestrado em Astrofísica) — Instituto Nacional de Pesquisas Espaciais (INPE), São José dos Campos, 2014. Available from: <sid.inpe.br/mtc-m21b/2014/04.04.19.26-TDI>. Access in: 04 jul. 2016. 91
- FIROUZJAH, H.; GORJI, M. A.; MANSOORI, S. A. H. Instabilities in mimetic matter perturbations. **Journal of Cosmology and Astroparticle Physics**, v. 7, p. 031, jul. 2017. 66
- FLEISCHHACK, C. On ashtekar's formulation of general relativity. **Journal of Physics**, v. 320, 2012. 38, 40
- FOFFANO, L. **Cosmological perturbations in mimetic gravity models**. 110 p. Thesis (Laurea Magistrale in Fisica) — Università degli Studi di Padova, Padova, 2016. Available from: <http://tesi.cab.unipd.it/53513/1/Tesi_LM_Foffano.pdf>. Access in: 21 mar. 2019. 55, 58, 60
- GALLI, S. **Cosmic Microwave Background - Lecture I**. Paris: [s.n.], 2015. Available from: <http://isapp2015.in2p3.fr/talks/Galli_CMB1.pdf>. Access in: 11 jun. 2019. 126
- GAMBINI, R.; PULLIN, P. **A first course in loop quantum gravity**. New York: Oxford University Press, 2011. 179 p. 2, 21, 25, 32, 33, 34, 35, 37, 39, 123

- GANZ, A.; BARTOLO, N.; KARMAKAR, P.; MATARRESE, S. Gravity in mimetic scalar-tensor theories after GW170817. **Journal of Cosmology and Astroparticle Physics**, v. 1, p. 056, jan. 2019. [96](#)
- GAO, C.; GONG, Y.; WANG, X.; CHEN, X. Cosmological models with Lagrange multiplier field. **Physics Letters B**, v. 702, p. 107–113, aug. 2011. [53](#)
- GOLOVNEV, A. On the recently proposed mimetic Dark Matter. **Physics Letters B**, v. 728, p. 39–40, jan. 2014. [57](#), [58](#)
- GORJI, M. A.; MANSOORI, S. A. H.; FIROUZJAH, H. Higher derivative mimetic gravity. **Journal of Cosmology and Astroparticle Physics**, v. 1, p. 020, jan. 2018. [56](#), [57](#), [61](#), [62](#)
- GOURGOULHON, E. 3+1 Formalism and Bases of Numerical Relativity. **arXiv gr-qc/0703035**, mar. 2007. [28](#)
- GRIBEL, C. **Connecting the cosmic star formation rate with the local star formation rate**. 2018. 101 p. Tese (Doutorado em Astrofísica) — Instituto Nacional de Pesquisas Espaciais (INPE), São José dos Campos, 2018. Available from: sid.inpe.br/mtc-m21b/2018/02.05.17.02-TDI. Access in: 26 mar. 2019. [56](#)
- GRON, O.; HERVIK, S. **Einstein’s general theory of relativity with modern applications in cosmology**. New York, USA: Springer, 2007. [2](#), [5](#), [6](#), [7](#)
- GUZZETTI, M. C.; BARTOLO, N.; LIGUORI, M.; MATARRESE, S. Gravitational waves from inflation. **ArXiv e-prints**, may 2016. [7](#), [12](#), [15](#), [16](#), [17](#), [18](#), [91](#)
- HARO, J. de; AMORÓS, J. Bouncing cosmologies via modified gravity in the ADM formalism: application to loop quantum cosmology. **Physical Review D**, v. 97, n. 6, p. 064014, mar. 2018. [62](#)
- HARO, J. de; ODINTSOV, S. D.; OIKONOMOU, V. K. Viable inflationary evolution from Einstein frame loop quantum cosmology. **Physical Review D**, v. 97, n. 8, p. 084052, apr. 2018. [21](#), [22](#)
- HARO, J. de; SALÓ, L. A.; ELIZALDE, E. Cosmological perturbations in a class of fully covariant modified theories: application to models with the same background as standard LQC. **ArXiv e-prints**, jun. 2018. [62](#)

- HARO, J. de; SALÓ, L. A.; PAN, S. Mimetic loop quantum cosmology. **ArXiv e-prints**, mar. 2018. 62
- HIRANO, S.; NISHI, S.; KOBAYASHI, T. Healthy imperfect dark matter from effective theory of mimetic cosmological perturbations. **Journal of Cosmology and Astroparticle Physics**, v. 2017, n. 07, p. 009, 2017. 96
- KAMIONKOWSKI, M.; KOSOWSKY, A.; STEBBINS, A. Statistics of cosmic microwave background polarization. **Physical Review D**, v. 55, n. 12, p. 7368, 1997. 127
- KEHAGIAS, A.; DIZGAH, A. M.; RIOTTO, A. Remarks on the starobinsky model of inflation and its descendants. **Physical Review D**, v. 89, n. 4, p. 043527, 2014. 74
- KINNEY, W. H. Cosmology, inflation, and the physics of nothing. **ArXiv 0301448**, jan. 2003. 10, 125
- _____. TASI lectures on inflation. **arXiv 0902.1529**, feb. 2009. 17
- KOLB, E. W.; TURNER, M. S. **The early universe**. [S.l.: s.n.], 1990. 71
- KROON, J. **Mathematical problems of General Relativity - Lecture 2**. London: [s.n.], 2013. Available from: <<http://www.maths.qmul.ac.uk/~jav/LTCCmaterial/LTCCslidesLecture2.pdf>>. Access in: 11 jun. 2019. 119
- LANGLOIS, D.; LIU, H.; NOUI, K.; WILSON-EWING, E. Effective loop quantum cosmology as a higher-derivative scalar-tensor theory. **Classical and Quantum Gravity**, v. 34, n. 22, p. 225004, nov. 2017. ix, xi, 23, 37, 38, 39, 40, 42, 43, 44, 45, 46, 47, 48, 55, 58, 61, 62, 63, 64, 65, 67, 77, 78, 89, 93, 99, 100, 101
- LANGLOIS, D.; MANCARELLA, M.; NOUI, K.; VERNIZZI, F. Mimetic gravity as DHOST theories. **Journal of Cosmology and Astroparticle Physics**, v. 2, p. 036, feb. 2019. 58, 62
- LIDDLE, A. R. **An introduction to cosmological inflation**. London, Jan 1999. Available from: <<https://cds.cern.ch/record/376174>>. 12
- LIDSEY, J. E.; MULRYNE, D. J.; NUNES, N. J.; TAVAKOL, R. Oscillatory universes in loop quantum cosmology and initial conditions for inflation. **Physical Review D**, v. 70, n. 6, p. 063521, sep. 2004. 102

LIGO COLLABORATION. **Gravitational waves**. California Institute of Technology: [s.n.], 2019. Available from: <https://www.ligo.caltech.edu/page/gravitational-waves>. Access in: 08 apr. 2019. 89, 90

LIM, E. A.; SAWICKI, I.; VIKMAN, A. Dust of dark energy. **Journal of Cosmology and Astroparticle Physics**, v. 5, p. 012, may 2010. 53

LIN, T. Tasi lectures on dark matter models and direct detection. **ArXiv 1904.07915**, 2019. 53

LINDE, A. Inflationary cosmology. In: LEMOINE, M.; MARTIN, J.; PETER, P. (Ed.). **Inflationary Cosmology**. [S.l.]: Springer, 2007. v. 738, p. 1–54. 72

LUC, J.; MIELCZAREK, J. Slow-roll approximation in loop quantum cosmology. **Journal of Cosmology and Astroparticle Physics**, v. 1, p. 045, jan. 2017. 49, 71, 102

MARTINS, G. L. **Sobre a quantização de laços de teorias topológicas em 2 + 1 dimensões: gravitação e Chern-Simons**. 2009. 238 p. Dissertação (Mestrado em Física) — Universidade Federal do Espírito Santo (UFES), Vitória, 2009. Available from: http://www.ifsc.usp.br/~gabriel.luchini/master_thesis.pdf. Access in: 19 mar. 2016. 2, 3, 6, 25, 26, 28, 32, 35, 36, 38, 119

MEISSNER, K. A. Black-hole entropy in loop quantum gravity. **Classical and Quantum Gravity**, v. 21, p. 5245–5251, nov. 2004. 39

MIELCZAREK, J. Gravitational waves from the big bounce. **Journal of Cosmology and Astroparticle Physics**, v. 11, p. 011, nov. 2008. 91

_____. Tensor power spectrum with holonomy corrections in loop quantum cosmology. **Physical Review D**, v. 79, n. 12, p. 123520, jun. 2009. 43

_____. Possible observational effects of loop quantum cosmology. **Physical Review D**, v. 81, n. 6, p. 063503, mar. 2010. 39, 43, 94, 95

_____. Signature change in loop quantum cosmology. In: BIČÁK, J.; LEDVINKA, T. (Ed.). **Springer proceedings in physics**. [S.l.: s.n.], 2014. (Springer proceedings in physics, v. 157), p. 555. 39, 40, 42, 45, 46, 52

- MIELCZAREK, J.; CAILLETEAU, T.; BARRAU, A.; GRAIN, J. Anomaly-free vector perturbations with holonomy corrections in loop quantum cosmology. **Classical and Quantum Gravity**, v. 29, n. 8, p. 085009, 2012. 124
- MIELCZAREK, J.; HRYCYNA, O.; SZYDŁOWSKI, M. Effective dynamics of the closed loop quantum cosmology. **Journal of Cosmology and Astroparticle Physics**, v. 11, p. 014, nov. 2009. 21, 48, 81, 83
- MILGROM, M. A modification of the newtonian dynamics as a possible alternative to the hidden mass hypothesis. **The Astrophysical Journal**, v. 270, p. 365–370, 1983. 53
- MOKHTAR, W. M. H. W. **An introduction to loop quantum gravity with application to cosmology**. 2014. 51 p. Dissertation (Master of Science) — Imperial College London, London, 2014. Available from: <<https://pdfs.semanticscholar.org/f6d7/9dd30ddea7a5e41cb1fb2031a08c9d205f65.pdf>>. Access in: 09 feb. 2019. 27
- MOSS, I. G. Covariant one-loop quantum gravity and Higgs inflation. **ArXiv e-prints**, sep. 2014. 72, 74
- MUKHANOV, V. F.; FELDMAN, H. A.; BRANDENBERGER, R. H. Theory of cosmological perturbations. **Review Section of Physics Letters**, v. 215, p. 203–333, 1992. 12, 18, 90
- NAGATANI, Y.; SHIGETOMI, K. Effective theoretical approach to back reaction of the dynamical Casimir effect in 1+1 dimensions. **Physical Review A**, v. 62, n. 2, p. 022117, aug. 2000. 103
- NASA/JAMES WEBB SPACE TELESCOPE. **First Light & Reionization**. 2019. Available from: <<https://jwst.nasa.gov/firstlight.html>>. Access in: 16 may 2019. 10
- NASA/WMAP SCIENCE TEAM. **Timeline of the universe**. 2012. Available from: <<https://map.gsfc.nasa.gov/media/060915/index.html>>. Access in: 05 feb. 2019. 4
- NI, S.; LI, H.; QIU, T.; ZHENG, W.; ZHANG, X. Probing signatures of bounce inflation with current observations. **European Physical Journal C**, v. 78, p. 608, aug. 2018. 94
- PAPAPETROU, A. **Lectures on general relativity**. Dordrecht: D. Reidel Publishing, 1974. 203 p. 6

PEREIRA, T. A. **3+ 1 formalism in General Relativity**. 2018. 89 p.
Dissertation (Mestrado em Física) — Universidade Federal do Rio Grande do Norte (UFRN), Natal, 2018. Available from:
<<https://repositorio.ufrn.br/jspui/handle/123456789/25308>>. Access in:
08 feb. 2019. 25, 26, 29, 30

POSTMA, M.; VOLPONI, M. Equivalence of the Einstein and Jordan frames. **Physical Review D**, v. 90, n. 10, p. 103516, nov. 2014. 72, 73, 74

PRASAD, J. **Cosmic Microwave Background Radiation - Lecture 1 : Physics of CMB**. Pilani: [s.n.], 2013. Available from:
<<http://www.iucaa.in/~jayanti/docs/cmb-part1.pdf>>. Access in: 11 jun. 2019. 126

QUINTIN, J. **Quick review of the ADM formalism in General Relativity**. 2015. Available from:
<<http://www.physics.mcgill.ca/~jquintin/GradSeminar2015.pdf>>. Access in: 08 feb. 2019. 26

RABOCHAYA, Y.; ZERBINI, S. A note on a mimetic scalar-tensor cosmological model. **European Physical Journal C**, v. 76, p. 85, feb. 2016. 54, 58

RUBIO, J. Higgs inflation and vacuum stability. **Journal of Physics: Conference Series**, v. 631, n. 1, p. 012032, 2015. 75, 100

RYDEN, B. **Introduction to cosmology**. San Francisco: Addison Wesley, 2003. 244 p. 20

SADJADI, H. M. On solutions of loop quantum cosmology. **European Physical Journal C**, v. 73, p. 2571, sep. 2013. 43, 82, 83, 85, 86, 87

SALIWANCIK, B. **Multichroic TES Bolometers and Galaxy Cluster Mass Scaling Relations with the South Pole Telescope**. 2015. 188 p.
Dissertation (Doctor of Philosophy) — Case Western Reserve University, Cleveland, 2015. Available from: <<https://arxiv.org/pdf/1601.05452.pdf>>. Access in: 13 jun. 2019. 128

SALTAS, I. D. Higgs inflation and quantum gravity: an exact renormalisation group approach. **Journal of Cosmology and Astroparticle Physics**, v. 2, p. 048, feb. 2016. 71

SEBASTIANI, L.; VAGNOZZI, S.; MYRZAKULOV, R. Mimetic gravity: a review of recent developments and applications to cosmology and astrophysics. **Advances in High Energy Physics**, v. 2017, dec. 2017. 2, 21, 53, 54, 55, 56, 57, 58, 100

SHAPOSHNIKOV, M. The Higgs boson and cosmology. **Philosophical Transactions of the Royal Society of London Series A**, v. 373, p. 20140038–20140038, nov. 2015. 23, 71

SINGH, P. Viewpoint: a glance at the earliest universe. **Physics**, v. 5, p. 142, 2012. 51

SINGH, P.; VANDERSLOOT, K.; VERESHCHAGIN, G. V. Nonsingular bouncing universes in loop quantum cosmology. **Physical Review D**, v. 74, n. 4, p. 043510, aug. 2006. 102

SIRUNYAN, A. M. et al. Observation of $t\bar{t}H$ production. **Physical Review Letters**, v. 120, n. 23, p. 231801, 2018. 71

TAKAHASHI, K.; KOBAYASHI, T. Extended mimetic gravity: Hamiltonian analysis and gradient instabilities. **Journal of Cosmology and Astroparticle Physics**, v. 11, p. 038, nov. 2017. 97

TAKAHASHI, K.; MOTOHASHI, H.; SUYAMA, T.; KOBAYASHI, T. General invertible transformation and physical degrees of freedom. **Physical Review D**, APS, v. 95, n. 8, p. 084053, 2017. 54

TAVAKOLY, Y. **Lecture II: Hamiltonian formulation of general relativity**. 2014. Available from: <<http://www.cosmo-ufes.org/uploads/1/3/7/0/13701821/lect.notes-2.pdf>>. Access in: 05 feb. 2019. 25, 26, 27, 29, 30, 35, 36

THIEMANN, T. **Modern canonical quantum general relativity**. [S.l.]: Cambridge University Press, 2007. 41

TONG, D. **Lectures on string theory**. 2012. Available from: <<http://www.damtp.cam.ac.uk/user/tong/string/four.pdf>>. Access in: 18 mar. 2019. 54

TONG, F. **A Hamiltonian formulation of general relativity**. 2006. Available from: <<http://www.math.toronto.edu/mccann/assignments/426/Tong.pdf>>. Access in: 07 feb. 2019. 28

- WALLACE, D. The quantization of gravity-an introduction. **arXiv preprint gr-qc/0004005**, 2000. 42
- WAN, Y.; QIU, T.; HUANG, F. P.; CAI, Y.; LI, H.; ZHANG, X. Bounce inflation cosmology with standard model higgs boson. **Journal of Cosmology and Astroparticle Physics**, v. 2015, n. 12, p. 019, 2015. 99
- WANG, Y. Inflation, cosmic perturbations and non-gaussianities. **Commun. Theor. Phys.**, v. 62, p. 109–166, 2014. 11, 14
- WATSON, G. S. An exposition on inflationary cosmology. **ArXiv 0005003v2**, 2000. Available from: <<http://xxx.lanl.gov/pdf/astro-ph/0005003v2>>. Access in: 16 aug. 2016. 14
- WEINBERG, S. Gravitation and Cosmology: Principles and Applications of the General Theory of Relativity. **American Journal of Physics**, v. 41, n. 4, p. 598–599, 1973. 2
- YOKOYAMA, J. Inflation: 1980–201x. **Progress of Theoretical and Experimental Physics**, v. 2014, n. 6, 2014. 85
- YOSHIDA, D.; QUINTIN, J.; YAMAGUCHI, M.; BRANDENBERGER, R. H. Cosmological perturbations and stability of nonsingular cosmologies with limiting curvature. **Physical Review D**, v. 96, n. 4, p. 043502, aug. 2017. 66
- ZHANG, X.; LING, Y. Inflationary universe in loop quantum cosmology. **Journal of Cosmology and Astroparticle Physics**, v. 8, p. 012, aug. 2007. 39, 47
- ZHENG, Y.; SHEN, L.; MOU, Y.; LI, M. On (in)stabilities of perturbations in mimetic models with higher derivatives. **Journal of Cosmology and Astroparticle Physics**, v. 8, p. 040, aug. 2017. 66, 97

APPENDIX A - How to obtain the ADM Lagrangian?

Basically, \mathcal{L}_{ADM} is just a different way to write \mathcal{L}_{EH} in which the variables N , N_a and q_{ab} are used to reproduce the evolution of the space-time metric $g_{\mu\nu}$. First, let us start with S_{EH} defined in the simplest form

$$S_{\text{EH}} = \int d^4x \sqrt{-g} R, \quad (\text{A.1})$$

and identify the ADM variables with the $g_{\mu\nu}$ components as

$$N = \sqrt{-g^{00}}, \quad N_a = g_{a0} \quad \text{and} \quad q_{ab} = g_{ab}. \quad (\text{A.2})$$

The term $\sqrt{-g}$ can be obtained from (2.4), however, the space-time Ricci scalar will require more effort to be rewritten in a suitable way to derive (2.9).

In other words, to build \mathcal{L}_{ADM} , it is necessary to relate the space-time curvature with the Σ one. In order to achieve this goal we follow the development presented in (MARTINS, 2009), starting with the Gauss-Codazzi equations:

$${}^{(3)}R_{\rho\sigma\eta}^{\theta} = q_{\rho}^{\alpha} q_{\sigma}^{\beta} q_{\eta}^{\gamma} q_{\mu}^{\theta} R_{\alpha\beta\gamma}^{\mu} - K_{\rho\eta} K_{\sigma}^{\theta} + K_{\sigma\eta} K_{\rho}^{\theta} \quad (\text{A.3})$$

and

$$D_{\mu} K_{\nu}^{\mu} - D_{\nu} K_{\mu}^{\mu} = R_{\alpha\beta} n^{\beta} q_{\nu}^{\alpha}. \quad (\text{A.4})$$

Note that (A.3) establishes a relation between the spatial projection of the spacetime curvature with the hypersurface analog. Moreover, (A.4) describes the behavior of the 4-dimensional Riemann tensor projected along the normal direction (KROON, 2013; MARTINS, 2009).

The next step is to rewrite the Einstein tensor in term of N and N_a . This can be performed by writing it as $G_{\mu\nu} = A_{\mu} B_{\nu}$, where each vector is decomposed into the orthogonal base like

$$A_{\mu} = N n_{\mu} + q_{\mu}^{\alpha} N_{\alpha}. \quad (\text{A.5})$$

As a tensor, $G_{\mu\nu}$ has time, space and mixed components:

$$G_{\perp\perp} = G_{\mu\nu}n^\mu n^\nu, \quad G_{\perp\beta} = -G_{\mu\nu}n^\mu q_\beta^\nu, \quad G_{\alpha\perp} = -G_{\mu\nu}n^\nu q_\alpha^\mu \quad \text{and} \quad G_{\alpha\beta} = G_{\mu\nu}q_\alpha^\mu q_\beta^\nu, \quad (\text{A.6})$$

where \perp indicates the perpendicular component regarding the hypersurface. Thus, $G_{\mu\nu}$ can be expressed in the form

$$G_{\mu\nu} = G_{\perp\perp}n_\mu n_\nu + G_{\perp\beta}n_\mu q_\nu^\beta + G_{\alpha\perp}n_\nu q_\mu^\alpha + G_{\alpha\beta}q_\mu^\alpha q_\nu^\beta. \quad (\text{A.7})$$

In GR, $G_{\mu\nu}$ is diagonal as a result of the homogeneity and isotropy feature of the FRW universe. Therefore, considering that the same applies to this case, the mixed components will be null since $n_\nu q_\mu^\alpha = 0$. Remember from chapter 2 that $q_\mu^\alpha = q_b^a$ and $n_\nu = n_0$, consequently,

$$G_{\mu\nu}n^\mu q_\beta^\nu = 0. \quad (\text{A.8})$$

Substituting (1.4) into (A.8), the result is the equality

$$q_\alpha^\mu R_{\mu\nu}n_\nu = 0, \quad (\text{A.9})$$

which enables us to rewrite (A.4) as

$$D_b K_a^b - D_a K_b^b = 0. \quad (\text{A.10})$$

The time component of Einstein's tensor can be obtained by working with the Riemann tensor and equation (2.3) as it follows

$$R_{\mu\nu\rho\sigma}q^{\mu\rho}q^{\nu\sigma} = R + 2R_{\mu\rho}n^\mu n^\rho = 2G_{\mu\rho}n^\mu n^\rho. \quad (\text{A.11})$$

If we try to derive the term $R_{\mu\nu\rho\sigma}q^{\mu\rho}q^{\nu\sigma}$ from (A.3), the result is determined by the expression

$$R_{\mu\nu\rho\sigma}q^{\mu\rho}q^{\nu\sigma} = {}^{(3)}R + K^2 - K_{\mu\nu}K^{\mu\nu}. \quad (\text{A.12})$$

Thus, comparing (A.11) and (A.12), the obtained relation must be

$$G_{\mu\nu}n^\mu n^\nu = \frac{1}{2} \left[{}^{(3)}R + K^2 - K_{\mu\nu}K^{\mu\nu} \right]. \quad (\text{A.13})$$

Just like in the previous procedure, $G_{\mu\nu}n^\mu n^\nu$ is rewritten considering the equation (1.4) which results in

$$G_{\mu\nu}n^\mu n^\nu = R_{\mu\nu}n^\mu n^\nu + \frac{1}{2}R. \quad (\text{A.14})$$

Once (A.13) and (A.14) must be equal, the 4-dimensional Ricci scalar can be described by

$$R = {}^{(3)}R + K^2 - K_{\mu\nu}K^{\mu\nu} - 2R_{\mu\nu}n^\mu n^\nu. \quad (\text{A.15})$$

The idea is to write $R_{\mu\nu}n^\mu n^\nu$ in terms of $K_{\mu\nu}$ which is performed through the relation

$$(R_{\mu\rho\nu}^{\rho}n^\mu)n^\nu = \nabla_\rho(n^\nu\nabla_\nu n^\rho) - \nabla_\rho n^\nu\nabla_\nu n^\rho - \nabla_\nu(n^\nu\nabla_\rho n^\rho) + \nabla_\nu n^\nu\nabla_\rho n^\rho. \quad (\text{A.16})$$

Since $K_{\mu\nu}K^{\mu\nu}$ does not have time component, from (2.6), (A.16) can be expressed as

$$R_{\mu\rho\nu}^{\rho}n^\mu n^\nu = K^2 - K_{\mu\nu}K^{\mu\nu}. \quad (\text{A.17})$$

Finally, by plugging (A.17) into (A.16), the 4-dimension Ricci scalar can be written in the form

$$R = {}^{(3)}R - K^2 + K_{ab}K^{ab}. \quad (\text{A.18})$$

Thus, the ADM Lagrangian corresponds to the equation

$$\mathcal{L}_{\text{ADM}} = \sqrt{-g}R = N\sqrt{q}[K_{ab}K^{ab} - K^2 + {}^{(3)}R]. \quad (\text{A.19})$$

APPENDIX B - Some details about the Hamiltonian constraint of Loop Quantum Cosmology and the sine function

As mentioned before, $\Omega_{ab}{}^k = 0$ since the space-time is a flat FRW one. Moreover, $q_{ab} = g_{ab}$ implies that $q_{ab} = \text{diag}(a^2, a^2, a^2) = \text{diag}(p, p, p)$. Therefore, (2.46) can be written as

$$\mathcal{H} = -\frac{E_i^a E_j^b}{16\pi G \gamma^2 p^{3/2}} \epsilon^{ij}{}_k F_{ab}{}^k + \frac{\pi_\varphi^2}{2p^{3/2}} + p^{3/2} V(\varphi). \quad (\text{B.1})$$

Plugging (2.52) into (2.47) and working with the properties of the Levi-Civita symbol and the symmetry associated with the Ashtekar connection, $\epsilon^{ij}{}_k F_{ab}{}^k$ could be described by the relation

$$\epsilon^{ij}{}_k F_{ab}{}^k = 6c^2 (dx^i)_a (dx^j)_b. \quad (\text{B.2})$$

The final step is to substitute the LQC densitized triad definition (2.51) and (B.2) in (B.1) which enables us to obtain the LQC Hamiltonian constraint

$$\mathcal{H} = -\frac{3}{8\pi G \gamma^2} p^{1/2} c^2 + \frac{\pi_\varphi^2}{2p^{3/2}} + p^{3/2} V(\varphi). \quad (\text{B.3})$$

At this point, the Hamiltonian constraint cannot be promoted to operator level due to the absence of an analog operator for c . In order to overcome this situation, the strategy implemented was to replace c as it follows

$$c \rightarrow \frac{\sin \bar{\mu} c}{\bar{\mu}}. \quad (\text{B.4})$$

The sine function can be expanded in terms of holonomies (GAMBINI; PULLIN, 2011). Remember that, as an exponential function, holonomy can be decomposed in sine and cosine functions. Thus, considering (B.4) and (2.56), the Hamiltonian constraint acquires the effective structure

$$\mathcal{H}_{eff} = -\frac{3p^{3/2}}{8\pi G \Delta \gamma^2} \sin^2 \bar{\mu} c + \frac{\pi_\varphi^2}{2p^{3/2}} + p^{3/2} V(\varphi). \quad (\text{B.5})$$

In other words, introducing the sine function within the Hamiltonian can be interpreted as a direct consequence of the holonomy corrections since they are used to regularize the classical constraints to incorporate the Ashtekar connection (MIEL-

CZAREK et al., 2012).

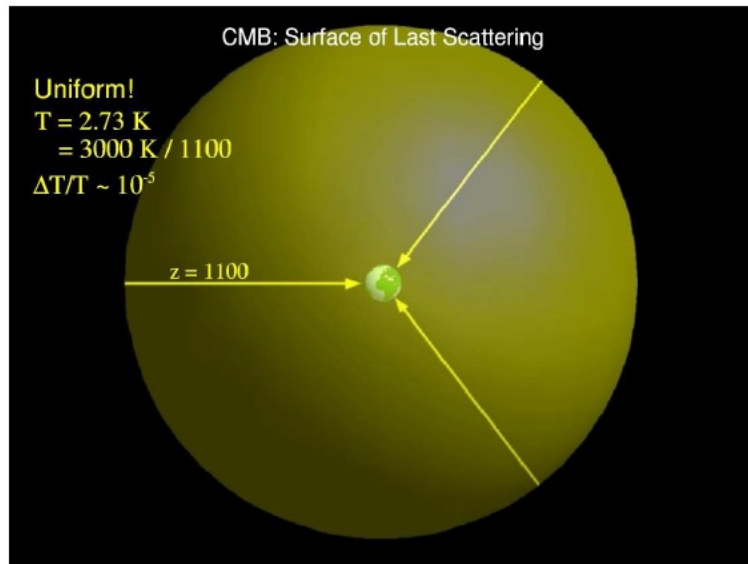
In principle, the use of the sine function should be restricted to small values of its argument which would exclude the bounce phase. Notwithstanding, for an isotropic universe dominated by a massless-free scalar field, the Ashtekar connection can also be replaced during the bounce stage too (BOJOWALD; HOSSAIN, 2008).

Another key aspect to be emphasized is the fact that the sine function contains higher order terms of the extrinsic curvature which should be understood as a short way to express the leading order corrections (BOJOWALD; HOSSAIN, 2008). Therefore, the sine function from MG representation of LQC could also hide higher terms related to the higher derivative scalar-tensor theory.

APPENDIX C - Cosmic Microwave Background: physics and statistics

As an electromagnetic wave, CMB can be explored through the Stokes parameters. Basically, an observer on Earth receives CMB photons from all directions at the same time. From Figure C.1, see that SLS is considered from a geocentric perspective. The strategy implemented was to use the properties of the photons (temperature and polarization) to obtain information about how the universe was during its primordial evolutionary stages. The intensity parameter I is related to CMB temperature, while Q and U parameters can be used to determine the CMB linear polarization pattern (CHANDRASEKHAR, 1960; BESSADA, 2010).

Figure C.1 - Cosmic Microwave Background



SOURCE: Kinney (2003)

CMB has a blackbody spectrum and its temperature $T \simeq 2,73K$ is almost uniform at one part in ten hundred (DODELSON, 2003; KINNEY, 2003). According to the SCM, this slightly anisotropies occur due to scalar perturbations produced during the inflationary period and enables one to study the epochs before decoupling. Moreover, any kind of polarization is also a signature that CMB photons are not an isotropic radiation beam (CHANDRASEKHAR, 1960; BESSADA, 2010).

The standard procedure to measure CMB anisotropies is through the two-point

correlation function of the temperature distribution. Since temperature corresponds to a two-dimensional field, it can be expanded in a spherical harmonics base Y_m^ℓ . So, we are dealing with a function of multipole momentum ℓ (DODELSON, 2003). Therefore, the fractional temperature variation can be defined by

$$\frac{\Delta T(\mathbf{n})}{T} = \sum_{\ell m} a_{\ell m} Y_m^\ell(\mathbf{n}), \quad (\text{C.1})$$

where \mathbf{n} is the unitary vector associated to the direction in which the measurement was taken.

For simplest inflationary models, $\frac{\Delta T(\mathbf{n})}{T}$ corresponds to a Gaussian random field. In this case, the statistical properties can be obtained from the mean and variance of the field. The first is zero by definition and the second one is determined through the two-point correlation function in the real space. This means that the variance is computed from the angular power spectrum in harmonic space (GALLI, 2015). Both definitions can be summarized by the relations

$$\langle a_{\ell m} \rangle = 0 \quad \text{and} \quad \langle a_{\ell m} a_{\ell' m'}^* \rangle = \delta_{\ell \ell'} \delta_{m m'} C_\ell, \quad (\text{C.2})$$

in which C_ℓ is usually referred to as angular power spectrum. Moreover, C_ℓ can be directly expressed in terms of the two point angular correlation function (PRASAD, 2013):

$$\left\langle \frac{\Delta T(\mathbf{n})}{T} \frac{\Delta T(\mathbf{n}')}{T} \right\rangle = C(\theta) = \sum_{\ell} \frac{2\ell + 1}{4\pi} C_\ell P_\ell(\cos \theta), \quad (\text{C.3})$$

where P_ℓ are Legendre polynomials and θ is the angle separation between the directions \mathbf{n} and \mathbf{n}' that increases as ℓ becomes smaller ($\ell \propto \theta^{-1}$).

Another way to obtain the term $a_{\ell m}^T$ associated with temperature is straight from the Stokes parameter I ,

$$I(\theta, \varphi) = \sum_{\ell=0}^{\infty} \sum_{m=-\ell}^{\ell} a_{\ell m}^T Y(\theta, \varphi)_{\ell m}, \quad (\text{C.4})$$

with θ and φ determining a given region in the sky (BESSADA, 2010). Both sides of C.4 are multiplied by $Y(\theta, \varphi)_{\ell m}$ and integrated with respect to the solid angle Ω , resulting in the expression

$$a_{\ell m}^T = \int I(\theta, \varphi) Y_{\ell m}^*(\theta, \varphi) d\Omega. \quad (\text{C.5})$$

This procedure can also be performed to get information about the CMB polarization. Here, we restrict ourselves to linear case since until the moment there is no evidence of circular polarization from CMB photons.

Before we start the discussion of the correlation function for polarization, first, it must be clear that this process is slightly different from the temperature case. The Stokes parameters Q and U are not directly related to the term $a_{\ell m}$. In fact, they are combined into the so-called E- and B-modes through the expressions (BASKARAN et al., 2006)

$$E(\theta, \varphi) = -2\nabla^a \nabla^b \mathcal{P}_{ab} \quad \text{and} \quad B(\theta, \varphi) = -2\nabla^a \nabla^c \mathcal{P}_{ab} \epsilon^a{}_c, \quad (\text{C.6})$$

where \mathcal{P}_{ab} corresponds to the symmetric-trace-free part of the polarization tensor given by (KAMIONKOWSKI et al., 1997; CABELLA; KAMIONKOWSKI, 2004; BESSADA, 2010)

$$\mathcal{P}_{ab}(\theta, \varphi) = \frac{1}{2} \begin{pmatrix} Q & -U \sin \theta \\ -U \sin \theta & -Q \sin^2 \theta \end{pmatrix}. \quad (\text{C.7})$$

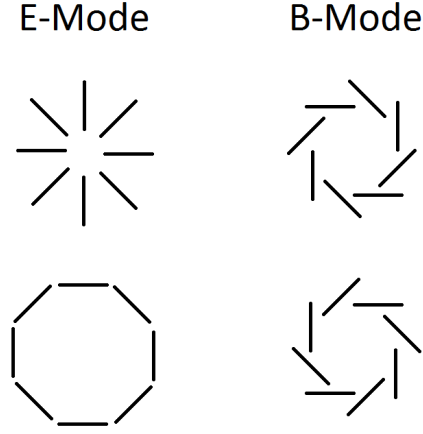
In terms of the harmonic spherical base, equation (C.6) can be written in the following form

$$E(\theta, \varphi) = \sum_{\ell=2}^{\infty} \sum_{m=-\ell}^{\ell} \left[\frac{(\ell+2)!}{(\ell-2)!} \right]^{\frac{1}{2}} a_{\ell m}^E Y(\theta, \varphi)_{\ell m}, \quad (\text{C.8})$$

$$B(\theta, \varphi) = \sum_{\ell=2}^{\infty} \sum_{m=-\ell}^{\ell} \left[\frac{(\ell+2)!}{(\ell-2)!} \right]^{\frac{1}{2}} a_{\ell m}^B Y(\theta, \varphi)_{\ell m}. \quad (\text{C.9})$$

Figure C.2 shows the specific pattern caused only by one mode or another. E-mode describes a divergent pattern, while the B-mode would determine a curl of the observed radiation beam. This is the reason why the modes are named with the letters E and B , analogously to electromagnetic case.

Figure C.2 - CMB polarization patterns



SOURCE: Saliwanchik (2015)

The equations (C.4), (C.8) and (C.9) can be worked until the invariant functions $I(\theta, \varphi)$, $E(\theta, \varphi)$ and $B(\theta, \varphi)$ achieve a suitable structure to solve the Boltzmann equations for the radiative transfer equation considering the weak gravitational field case (BESSADA; MIRANDA, 2009a). This allows one to obtain an expression for $a_{\ell m, nr}^X$ ($X = T, E, B$) where n is the wavenumber and $r = 1$ and $r = 2$ represent the left and right-hand polarization states, respectively. As a result the general correlation function can be expressed as (BASKARAN et al., 2006)

$$C_{\ell}^{XX'} = \frac{\mathcal{C}^2}{4\pi^2(2\ell + 1)} \int ndn \sum_{r=1,2} \sum_{m=-\ell}^{\ell} \left[a_{\ell m, nr}^X a_{\ell m, nr}^{X'*} + a_{\ell m, nr}^{X*} a_{\ell m, nr}^{X'} \right], \quad (\text{C.10})$$

with \mathcal{C} referring to a constant value. Therefore, at CMB area, the power spectrum consists in the plot $C_{\ell}^{XX'} \times \ell$ like Figures 5.1, 5.2 and so on. The range associated with the values of ℓ provides information from particular evolutionary stages. In case of the very early times, the values $\ell < 30$ are the most relevant part of the spectrum.

PUBLICAÇÕES TÉCNICO-CIENTÍFICAS EDITADAS PELO INPE

Teses e Dissertações (TDI)

Teses e Dissertações apresentadas nos Cursos de Pós-Graduação do INPE.

Manuais Técnicos (MAN)

São publicações de caráter técnico que incluem normas, procedimentos, instruções e orientações.

Notas Técnico-Científicas (NTC)

Incluem resultados preliminares de pesquisa, descrição de equipamentos, descrição e ou documentação de programas de computador, descrição de sistemas e experimentos, apresentação de testes, dados, atlas, e documentação de projetos de engenharia.

Relatórios de Pesquisa (RPQ)

Reportam resultados ou progressos de pesquisas tanto de natureza técnica quanto científica, cujo nível seja compatível com o de uma publicação em periódico nacional ou internacional.

Propostas e Relatórios de Projetos (PRP)

São propostas de projetos técnico-científicos e relatórios de acompanhamento de projetos, atividades e convênios.

Publicações Didáticas (PUD)

Incluem apostilas, notas de aula e manuais didáticos.

Publicações Seriadas

São os seriados técnico-científicos: boletins, periódicos, anuários e anais de eventos (simpósios e congressos). Constam destas publicações o International Standard Serial Number (ISSN), que é um código único e definitivo para identificação de títulos de seriados.

Programas de Computador (PDC)

São a seqüência de instruções ou códigos, expressos em uma linguagem de programação compilada ou interpretada, a ser executada por um computador para alcançar um determinado objetivo. Aceitam-se tanto programas fonte quanto os executáveis.

Pré-publicações (PRE)

Todos os artigos publicados em periódicos, anais e como capítulos de livros.